RECYCLING STRATEGIES FOR PEROVSKITE PHOTOVOLTAIC MODULES: LIFE CYCLE ASSESSMENT OF ENERGY USE AND ENVIRONMENTAL IMPACTS

A Thesis

Presented to the Faculty of the Graduate School

of Cornell University

In Partial Fulfillment of the Requirements for the Degree of

Master of Science

by

Xueyu Tian

August 2019

ABSTRACT

Energy use and environmental impacts of perovskite solar cells (PSCs) have been extensively investigated over the past few years, driven by three major scientific questions. The first question lies in what components or processing steps play critical roles in PSC production. In order to identify hotspots in terms of embedded energy and environmental impacts, “cradle-to-grave” comparative life cycle analyses are conducted for five types of state-of-the-art PSC device architectures. We find that the use of substrate and precious metal, as well as energy-intensive heating processes, such as thermal evaporation and calcining, are the major contributors to the primary energy consumption, carbon footprint, and other environmental impact categories. The second key question is whether recycling is worthwhile for PSCs. To this end, the system boundary is expanded to a “cradle-to-cradle” counterpart, with recycling as the end-of-life scenario. The outcome indicates that the suggested recycling strategy results in at least 47% shorter energy payback time (EPBT) and over 44% reduction of greenhouse gas (GHG) emission factor for the energy-intensive and environmentally expensive PSCs. Finally, we quantify the impacts of uncertainty induced by the immaturity of manufacturing processes and the fluctuation of operating conditions. The results emphasize the importance of prolonging the device lifetime (higher stability). Simultaneous consideration of high stability and recycling strategies could more efficiently improve the energy and environmental performance of PSCs.

BIOGRAPHICAL SKETCH

Xueyu Tian was born and raised in Wuhan, China. He graduated with a Bachelor's degree in Chemical Engineering from Xi'an Jiaotong University, China in June 2016. In August 2016, he enrolled in the Master of Science Program in Chemical Engineering at Cornell University. During his graduate study, he focused on the sustainable design and optimization of energy systems using systematic tools. He participated in several research projects on sustainable energy systems with two publications in I&EC Research and Applied Energy, respectively. Motivated by the great potential of perovskite solar cells for power generation, he then dedicated himself to the life cycle assessment of energy use and environmental impacts of state-of-the-art perovskite photovoltaic modules. He plans to pursue his PhD degree in Systems Engineering at Cornell University later in 2019.

ACKNOWLEDGMENTS

First and foremost, I would like to express my sincerest gratitude to my parents, who supported me unconditionally and constantly over the past few years. It would be impossible for me to have come this far without their encouragement and love.

I would like to thank my advisor, Professor Fengqi You, for his constant support and invaluable instruction throughout the past few years. His meticulous attention to detail and dedication to research will cast a life-long impact on my future work. It is a great honor to work with him and learn from his pursuit of excellence.

I am grateful for my committee member, Professor Jefferson Tester, for his patience and guidance. He offered very constructive comments and thoughtful feedback to make this thesis possible. I would like to thank Dr. Sam Stranks from Cambridge University for his pertinent suggestions and prompt replies during the perovskite project, despite his hectic schedule.

Last but not least, I want to thank all my current and past colleagues, who provided a colorful experience during my M.S. life. Dr. Jian Gong, Dr. Jiyao Gao, Chao Ning, and Dr. Chao Shang set great examples about high-level research, and they were always the go-to people when I came across any question or confusion. Dr. Minbo Yang helped me a lot by raising critical comments about my manuscript and presentation. Dr. Inkyu Lee spared no efforts to answer my questions about ASPEN simulation and figure drawing. Most importantly, they were all fantastic friends of mine and I would never forget the wonderful time we spent together. My thanks also go to other visiting scholars including Dr. Hua Zhou, Dr. Liang Zhao, Dr. Zuwei Liao, among others. Shipu Zhao, Ning Zhao, Yanqiu Tao, Shuwen Lu, Jiwei Yao, Wei-Han Chen, Akshay Ajagekar, and Raaj Bora, thank you guys for the wonderful time with me.

All of you are of paramount importance in my life!

TABLE OF CONTENTS

LIST OF FIGURES

LIST OF TABLES

LIST OF ABBREVIATIONS

Abbreviation	Full name
BL	Blocking layer
CdTe	Cadmium telluride
c-Si	Mono-crystalline silicon
DMF	Dimethylformamide
EPBT	Energy payback time
ETL	Electron-transport layer
GHG	Greenhouse gas
HTL	Hole-transport layer
IPCC	Intergovernmental Panel on Climate Change
ITO	Indium tin oxide
La	Lanthanum
LCA	Life cycle assessment
LCI	Life cycle inventory
LCIA	Life cycle impact assessment
MP	Mesoporous
OPV	Organic photovoltaics
PCE	Power conversion efficiency
PL	Perovskite layer
PSC	Perovskite solar cell
p-Si	Poly-crystalline silicon
PV	Photovoltaic
UV	Ultraviolet

CHAPTER 1

INTRODUCTION

Photovoltaic (PV) technologies are capable of converting solar energy into electricity without inducing significant environmental burden.[1] During the past few decades, PV technologies have demonstrated remarkable progress and become sufficiently competent to play an unrivalled role in renewable energy production. PV deployment is currently booming across the world, and the PV industry is gradually becoming a central player in the global electricity market. With power conversion efficiency (PCE) up to 27.6%,[2] the first-generation solar cells are primarily based on silicon wafers, which still dominate the current PV market.[3] For the second generation of PV technologies, amorphous silicon or non-silicon materials, such as cadmium telluride (CdTe), serve as the active material, and they are usually referred to as thin-film solar cells.[4, 5] The third-generation PV technologies adopt a variety of novel materials, including solar dye, ink, and conductive plastics, to replace the traditional active materials. The advent of the third generation of PV modules enables further cost reduction, higher scalability, and flexibility in solar cell development.[6]

With methylammonium lead iodide being the prototype,[7] perovskite PV modules demonstrate both low manufacturing cost and high PCE among the wide range of third-generation solar cells.[1] From 3.8% in 2009 to a recent certified record PCE as high as 24.2% in 2019,[2] the PCE of perovskite solar cells (PSCs) has increased substantially over a decade. Perovskite materials involve abundant elements and present low formation energy during the deposition.[8] Therefore, PSCs hold great potential to be compatible with high-volume manufacturing, such as roll-to-roll production, that would ultimately facilitate wide adoption and deployment.

Recent research efforts on perovskite PVs are directed toward enhancing the PCE, prolonging

the lifetime, and reducing the use of energy-intensive materials and processes.[9-17] There is a growing recognition of the significance of the device lifetime, and there are increasing efforts to explore new device architectures to enhance the long-term stability of PSCs.[18-22] The mesoporous (MP)-TiO_2 electron-collecting layer negatively influences the device stability when exposed to ultraviolet (UV) illumination, which is circumvented by substituting MP-TiO_2 with new electron transporting materials.[18] Organic molecules are often replaced with inorganic materials to avoid degradation when exposed to heat.[20] Multiple cation mixtures within the perovskite layer (PL) endow the PSCs with better performance, increased robustness against variation during fabrication,[21, 23, 24] and enhanced thermal stability during operation. Recent literature on perovskite PVs shows that the identified environmental hotspot materials and processes, such as gold and thermal evaporation, remain popular in the perovskite PV module fabrication,[12, 22, 25, 26] because they can facilitate easy prototyping of PSCs in academic laboratories. However, these materials or processes may encounter technical or economic challenges in scaling-up and large-scale commercialization. In order to pursue sustainable PSC production, there are two potential approaches: 1) exploring appropriate materials and processing steps with lower environmental impacts and energy consumption for PSC fabrication and 2) recycling the hotspot materials. Before we find the most suitable materials or processing steps to fabricate scaled PSC modules in industry, recycling is an effective approach for energy saving and environment protection.

The recycling procedure of PSCs would in principle be straightforward.[11, 27] Recent works reveal that the environmental hotspots in manufacturing PSCs should also be the focus in recycling phases,[10, 11, 27] because successful reuse of hotspot materials would significantly reduce energy consumption and environmental impacts in the re-manufacturing process of the recycled PSCs. Dang et al. proposed a recycling strategy to retrieve indium tin oxide (ITO)-coated glass from

decommissioned devices by sonication in dilute aqueous NaOH.[27] Even though this recycling strategy may sacrifice the upper layers, the ITO substrate is efficiently recovered with minor loss of performance. Kim et al. and Kadro et al. presented a recycling method for reusing gold electrodes and transparent conducting glasses via selective dissolution.[11, 28]

Life cycle assessment (LCA) is a widely used methodology to systematically evaluate the environmental impacts of a certain product throughout the life cycle.[29, 30] As required by the systematic LCA framework, different end-of-life scenarios for PV modules should be carefully investigated. There are three typical end-of-life scenarios for PSCs, i.e., recycling, landfill, and failure of the modules with subsequent accidental release.[12] Unexpected module failure is dominated by numerous factitious and natural factors, which are quite difficult to forecast or prevent, so this scenario is excluded from our consideration. Even though ill-considered landfill may result in severe waste of materials and energy accompanied by environmental contamination, both municipal and hazardous wastes are widely disposed of in this way. Previous LCA studies of PSCs either focus on landfill as the end-of-life scenario,[10] or simply consider a "cradle-to-gate" system boundary.[16, 31] Therefore, it remains an unmet research challenge to systematically evaluate and highlight the advantages of PSC recycling over the landfill counterpart. Two ISO-compliant approaches to modeling the life cycle inventory (LCI) of recycling of materials, namely the cutoff approach (the recycled content approach) and the avoided burden approach (the end of life recycling approach), are frequently applied in LCA studies for end-of-life modeling.[32] The former supports risk-averse attitude without burden shifting to future generations, while the latter borrows environmental loans from future generations for man-made capital potentially being recycled in the future.

In this work, systematic LCA studies are performed to quantitatively assess and compare the

"cradle-to-grave" environmental impacts of five types of state-of-the-art PSCs, including three innovative modules developed at the laboratory scale and two prototyping architectures for scaled modules in industry. Specifically, 18 midpoint environmental impact categories are first evaluated, which are then aggregated into three endpoint indicators according to the ReCiPe methodology.[33] To obtain the complete life cycle impact assessment (LCIA) results for all relevant materials, comprehensive manufacturing routes are developed and modeled to determine the corresponding mass and energy balances for LCIs. This approach bridges undocumented substances with those well archived in the database. In addition, we calculate two prevalent sustainability metrics, namely energy payback time (EPBT) and greenhouse gas (GHG) emission factor, which are then compared with existing PV technologies to critically analyze the pros and cons of perovskite PVs and emphasize on the necessity of PSC recycling. A Monte Carlo simulation method is employed in the following step to decipher the uncertainty in input parameters, followed by a sensitivity analysis to quantify the influences of parameter deviation. Furthermore, module recycling is considered as the end-of-life scenario for PSCs to gauge the tremendous potential of recycling the environmental hotspots, where the system boundary is expanded as a "cradle-to-cradle" counterpart. The end-of-life recycling phase is modeled using the avoided burden approach. The effectiveness of recycling strategy on different levels are quantified for environmental hotspot materials. Ultimately, we provide insights about promising perovskite PV modules and recycling strategies for judicious decision making in perovskite PV research, development and manufacturing.

CHAPTER 2

MATERIALS AND METHODS

2.1 Goal and scope definition

The goal of this LCA study is to evaluate the life cycle environmental impacts of five types of state-of-the-art PSCs across all life cycle stages. The functional unit of this LCA is set as 1 m^2 of envisioned perovskite PV module, which follows the typical approach in the literature.[17, 34] All LCIs and LCIA results are converted by aligning with the functional unit. The geometric fill factor, defined as the ratio between the active area and the total area of the module, is assumed to be 80%. The module efficiency is determined by multiplying the certified PCE of the active area by the geometric fill factor.[10]

In this work, the system boundary is defined to embrace four life cycle stages: (1) raw material acquisition; (2) module assembly; (3) power generation; and (4) end of life. Raw material acquisition phase refers to the acquisition of all raw materials needed in the module assembly phase. The module assembly phase is defined as the layer-by-layer deposition procedures of functional layers, including the top metal contact, electron-transport layer (ETL), perovskite layer, hole-transport layer (HTL), and transparent conducting substrate, as well as the etching, drying and calcining process to produce functional PV modules. Completed perovskite PV modules are then installed for power generation. After module use, perovskite PV modules are decommissioned from the local facilities and go to the end of life. Even though landfill is commonly chosen to dispose of the worn-out PV modules, it is clearly not the best choice from an environmental perspective. Alternative disposal approaches, such as incineration, are also feasible. Nevertheless, we do not consider these disposal methods in this work because of either intensive energy consumption or a lack of data. The module-use phase and transportation phase are both excluded

from the system boundary following assumptions made in the existing literature.[10, 35-38] Note that solvent recycling is not considered due to the complicated composition of used solvents and a lack of data. In order to make intuitive comparison with the existing PV technologies in terms of EPBT and GHG emission factor, we initially consider landfill as the end-of-life scenario in Subsections 3.1 to 3.2, where the decommissioned PSCs are regarded as inert waste in the disposal stage. Next, we quantify the influence of recycling strategies in Subsection 3.3 to 3.4, where the "cradle-to-grave" system boundary (in Figure 2) is modified to consider recycling as the end-of-life scenario (vide infra) in Figure 10.

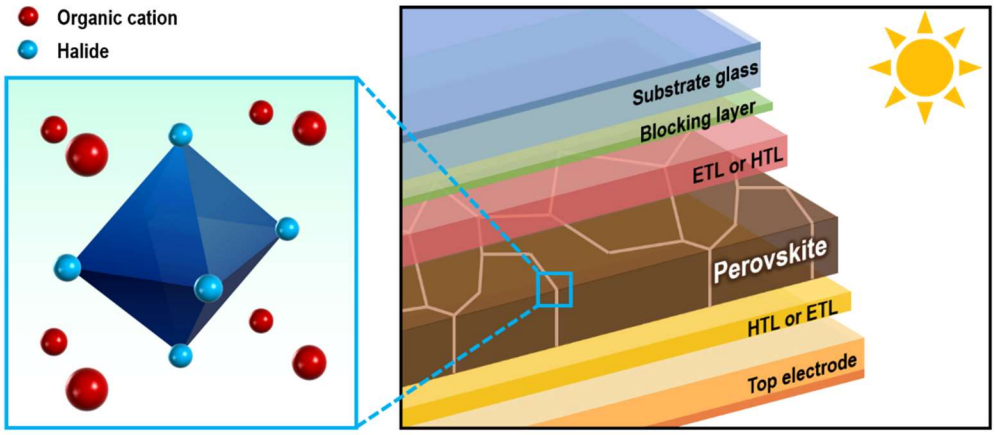

Figure 1. Schematic of perovskite solar cells.

Recently, new perovskite PV modules with various device architectures have been reported to present either continuous record-breaking PCE or enhanced stability. However, not all these innovative device architectures are suitable for scaling-up. Therefore, we classify them into two groups: one refers to laboratory-scale modules, which use efficient but niche materials in device fabrication; the other group refers to device architectures that serve as promising prototypes for scaled modules in industry. An illustration of a typical perovskite PV cell is shown in Figure 1.

Among numerous options, we pay special attention to two commercial-scale single-junction modules and three laboratory-scale modules due to their promising module efficiency and stability. For the laboratory-scale modules, widely adopted processing steps, such as spin coating and thermal evaporation, are considered according to the reported experimental procedures. However, the encapsulation step is not adopted as a standard approach for the laboratory-scale modules, while it is imperative for the scaled modules in industry to prolong their lifetime. Since there is no consistent method for PSC encapsulation, we use a typical encapsulation approach for organic PV (OPV) as a preliminary approximation. Moreover, slot-die coating, a scalable deposition method with higher material utilization efficiency, is employed to replace spin coating in manufacturing commercial-scale modules; thermal evaporation is substituted with sputtering as the latter is less dependent on the vacuum level, and generally has shorter processing time than thermal evaporation.[8] The technical details are illustrated in Table 1, from which we can differentiate among the five device architectures. Each PSC is named according to the unique materials used in device fabrication or other novelties. The system boundary of manufacturing the Lanthanum (La)–doped $BaSnO_3$ (LBSO) module with landfill as the end-of-life scenario is shown in Figure 2.

Table 1. Technical details of five types of state-of-the-art perovskite PV modules.

	LBSO module[18]	Metal oxide module[20]	Mixed-cation module [a 23]
Module efficiency [b]	16.96%	11.68%	16.64%
Substrate	FTO glass	ITO glass	FTO glass
ETL/HTL	LBSO/PTAA	ZnO/NiO_x	TiO_2/spiro-OMeTAD
Electrode	Gold	Aluminum	Gold
	Defect-engineered module[39]	SnO_2 module[40]	

Module efficiency [b]	17.68%	17.28%
Substrate	FTO glass	ITO glass
ETL/HTL	TiO_2/PTAA	SnO_2/spiro-OMeTAD
Electrode	Gold	Gold

[a] The mixed-cation module refers to the PSC using perovskite materials that involve mixed organic cations.

[b] The module efficiency is derived by multiplying the laboratory-scale efficiency with the geometric fill factor.

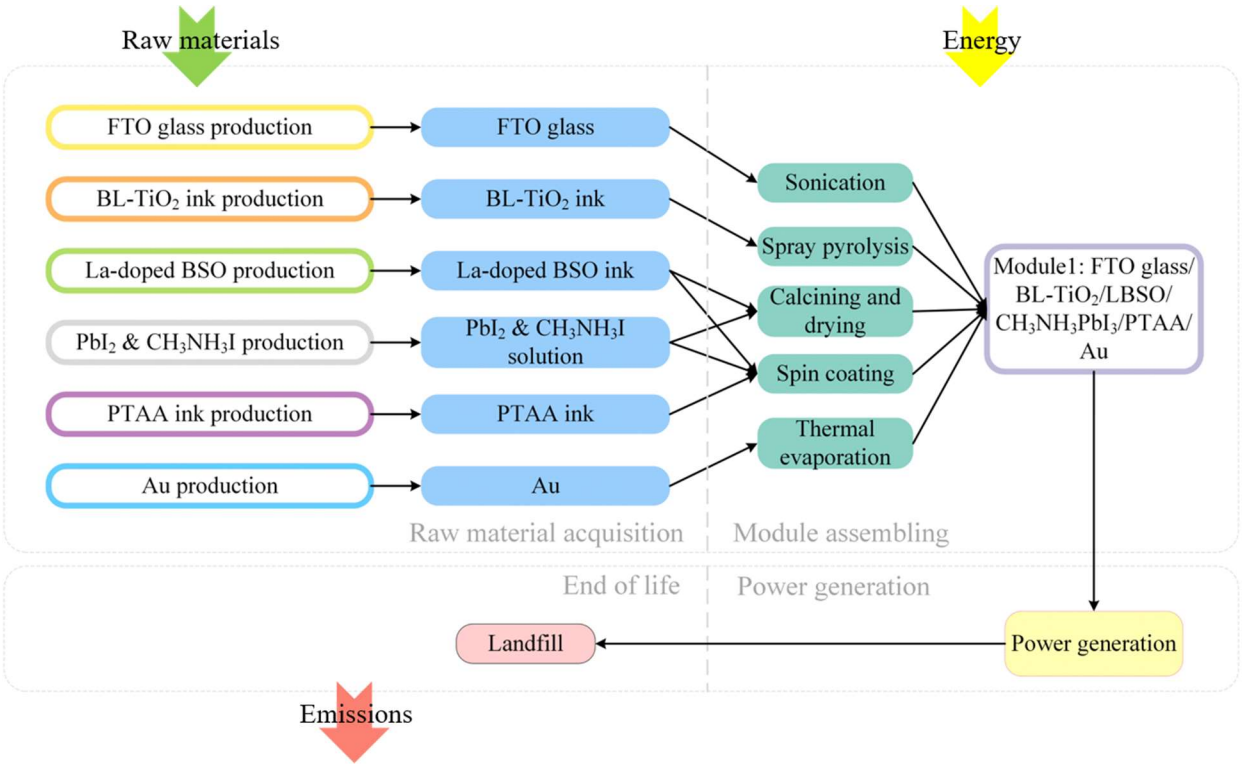

Figure 2. System boundary of manufacturing LBSO perovskite solar modules with landfill as the end-of-life scenario.

2.2 Life cycle inventory analysis

Data acquisition is an important step in LCA. Key data for LCA can be classified into two categories, namely, LCIs and characterization factors. There are various sources of LCI data, such as literature, simulation results, experimental reports, and patents. In this study, most LCI data are

extracted from relevant literature with high-fidelity source data.[18, 20, 23] Relevant characterization factors are typically extracted from the Ecoinvent database if available.[41] The data gap arises from the substances which are not archived in Ecoinvent database and are usually chemicals of which the production is not commercialized yet. For these substances, we comprehensively and rigorously model their manufacturing pathways, which produces the target components as main products, and analyze the corresponding mass and energy balances to establish the LCIs and characterization factors of these undocumented components. The derivation of these characterization factors mainly depends on the chemical reactions and separation processes, where many parameters from existing publications, such as stoichiometric coefficient, solubility, and yields are used, so the calculations of these characterization factors are relatively accurate. Several module-related input parameters, such as performance ratio (ratio between the actual and the theoretically possible energy output),[34] lifetime, and annual irradiation, are case-specific and subject to uncertainty.

LCI of this study can be classified into two categories, namely material inventory and energy inventory. The material inventory is comprised of three parts, i.e., mass of raw materials, direct emissions during assembly, and mass of module to be disposed of during end of life. Table 2 illustrates the mass inventory of 1 m^2 of the LBSO module with an 80% geometric fill factor. The mass of cleanser and substrate glass are extracted from the literature.[10, 35] We calculate the mass of BL-TiO_2 ink, LBSO nanoparticles solution, PbI_2 ink, CH_3NH_3I ink, PTAA, and gold electrode based on the module active area, conversion efficiency, utilization efficiency, and thickness of the corresponding layer in the finished product. The amount of solvent is derived from the volume and solubility of solutes, as well as the density and concentration of the solution. Direct emissions mainly come from the wasted effective components in the raw materials and the evaporated

solvents during manufacturing. Following existing LCA studies of perovskite PVs,[10] the material utilization efficiencies of spin coating, spray pyrolysis, and thermal evaporation of electrode are fixed at 30%,[35] 80%,[42] and 82%,[43] respectively. The mass of module is estimated by summing up all effective components. Because the LCIA results of several key chemicals are not readily available in the known LCA databases, we establish comprehensive manufacturing routes for these components. By modeling manufacturing pathways for the key components whose LCIA results are not available in the Ecoinvent,[41] we can derive their energy balance and mass balance relationships from the well archived components. The manufacturing routes, LCIs, and corresponding LCIA results of LBSO nanoparticle solution and PTAA solution are available in the Supplementary Information.

Table 2. Material inventory of 1 m^2 of the LBSO module with an 80% active area.

	Mass (kg)	Notes
Substrate patterning		
FTO glass	5.040E+00	Substrate
Zinc power	7.130E-05	Chemical etching
Dilute HCl	1.868E-04	$Zn+2HCl \rightarrow ZnCl_2+H_2$
Ethanol	2.577E-02	Cleaning solvent
Deionized water	3.266E-02	Cleaning solvent
BL deposition		
BL-TiO_2 ink	1.462E-02	70 nm of blocking layer
Ethanol	2.577E-02	Cleaning solvent
Deionized water	3.266E-02	Cleaning solvent
ETL deposition		
La-doped BSO NPs	2.317E-03	120 nm of ETL

2-Methoxyethanol	1.544E-03	Solvent of La-doped BSO NPs
Perovskite layer deposition		
PbI_2	2.313E-03	140 nm
Dimethylformamide	4.746E-03	Solvent of PbI_2
CH_3NH_3I	7.979E-04	300 nm
Isopropanol	6.253E-02	Solvent of CH_3NH_3I
Toluene	8.670E-04	Additive
HTL deposition		
PTAA solution	9.194E-03	HTL precursor
Cathode deposition		
Au	1.883E-03	100 nm of electrode
Direct emissions		
$ZnCl_2$	1.044E-04	Resultants from chemical etching
H_2	1.536E-06	
Ethanol	1.328E-02	Solvent in BL-TiO_2 ink
$TiCl_4$	1.406E-04	Wasted effective component of BL-TiO_2 ink
Isopropanol	6.342E-02	Solvent in BL-TiO_2 ink and solvent of CH_3NH_3I
Acetone	4.298E-04	Solvent in BL-TiO_2 ink
Acetic anhydride	7.573E-04	Solvent in BL-TiO_2 ink
La-doped BSO NPs	1.622E-03	Wasted effective component of LBSO ink
2-Methoxyethanol	1.544E-03	Solvent in LBSO ink
PbI_2	1.619E-03	Wasted PbI_2
Dimethylformamide	4.746E-03	Solvent of PbI_2
CH_3NH_3I	5.585E-04	Wasted CH_3NH_3I
PTAA	1.050E-05	Wasted effective component of PTAA solution
LiTFSI	1.190E-04	Wasted effective component of PTAA solution
Toluene	2.168E-03	Solvent in PTAA solution and waste from spin coating

Acetonitrile	7.860E-04	Solvent in PTAA solution
4-tert-butylpyridine	6.923E-03	Solvent in PTAA solution
Au	3.389E-04	Wasted gold
Mass of module	**5.043**	Landfill

Table 3. Energy inventory of 1 m^2 of the LBSO module with an 80% active area.

	Power (W)	Time (s)	Electricity (kWh)
Substrate patterning			
Sonication	1.449E+03	1,200	4.831E-01
BL deposition			
Spray pyrolysis	1.300E+02	19	6.691E-04
ETL deposition			
LBSO spin coating	2.020E+04	30	1.683E-01
Calcining	3.374E+03	3,600	3.374E+00
Perovskite layer deposition			
1^{st}-step spin coating	6.733E+03	10	1.870E-02
2^{nd}-step spin coating	3.367E+04	20	1.870E-01
Drying	5.327E+02	600	8.879E-02
HTL deposition			
PTAA spin coating	2.020E+04	30	1.683E-01
Electrode deposition			
Thermal evaporation			3.309E+00
Total			**7.797**

Table 3 presents the energy inventory during the assembly phase of 1m^2 of LBSO module. All devices used for assembling the LBSO modules are driven by electricity, and the amount of electricity consumption in each procedure is evaluated based on the power and corresponding

operational time. Electricity consumption for manufacturing 1 m^2 of the LBSO module amounts to 7.797 kWh.

Table 4. Material inventory of 1 m^2 of the defect-engineered module with an 80% active area.[39]

	Mass (kg)	Notes
Substrate		
FTO glass	5.040E+00	Substrate
BL deposition		
BL-TiO_2 ink	1.253E-02	60 nm of blocking layer
ETL deposition		
MP-TiO_2	5.076E-04	150 nm of ETL
2-Methoxyethanol	2.449E-03	Solvent of MP-TiO_2
Perovskite layer deposition		
PbI_2	7.672E-04	156 nm
$PbBr_2$	1.566E-05	3 nm
FAI	2.463E-04	286 nm
MABr	3.079E-05	55 nm
Dimethylformamide	9.709E-03	Solvent
DMSO	2.816E-04	Solvent
Isopropanol	2.420E-03	Solvent
HTL deposition		
PTAA solution	8.909E-04	HTL precursor
Cathode deposition		
Au	1.544E-03	100 nm of electrode
Encapsulation		
Adhesive	2.020E-02	

PET	6.170E-02	
Direct emissions		
$TiCl_4$	1.206E-04	Wasted effective component of BL-TiO_2 ink
Isopropanol	3.182E-03	Solvent
Acetone	3.684E-04	Solvent
Acetic anhydride	6.491E-04	Solvent
2-Methoxyethanol	2.449E-03	Solvent in MP-TiO_2 ink
Dimethylformamide	9.709E-04	Solvent
DMSO	2.816E-04	Solvent
Toluene	8.700E-04	Solvent in PTAA solution
Acetonitrile	5.895E-06	Solvent in PTAA solution
Mass of module	**5.123**	Landfill

Table 5. Energy inventory of 1 m^2 of the defect-engineered module with an 80% active area.

	Power (W)	Time (s)	Electricity (kWh)
BL deposition			
Spray pyrolysis	1.300E+02	16	5.736E-04
ETL deposition			
MP-TiO_2 slot-die coating	1.500E+03	60	2.500E-02
Calcining	3.374E+03	3,600	3.374E+00
Perovskite layer deposition			
1^{st}-step slot-die coating	1.500E+03	60	2.500E-02
2^{nd}-step slot-die coating	1.500E+03	60	2.500E-02
1^{st}-step drying	5.327E+02	1800	2.664E-01
2^{nd}-step drying	8.879E+02	1800	4.439E-01
Annealing	5.327E+02	1800	2.664E-01
HTL deposition			

PTAA slot-die coating	1.500E+03	60	2.500E-02
Electrode deposition			
Sputtering	5.000E+01	400	5.556E-03
Encapsulation			
Lamination	1.500E+03	30	1.250E-02
Total			**4.469**

Table 4 and Table 5 summarize the material and energy inventories of the defect-engineered module. Power consumption of the defect-engineered module is 4.469 kWh. The LCIs and LCA results of NiO_x precursor solution, ZnO precursor solution, FAI, MABr, and $PbBr_2$ are available in the Supplementary Information. The LCIs of other key components, such as FTO glass, ITO glass, PbI_2 ink, CH_3NH_3I ink, BL-TiO_2 ink, and spiro-OMeTAD are extracted from the literature,[10] and the corresponding LCA results are calculated according to ReCiPe LCIA method.[33] The relevant LCIs of the other investigated PSCs and the recycling processes are given in the Supplementary Information.

2.3 Life cycle impact assessment

The LCI data are converted into various impact categories by multiplying with the corresponding characterization factors. The individual impact assessment results for each entry in the LCIs are then summed up to reveal the overall environmental profile. The impact analysis results are allocated using mass-based allocation method. In this work, 18 midpoint indicators and three endpoint indicators are selected to give a comprehensive evaluation of the investigated perovskite PV modules according to the ReCiPe method.[33] In addition, primary energy consumption and carbon footprint are evaluated according to the cumulative energy consumption in Ecoinvent database,[41] and Intergovernmental Panel on Climate Change (IPCC) 2013 (climate

change) method.[44] Finally, two widely used sustainability indicators, namely EPBT and GHG emission factor, are calculated and compared with existing PV technologies.

In the state-of-the-art ReCiPe method, 18 categories of potential environmental impacts are taken into account, in order to provide a comprehensive estimation on the environmental profile over the lifetime of a certain product. The 18 metrics are agricultural land occupation, climate change, fossil depletion, freshwater ecotoxicity, freshwater eutrophication, human toxicity, ionizing radiation, marine ecotoxicity, marine eutrophication, metal depletion, natural land transformation, ozone depletion, particulate matter formation, photochemical oxidant formation, terrestrial acidification, terrestrial ecotoxicity, urban land occupation, and water depletion. To give a more intuitive assessment, the 18 midpoint indicators are aggregated into three endpoint impact scores regarding ecosystem quality, human health, and resources.

Similar to LCIA method Eco-indicator 99,[45] cultural perspectives theory is used to develop the ReCiPe method, and three subjective choices on time frame are proposed, which are identified as individualist (I), hierarchist (H), and egalitarian (E).[33] Following the assumption made in existing publications,[10, 37] perspective E is selected, which takes into account the longest time-frame, and thus is the most precautionary perspective.

Primary energy is the energy that has not been subjected to any human-engineered conversion process. Primary energy can be categorized into two groups, namely, renewable primary energy and non-renewable primary energy. Renewable primary energy embraces solar energy, wind energy, hydropower, biomass sources, primary forest, and geothermal energy, while non-renewable sources are exemplified by fossil fuels. By summing up all the primary energy demand, we can obtain the total cumulative energy demand for manufacturing raw materials, which is also known as the energy embedded within the feedstocks. Primary energy consumption is a prevailing

metric used by numerous LCA practitioners focusing on PV technologies.[10, 37, 46-48] The cumulative energy demand data for most raw materials are directly available in the Ecoinvent database.[41] There are, however, components whose relevant data are not reported. For these key chemicals, we establish the manufacturing pathways, and then derive the undocumented LCIA results. The end-of-life primary energy consumption refers to the energy consumed in landfill or recycling, as well as the embedded energy in the solvent used for selective solution during recycling.

As another prevailing environmental metric in numerous LCA on PV technologies,[36, 49, 50] carbon footprint reveals the GHG emissions across the lifetime of a product. In contrast to the primary energy consumption, there are four contributions to the total carbon footprint, namely raw materials, energy consumption, direct emissions, and end of life.

EPBT and GHG emission factor, derived from primary energy consumption and carbon footprint, respectively, are two widely used metrics in evaluating the sustainability of energy systems. These two prevailing metrics comprehensively consider many other factors such as annual irradiation, performance ratio, lifetime, and module efficiency.

2.4 Interpretation

The LCIA results demonstrate intuitive distribution of each impact category. Moreover, EPBT and GHG emission factor are calculated to evaluate the sustainability of the five investigated PSCs. The major impact contributors are identified as environmental hotspots, which provides guidance to determine the focus of the recycling work. Different recycling levels are then assigned to these environmental hotspots to quantify the effectiveness of recycling strategies. A momentary glimpse is given to envision the future of recycling PSCs from the perspectives of policy and infrastructure. By running Monte Carlo simulations, uncertainty analyses are performed to reflect the distribution of EPBT and GHG emission factor based on the assigned distribution patterns of input parameters.

In addition, sensitivity analyses are conducted to identify the input parameters contributing most to the variability of the primary energy consumption and carbon footprint during the manufacturing of recycled PSCs.

CHAPTER 3

RESULTS AND DISCUSSION

3.1 Environmental profile

Figure 3 and Figure 4 show the environmental profiles of the LBSO module and the defect-engineered module based on the ReCiPe LCIA method. All 18 midpoint impact categories and three endpoint indicators are normalized, which makes it intuitive to identify the major contributors for each impact category. The resulting environmental profiles serve as an important basis to identify the hotspot materials and processing steps and provide insights for the recycling work.

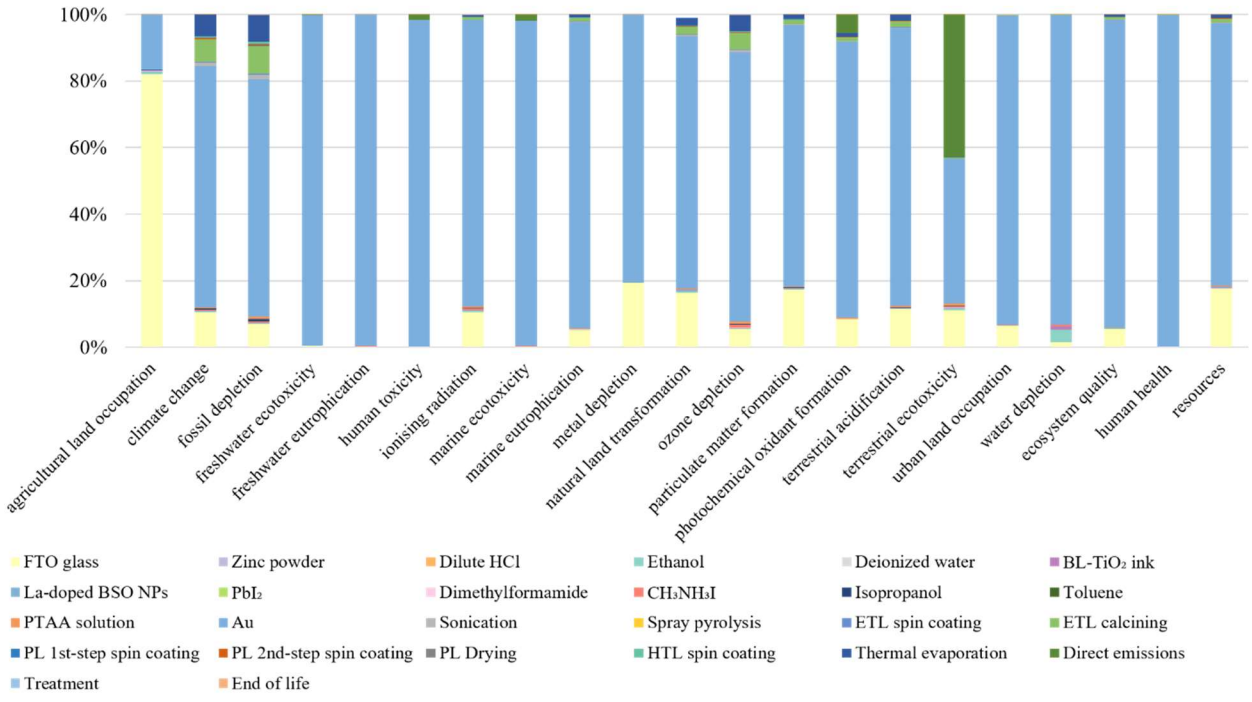

Figure 3. Environmental profile of a 1 m^2 LBSO module.

As shown in Figure 3, the use of gold electrode dominates most of the impact categories for the LBSO module even though the quantity of gold electrode is relatively small (1.54 g). To be

more specific, gold contributes to 72.4% of the climate change, 71.4% of the fossil depletion, 99.3% of the freshwater ecotoxicity, 99.6% of the freshwater eutrophication, 98.0% of the human toxicity, 85.9% of the ionising radiation, 97.8% of the marine ecotoxicity, 92.0% of the marine eutrophication, 79.9% of the metal depletion, 77.7% of the natural land transformation, 80.8% of ozone depletion, 78.4% of the particulate matter formation, 82.8% of the photochemical oxidant formation, 83.5% of the terrestrial acidification, 43.5%% of the terrestrial ecotoxicity, 92.8% of the urban land occupation, 93.0% of water depletion, 92.4% of the ecosystem quality, 99.5% of the human health, and 78.8% of the resources. Gold production always requires intensive consumption of various resources, including energy, water, cyanide, etc.[51] In addition, the resulting toxic mine drainage with residual cyanide and mercury can be highly detrimental to local ecosystems even at relatively low concentrations.[52] Furthermore, as the ore grades decline due to continuous mining, the unit resource consumption or release also increases, which makes the environmental issue of gold production even more acute.[51] Therefore, environmentally expensive electrode material, such as gold and silver, will not be compatible with scaled PSC production and thus exploration of substitute is of critical importance. To this end, non-precious transition metals, especially copper, are investigated to replace noble metals and utilized for laboratory-scale PSC fabrication.[53] When it comes to the defect-engineered module, a similar environmental profile dominated by FTO glass and gold can be observed in Figure 4.

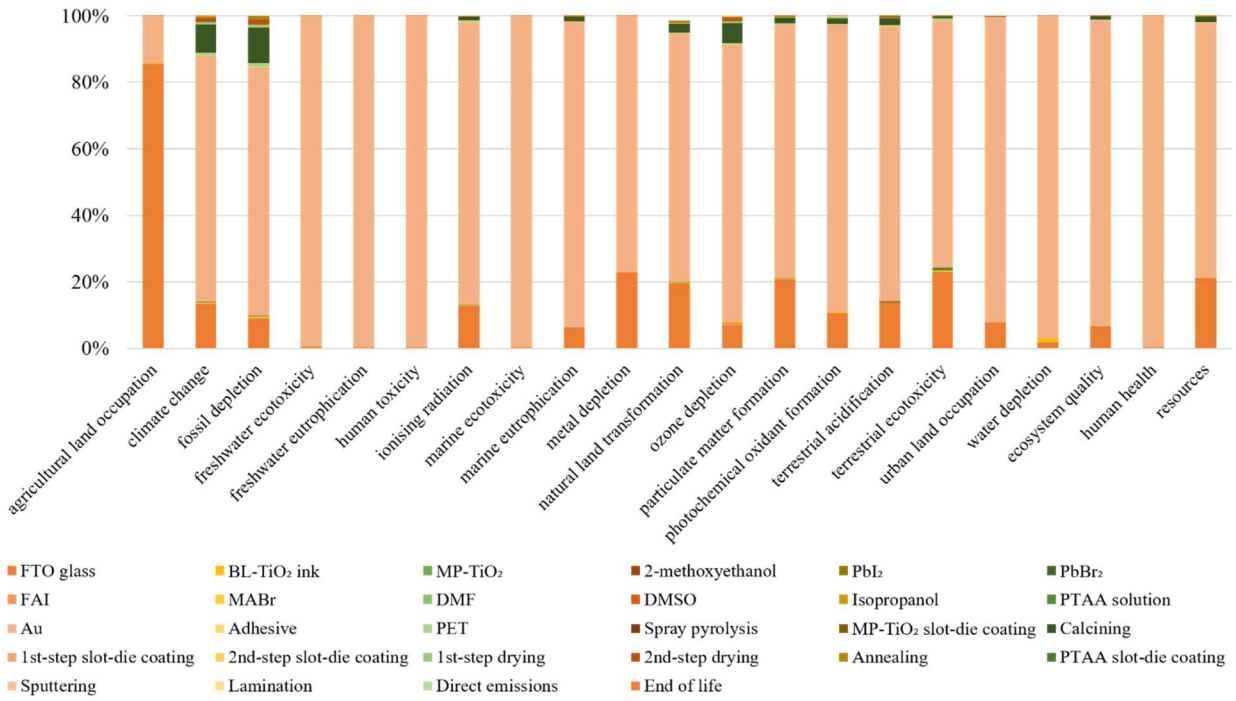

Figure 4. Environmental profile of a 1 m^2 defect-engineered module.

The environmental profiles of the other three modules including two laboratory-scale PSCs and one commercial-scale PSC are presented in the Supplementary Information. We then compare the LCIA results of the five investigated modules in Figure 5. The LBSO module is defined as the base case for normalization for all 21 impact categories. The metal oxide module employs metal oxide nanoparticle films as hole and electron transporting materials, which circumvent the toxic and environmentally expensive reagents to fabricate organic HTLs or ETLs. This module presents better environmental performance than the other four investigated PSC modules, because most impact categories of such PSC are maintained at relatively low levels.

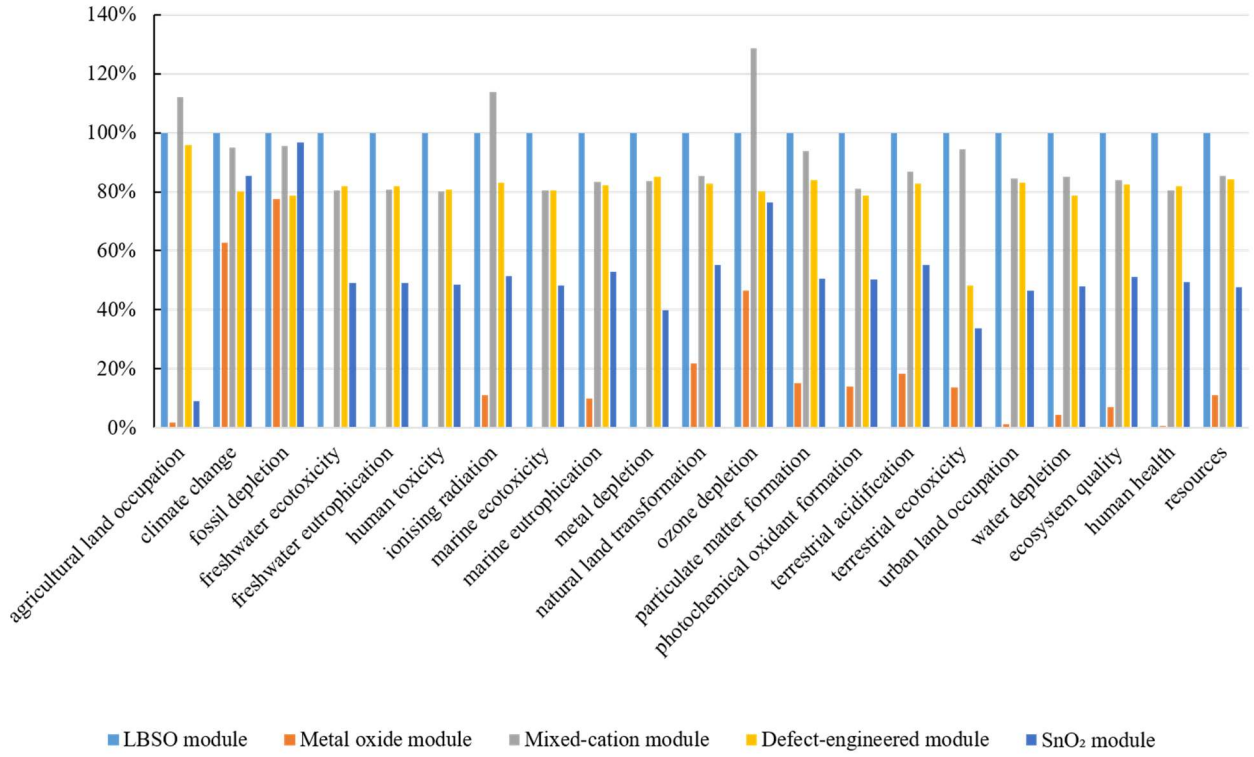

Figure 5. Comparative LCIA results among the five investigated modules (The LBSO module is defined as the base case for normalization).

3.2 Primary energy consumption and carbon footprint

Two attractive impact categories, namely primary energy consumption and carbon footprint, are calculated for the five perovskite PV modules based on the LCIA results and demonstrated in Figure 6 to Figure 9.

EPBT is an important metric for PV systems, which is defined as the time needed to generate as much energy as was consumed during manufacturing and operations of the system. There is little energy consumption during the operation phase of perovskite PV modules, so EPBT is dominated by the energy embedded in raw materials, as well as the energy consumption during

production and recycling processes. The GHG emission factor is obtained by dividing the life cycle GHG emissions by the total electric energy production during the lifetime of the given PSC system. When calculating the EPBT and GHG emission factor, we account for individual difference of PSCs and impacts of operating conditions on module performance and consider the fluctuation of parameters such as annual irradiation, module efficiency, performance ratio, lifetime, primary consumption, and carbon footprint.

As shown in Figure 6, during the lifetime of the three laboratory-scale perovskite PV modules, the LBSO module presents the highest primary energy consumption of up to 591.5 MJ/m^2-module, and the metal oxide module has the lowest primary energy consumption of 396.1 MJ/m^2-module. For all investigated modules, the energy embedded in the raw materials accounts for 76.2% to 85.4% of the total primary energy consumption, while energy consumption during the treatment phase and the end of life are negligible. Moreover, the breakdowns of the energy embedded in raw materials and energy consumed during module assembly vary significantly from module to module.

For both LBSO and mixed-cation modules, the embedded energy is dominated by FTO glass and gold, while ITO glass is the only major contributor in the metal oxide module due to the use of energy-intensive indium. Gold contributes 80% and 76% of the total primary energy consumption of the LBSO module and the mixed-cation module, respectively; FTO glass contributes 17% and 20% for the two modules, respectively. FTO glass accounts for a large proportion of the total primary energy consumption, mainly because it makes up over 90% of the total module mass. The dominance of gold and ITO glass to these metrics is fundamentally due to the use of precious metals, which consumes extremely large amounts of energy in smelting the metal ores, despite the small total mass used. Herein, we note that the use of precious metals and substrates are two significant environmental hotspots, which is consistent with the results reported

in the literature.[10] New materials and device architectures can be devised by reducing the consumption of these hotspot materials, which is likely to result in much lower primary energy consumption and carbon footprint. In addition, even though ITO glass is much more energy-intensive than FTO glass, the overall environmental impacts of ITO module would be lower if non-precious metal electrodes, such as aluminum, are employed.

Regarding the module assembly phase, the heating process is always the most energy-intensive aspect, typically covering over 80% of the total energy consumption. Specifically, thermal evaporation of the metal electrode accounts for 43%, 42%, and 47% of the total primary energy consumption of the fabrication of the LBSO, metal oxide, and mixed-cation modules, respectively. Annealing and drying are the other major contributors besides thermal evaporation. Even though several steps of module assembly involve spin coating, the total energy consumed by spinners is less pronounced. The energy consumption will be further reduced for other solution processing methods, such as slot-die coating, for fabricating scaled PSC modules in the future.

Figure 8 depicts the detailed breakdowns of carbon footprint during the lifetime of the three laboratory-scale perovskite PV modules. Distinct from primary energy consumption, there are five contributing phases to the total carbon footprint, i.e. material embedded, module assembly, direct emissions, treatment, and end of life. Similar to the results of primary energy consumption, gold, FTO glass, ITO glass, and heating processes are the major contributors. We notice that the carbon footprint distribution of module assembling phase is exactly the same as the primary energy distribution for each module because electricity is the only input during module assembling.

The comparative results of primary energy consumption and carbon footprint among the two commercial-scale PSCs are given in Figure 7 and Figure 9, respectively. For the primary energy consumption and carbon footprint embedded in the raw materials, the use of substrate and precious

metal are still the major contributors. However, the deposition of the metal electrode is no longer the most energy-intensive or environmentally expensive processing step in the assembling phase due to the use of sputtering. This result indicates that sputtering is more likely to be adopted for scaled PSCs fabrication with lower energy intensity than thermal evaporation.

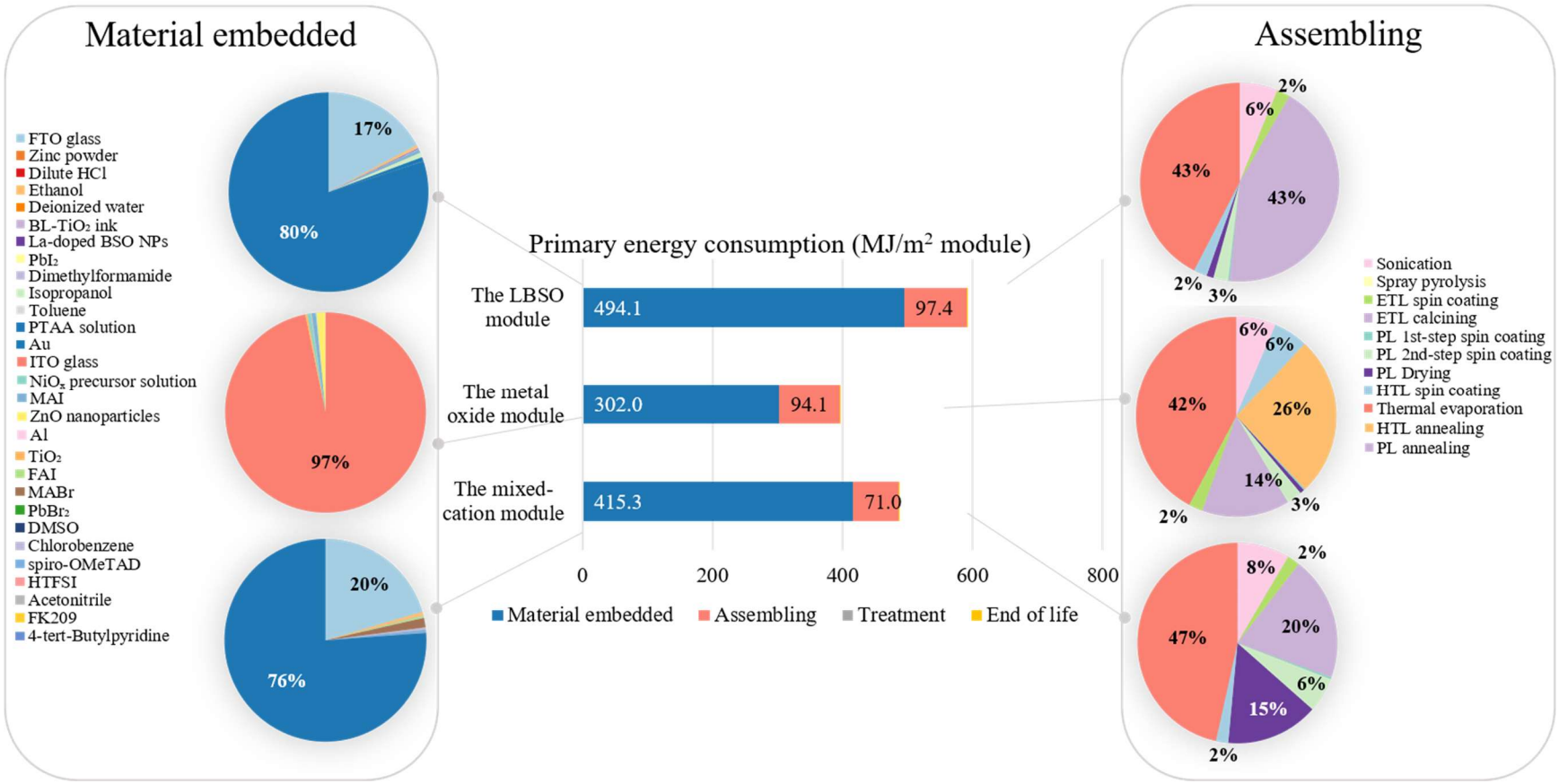

Figure 6. Profile of primary energy consumption of the three laboratory-scale perovskite PV modules (The bar charts in the middle reflect the breakdown of primary energy consumption during different phases ending up with landfill. The pie charts on the left reveal the energy embedded in various feedstocks for the three PSCs, while the pie charts on the right depict the energy consumption of different manipulations during assembling phase for the three PSCs).

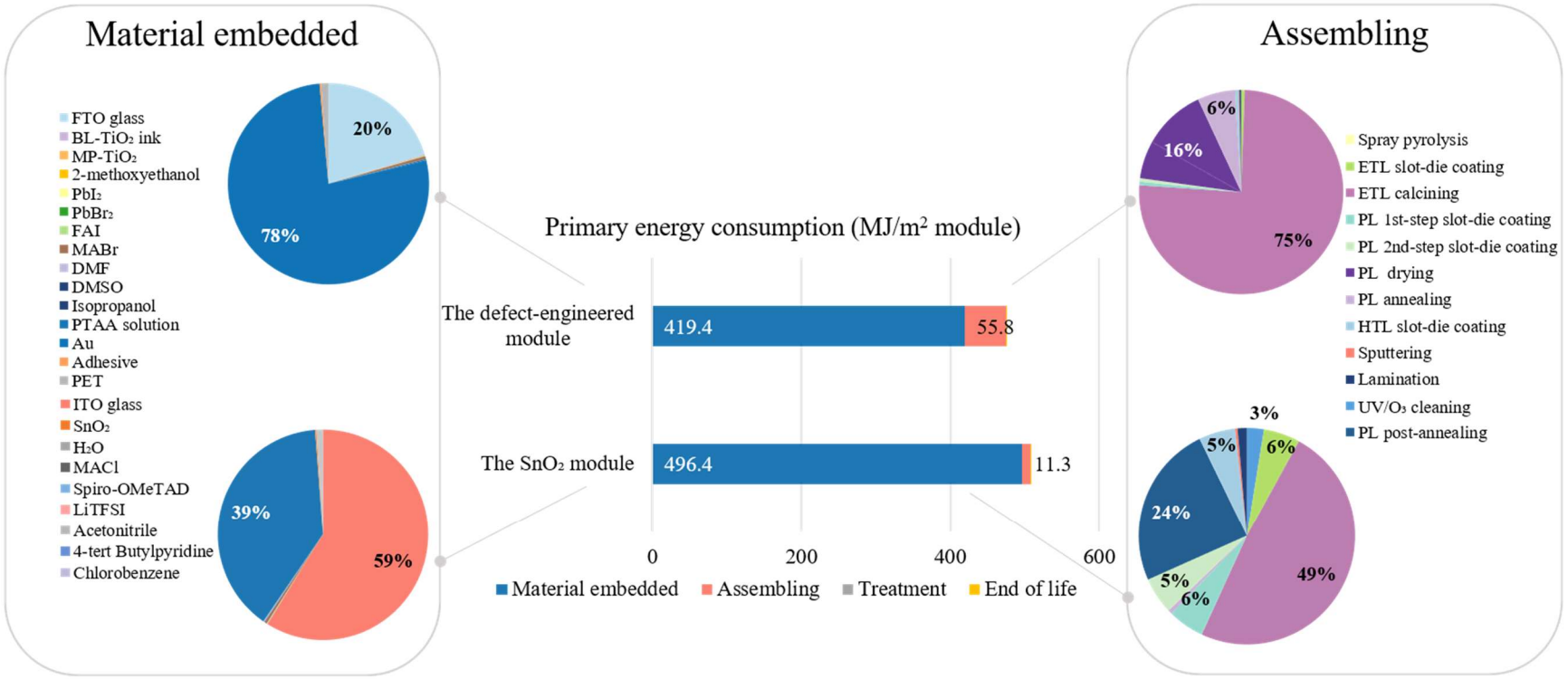

Figure 7. Profile of primary energy consumption of the two commercial-scale perovskite PV modules (The bar charts in the middle reflect the breakdown of primary energy consumption during different phases ending up with landfill. The pie charts on the left reveal the energy embedded in various feedstocks for the two PSCs, while the pie charts on the right depict the energy consumption of different manipulations during assembling phase for the two PSCs).

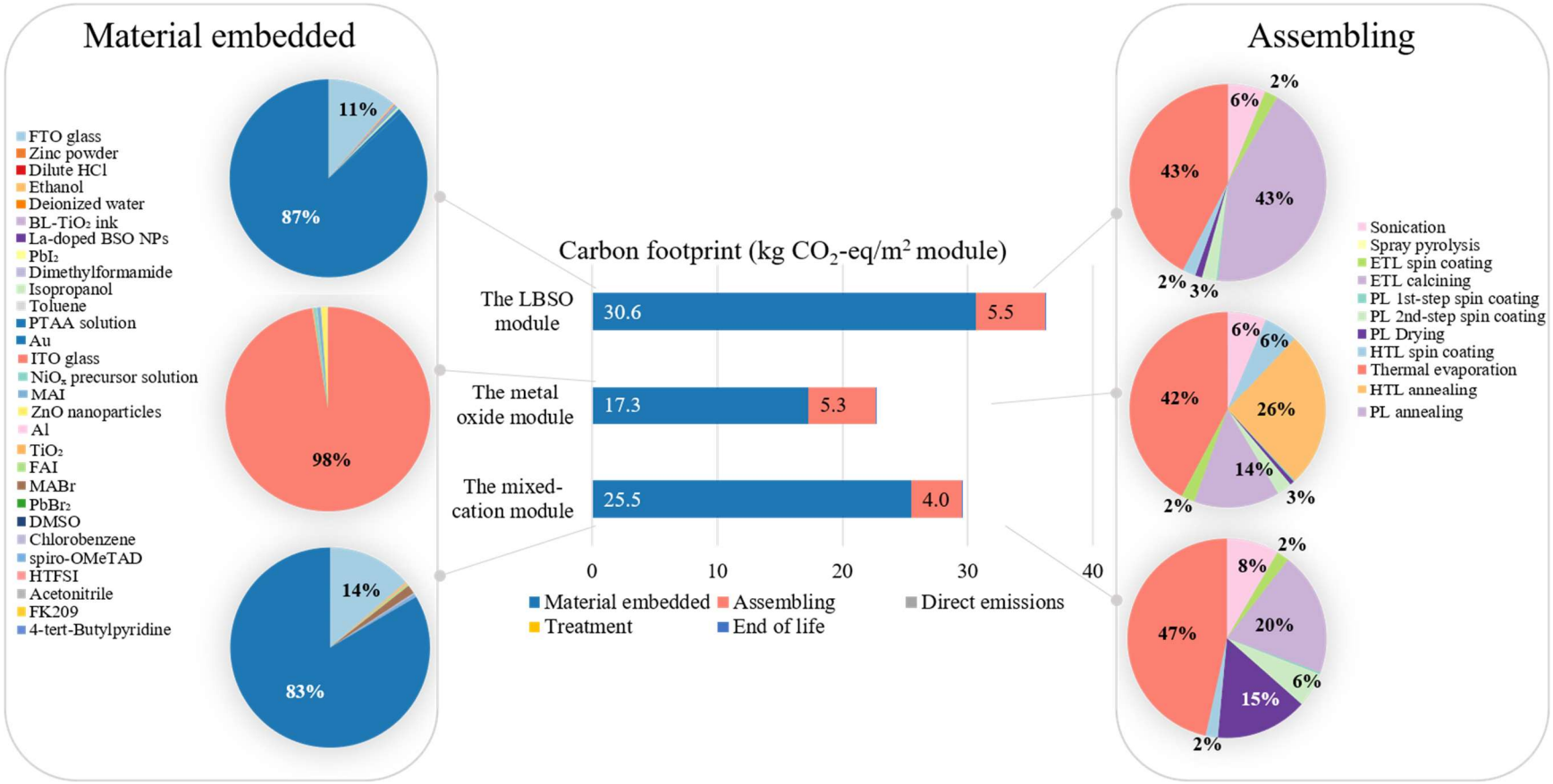

Figure 8. Profile of carbon footprint of the three laboratory-scale perovskite PV modules (The bar charts in the middle reflect the breakdown of carbon footprint during different phases ending up with landfill. The pie charts on the left reveal the GHG emissions embedded in various feedstocks for the three PSCs, while the pie charts on the right depict the carbon footprint of different manipulations during assembling phase for the three PSCs).

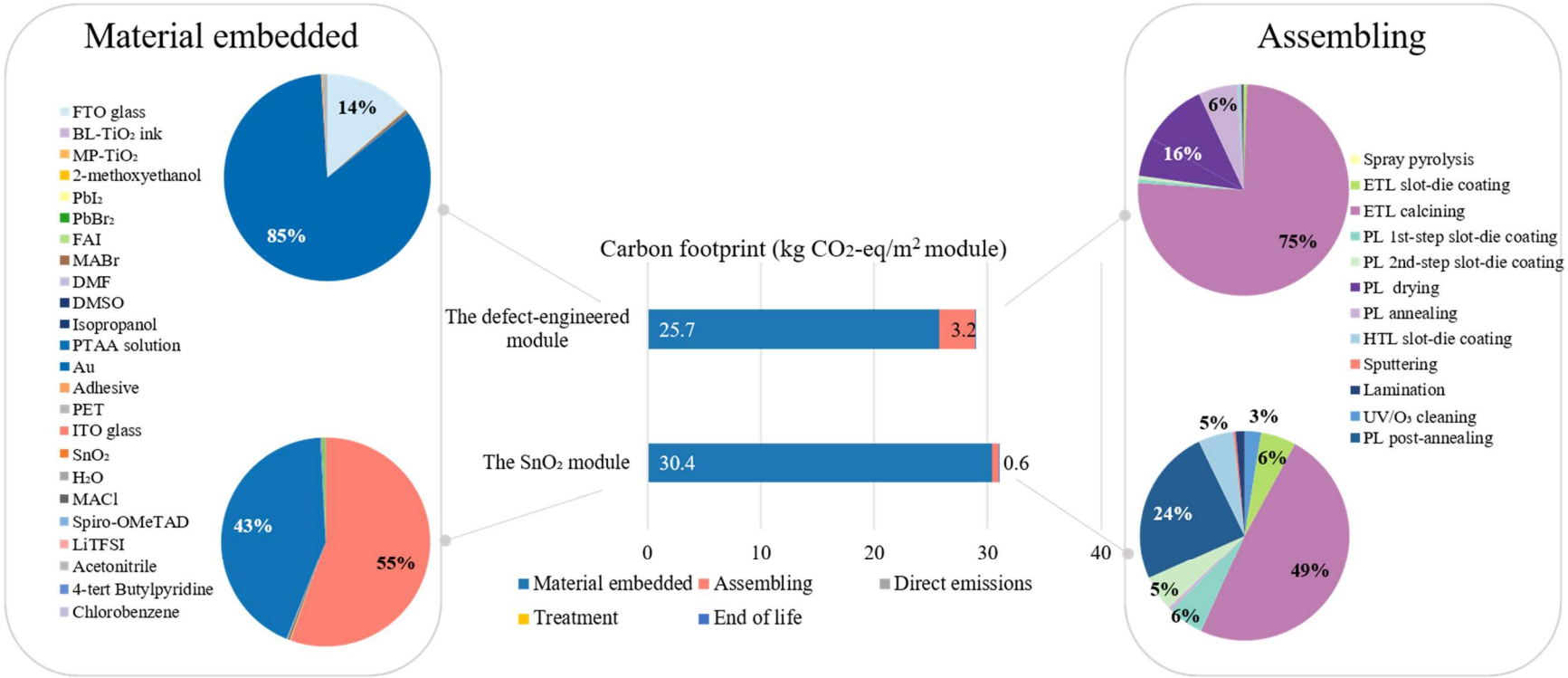

Figure 9. Profile of carbon footprint of the two commercial-scale perovskite PV modules (The bar charts in the middle reflect the breakdown of carbon footprint during different phases ending up with landfill. The pie charts on the left reveal the GHG emissions embedded in various feedstocks for the two PSCs, while the pie charts on the right depict the carbon footprint of different manipulations during assembling phase for the two PSCs).

3.3 The role of PSC recycling

From the previous LCA results, one environmental hotspot facet lies in the use of FTO glass, ITO glass, and precious metal. It is therefore vital to consider PSC recycling, provided that the hotspot materials can be refurbished at relatively lower emissions and energy intensity than PSC manufacturing using virgin feedstocks. Another environmental hotspot is the use of energy-intensive heating processes, such as thermal evaporation and calcining. Many of these processes are inevitable and would not be able to be engineered around in the short term. Therefore, it is critical to pursue recycling for PSC production. PSC recycling also finds favor with the reduction of solid waste as well as the scarcity of materials,[54] such as gold and indium, especially for the potential large-scale PSC future deployment scenario. One important measurement of the environmental viability of PSC fabrication is the difference of environmental performance between the cases with and without recycling. If the environmental performance of the recycling scenario is identical or very close to that of the case without recycling, a "breakeven" point is attained, which indicates that the investigated device architecture is sufficiently cheap or more advanced recycling approaches need to be explored.

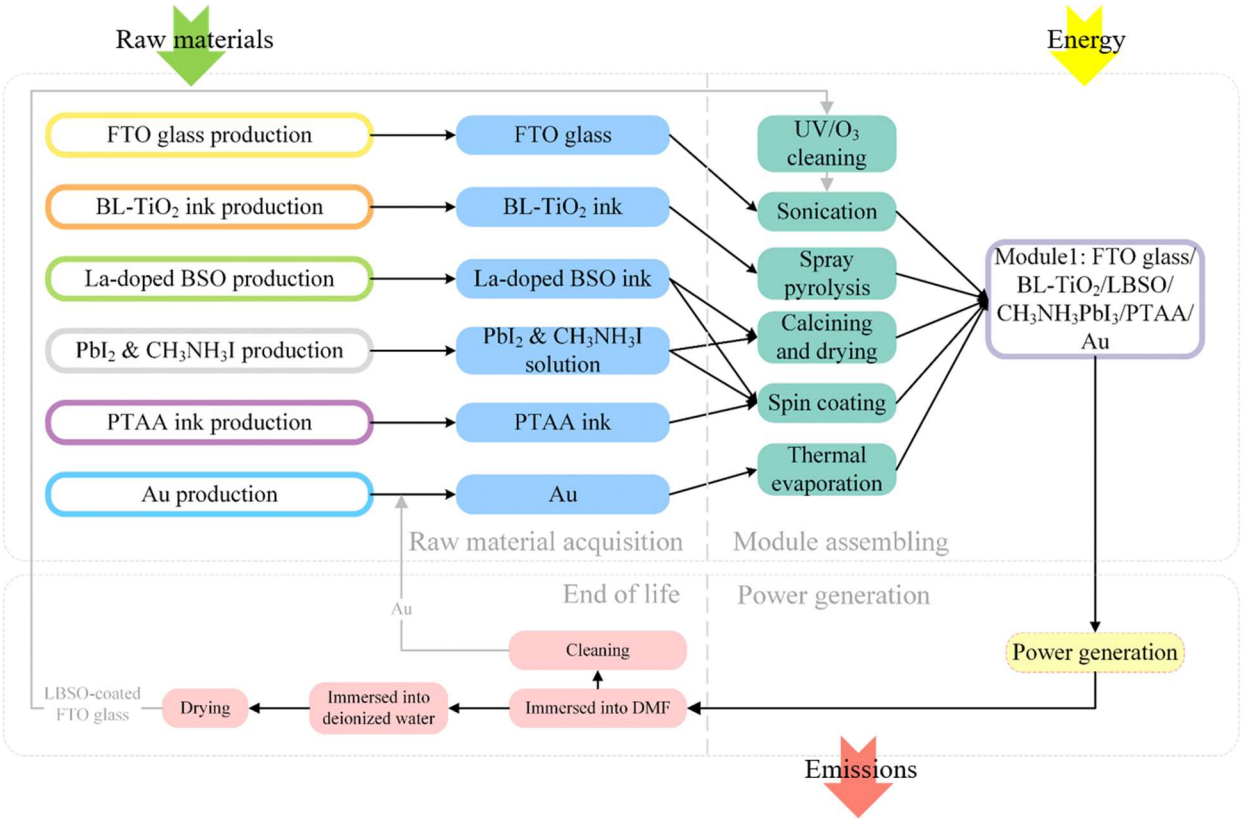

Figure 10. System boundary of manufacturing LBSO perovskite solar modules with recycling as the end-of-life scenario.

By switching the end-of-life scenario into its recycling counterpart, the system boundary is revised correspondingly, which is illustrated in Figure 10 for the LBSO modules. The recycling of PSCs is modeled based on the avoided burden approach, where the materials potentially being reused by future generations substitute a portion of the primary counterpart. In contrast to the intensive energy use and environmental impacts in the landfill scenario, significant melioration can be foreseen in both primary energy consumption and environmental profile if the hotspot materials are carefully recovered and reused for manufacturing PSCs. Compared with the recycling approaches for commercialized PV technologies, strategies for refurbishing perovskite PV modules are much more straightforward. One of the widely reported recycling strategies for

perovskite cells is to selectively dissolve the panel layers with suitable solvents.[11, 27, 28] The substrates are usually recovered and reused directly, instead of being smashed before reusing. Precious metal electrodes can also be directly retrieved after cleaning, because they are normally chemically stable and insoluble in the chosen solvent. According to the avoided burden approach, the shares of precious metal or substrates recycled after the use phase of PSCs determine the amount of primary metal or substrate feedstocks that can be potentially avoided.[32] In this way, the resulting energy consumption and environmental impacts of PSC manufacturing can be significantly reduced.

Figure 11, Figure 12, and Figure 13 show the changes in primary energy consumption during the material acquisition and assembling phases of three perovskite PV modules due to the recycling of hotspot module components. The results of the other two modules are given in the Supplementary Information. The pie charts on the left depict the primary energy consumption profile considering landfill as the end-of-life scenario, while the right-hand-side donut charts refer to the recycling counterpart.

As shown in Figure 11, by considering recycling as the end-of-life scenario of the LBSO module, the energy embedded within the raw materials is significantly reduced from 494.1 MJ/m^2-module to 81.5 MJ/m^2-module, accounting for about 83.5% of the primary energy consumption in the landfill scenario. The reasons are that the amount of gold use is reduced in the recycling scenario, and the FTO glass is assumed to be completely recycled and can be reused after surface treatment. Since the blocking layer (BL) and ETL are closely attached to the FTO substrate, these layers are recovered along with the substrate. The spray pyrolysis for depositing BL-TiO_2 layer onto the substrate as well as the spin coating and calcining of ETL is also excluded to produce the LBSO module from recycled materials. Energy consumption induced by the newly introduced

UV/O_3 cleaning process is relatively small compared with those of the aforementioned manipulations, so the overall primary energy consumption during the assembling phase decreases significantly by 45.2%. Even though both the LBSO module and defect-engineered module use FTO glass and gold, the effectiveness of recycling is drastically different, as shown in Figure 11 and Figure 13. For the commercial-scale module, a larger proportion of energy can be saved with a proper recycling process. Specifically, the embedded energy in the raw materials decreases by 97.8% to 9.4 MJ/m^2-module from the original 419.4 MJ/m^2-module, and the energy consumption during the module assembly decreases by 75.6% to 13.6 MJ/m^2-module from 55.8 MJ/m^2-module.

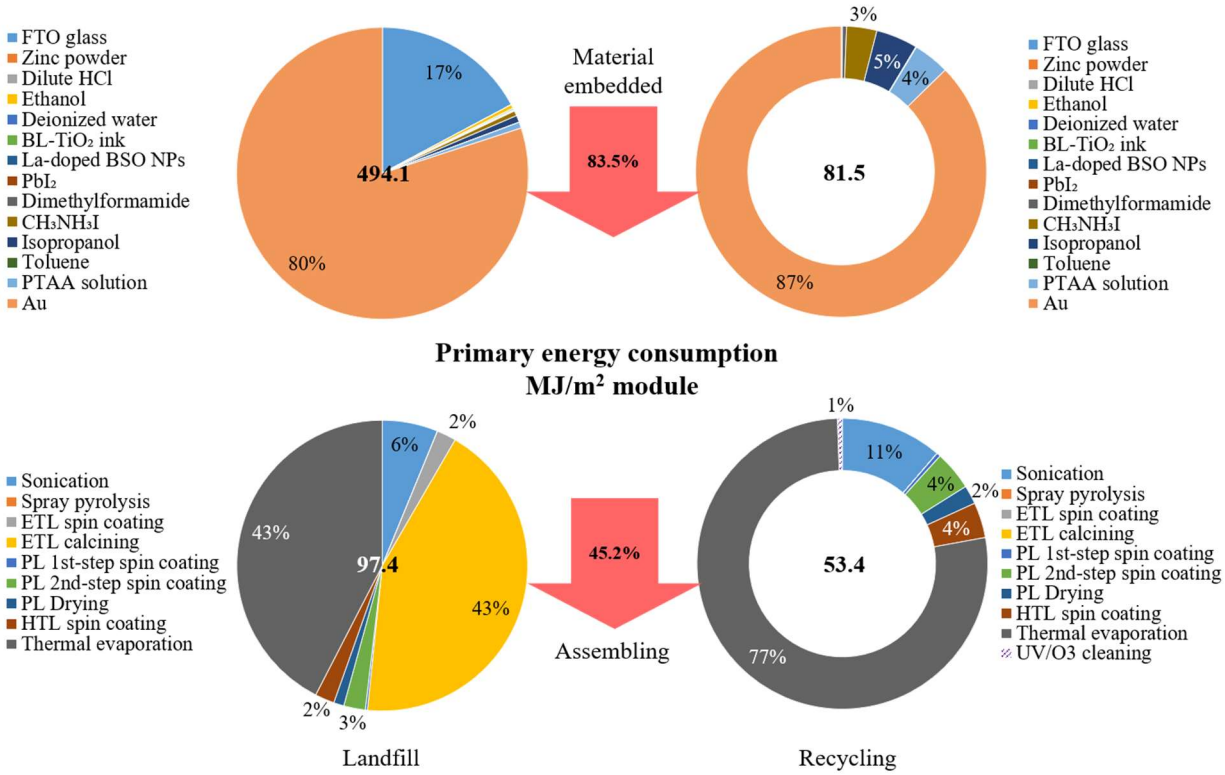

Figure 11. Primary energy consumption comparison between landfill (pie charts on the left) and recycling (donut charts on the right) end-of-life scenarios for the LBSO module (The upper two charts refer to the primary energy consumption in material acquisition, while the lower two charts represent the energy consumption during the assembling phase of PSC preparation. The

arrows in the middle reflect the variation of primary energy consumption relative to the landfill scenario).

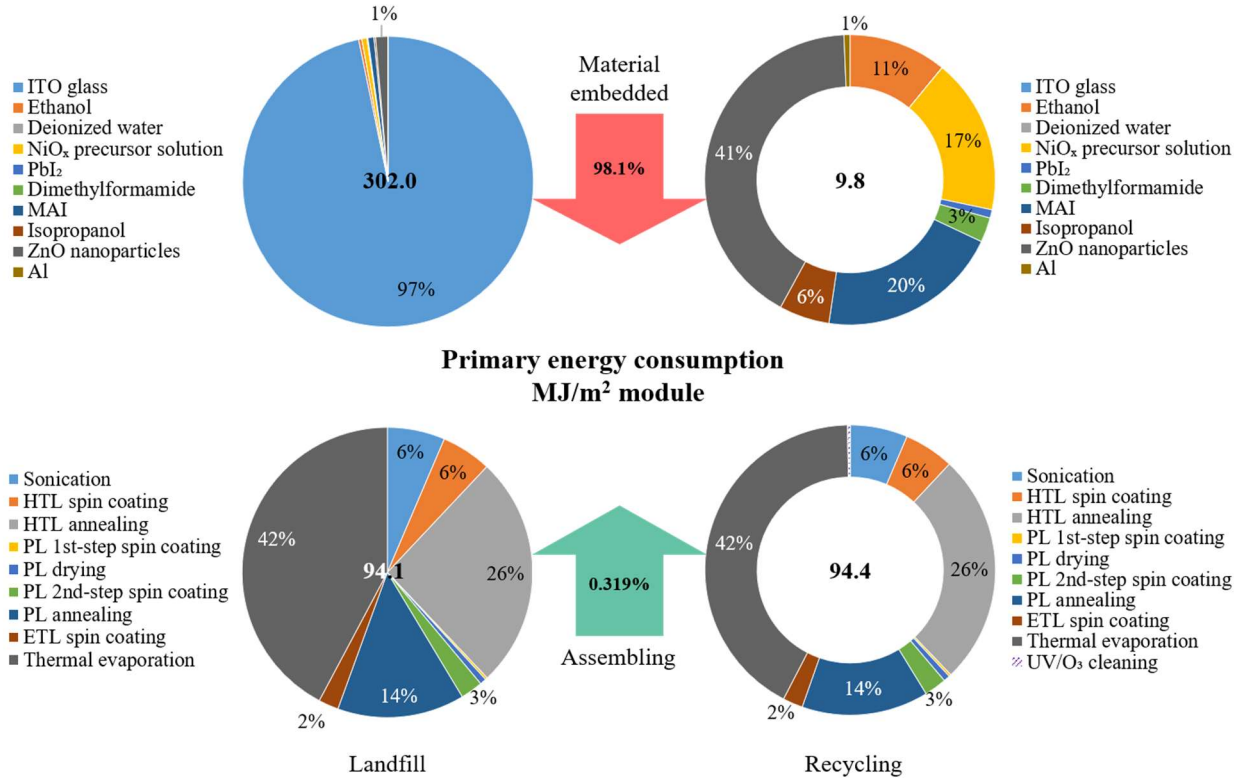

Figure 12. Primary energy consumption comparison between landfill (pie charts on the left) and recycling (donut charts on the right) end-of-life scenarios for the metal oxide module (The upper two charts refer to the primary energy consumption in material acquisition, while the lower two charts represent the energy consumption during the assembling phase of PSC preparation. The arrows in the middle reflect the variation of primary energy consumption relative to the landfill scenario).

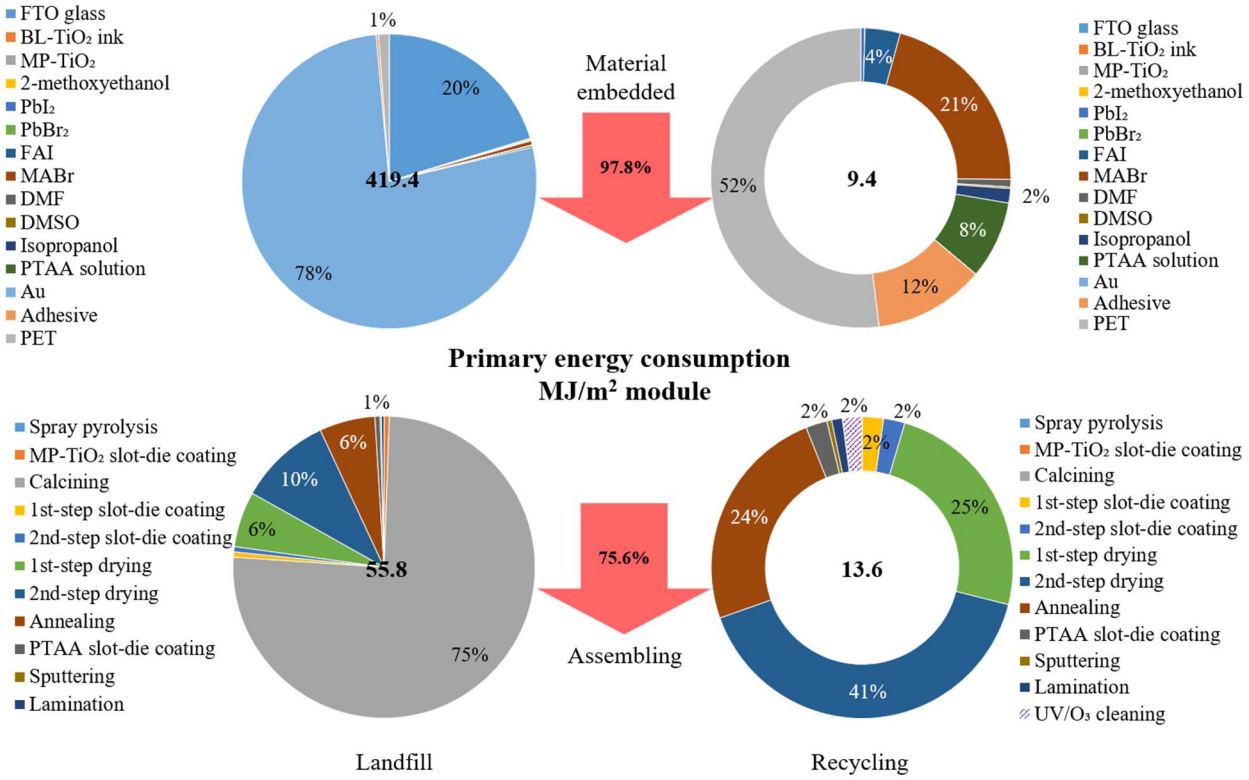

Figure 13. Primary energy consumption comparison between landfill (pie charts on the left) and recycling (donut charts on the right) end-of-life scenarios for the defect-engineered module (The upper two charts refer to the primary energy consumption in material acquisition, while the lower two charts represent the energy consumption during the assembling phase of PSC preparation. The arrows in the middle reflect the variation of primary energy consumption relative to the landfill scenario).

As shown in Figure 12, the metal oxide module demonstrates a totally different outcome for the recycling scenario. The ITO substrate is the only recycled material recovered via immersion in aqueous NaOH, with all other layers dissolved into the solution. Regarding primary energy embedded in raw materials, 98.1% of the primary energy consumption is eliminated by simply recycling and reusing ITO glass. The energy consumption in the assembling phase only

demonstrates a slight increase of around 0.319%. We note that such recycling methods only focus on the recycling of ITO glass, with all other active layers sacrificed and wasted. There is a critical need to develop alternative recycling strategies for more extensive material recovery and minimization of environmental consequences; it is likely such recycling strategies will be further developed and optimized as the ultimate scaled module compositions take form.

From the results of primary energy consumption change by considering recycling as the end-of-life scenario, we notice that tremendous energy saving can be achieved (even over 90% of the energy embedded in raw materials) by recovering and reusing the hotspot materials of perovskite PV modules. Meanwhile, the influence on the assembling phase is relatively small. Furthermore, considering that the raw materials contribute to over 76% of the primary energy consumption, the recycling of perovskite PV modules is of critical significance.

The aforementioned results would hold, on the major premise of ideal or exhaustive recycling for both substrates and precious metal electrodes, i.e., the recycling level is currently assumed to be almost 100%, which can be hardly guaranteed due to the limitation of current infrastructure. Recycling procedures, such as selective dissolution and sonication may cause irreversible damage to the morphology of the FTO and ITO substrates, resulting in drastic loss of performance. Despite the precious metal, such as Au and Ag, being chemically stable in the selected solvents, loss of mass is still inevitable during recycling. In addition, loss is also expected due to the metal migration during operation or other factors, indicating that the raw materials are not guaranteed to be in the original form or usable for refurbished devices. These issues reduce the effectiveness of recycling perovskite solar modules. To analyze these scenarios, a series of recycling levels are assigned to the investigated PSCs. The impacts of recycling levels on both primary energy consumption and carbon footprint for the LBSO module are illustrated in Figure 14. The recycling level variation

(from 70% to 100%) for the substrates is greater than the precious metal (from 90% to 100%), because the morphology completeness is relatively harder to be fulfilled. Note that the recycling of substrates is either successful or completely failed, i.e., the recycling rate for individual substrate is either 0 or 100%. Therefore, the recycling level of substrates refers to an average proportion of successfully recycled modules. The results of the other four perovskite PV modules are presented in the Supplementary Information.

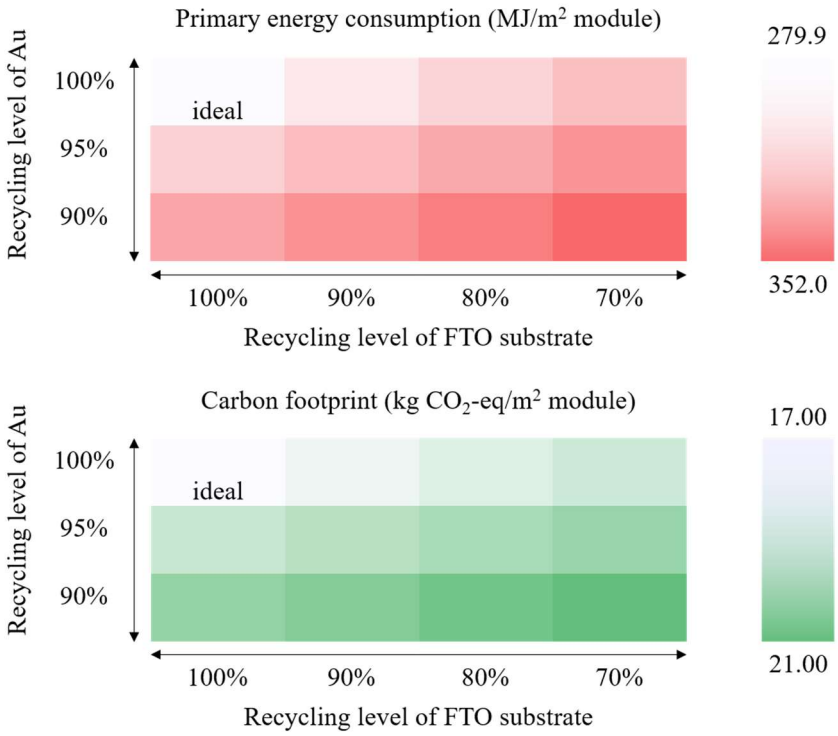

Figure 14. Impacts of recycling levels on the primary energy consumption and carbon footprint for the LBSO module (The ideal recycling scenario can be intuitively identified on upper left corner of this heat map; the lower right corner refers to the "worst" recycling strategy).

Because the recycling strategies are derived from laboratory-scale processing steps, they are likely to encounter technical challenges in scaling-up. Moreover, for recycling FTO glass via the selective dissolution, some of the solvents used to remove the layers other than the electrodes and

substrates can be retrieved from the solvent used to prepare the precursor solution. Earlier studies show that the direct emissions of these organic solvents have severe photochemical oxidation effect.[10] This detrimental effect would be mitigated if organic solvents are effectively recycled and reused in the selective dissolution phase, which will be significantly facilitated by policy against photochemical pollution. Furthermore, because the recovered substrates could be used for new device fabrication within four to five hours,[28] the recycling infrastructure co-located with the PSC manufacturing facilities would be an appropriate blueprint for efficient manufacturing of recycled PSCs in the future.

In spite of the relatively small environmental impacts induced by lead compounds according to the LCA results presented in this work, the use of lead is an extremely sensitive issue and may induce public concerns about the potential risks associated with lead leaking even at a relatively low concentration. The potential negative public perception motivates the recycling of lead even though lead is not an environmental hotspot. Future work should focus on the development of efficient solvent recycling and lead recovery approaches in the PSC industry, although it is beyond the scope of this study, because there is a lack of literature addressing how the used solvents (with lead) are disposed of and recovered.

3.4 Comparison between the landfill and recycling scenarios

In the previous subsection, we analyzed the primary energy consumption breakdown considering both material acquisition and assembling phases to reveal the relatively small influence of recycling for energy saving during PSC manufacturing. To conduct more systematic and comprehensive comparison between the landfill and recycling scenarios, all the life cycle stages must be fully covered, including material acquisition, assembling, recycling, and treatment of the waste. The treatment phase encompasses the wastewater treatment from the PSC

manufacturing as well as the incineration of the spent solvent from the recycling procedures. Figure 15 demonstrates the comparative results of the five investigated PSCs considering both landfill and recycling (ideal) end-of-life scenarios. Recycling strategies considered in this work present prominent effects on reducing the primary energy consumption for the investigated PSCs. For the LBSO module, up to 53.0% of primary energy is saved by reusing LBSO-coated FTO substrates and Au electrodes. Similar behavior can be observed for the mixed-cation module and the defect-engineered module, which demonstrate approximately 44.7% and 64.8% of energy savings, respectively. Moreover, the reduction of primary energy consumption for the metal oxide module and the SnO_2 module accounts for up to 73.7% and 97.1% of the total primary energy consumption in the landfill scenario, respectively. These two modules show more advantageous performance when recycling is implemented, because a low-cost inorganic solvent, sodium hydroxide solution, is employed in the recycling procedures. In contrast, an energy-intensive organic solvent, dimethylformamide (DMF), is utilized to recycle the LBSO, the mixed-cation module, and the defect-engineered module. A similar trend can be found for the carbon footprint behavior, as shown in Figure 16. Since EPBT is linearly dependent on the primary energy consumption, the EPBT drastically decreases by 53.0%, 73.7%, 44.7%, 64.8%, and 97.1% for the LBSO module, the metal oxide module, the mixed-cation module, the defect-engineered module, and the SnO_2 module, respectively. Similarly, the GHG emission factors for the five PV modules would demonstrate a drastic reduction of 52.8%, 73.0%, 44.8%, 64.7%, and 96.5%, respectively, compared with the landfill counterpart.

As mentioned above, ITO glass is more energy-intensive and environmentally expensive than FTO glass, so the FTO glass would be preferred for scaled modules. However, the recycling of FTO substrate induces more energy consumption and environmental impacts compared with the

ITO counterpart. Pursuing effective recycling and selecting proper materials for commercial-scale modules become conflicting objectives in this case, and the trade-off relationship should be carefully excavated to find a balanced choice.

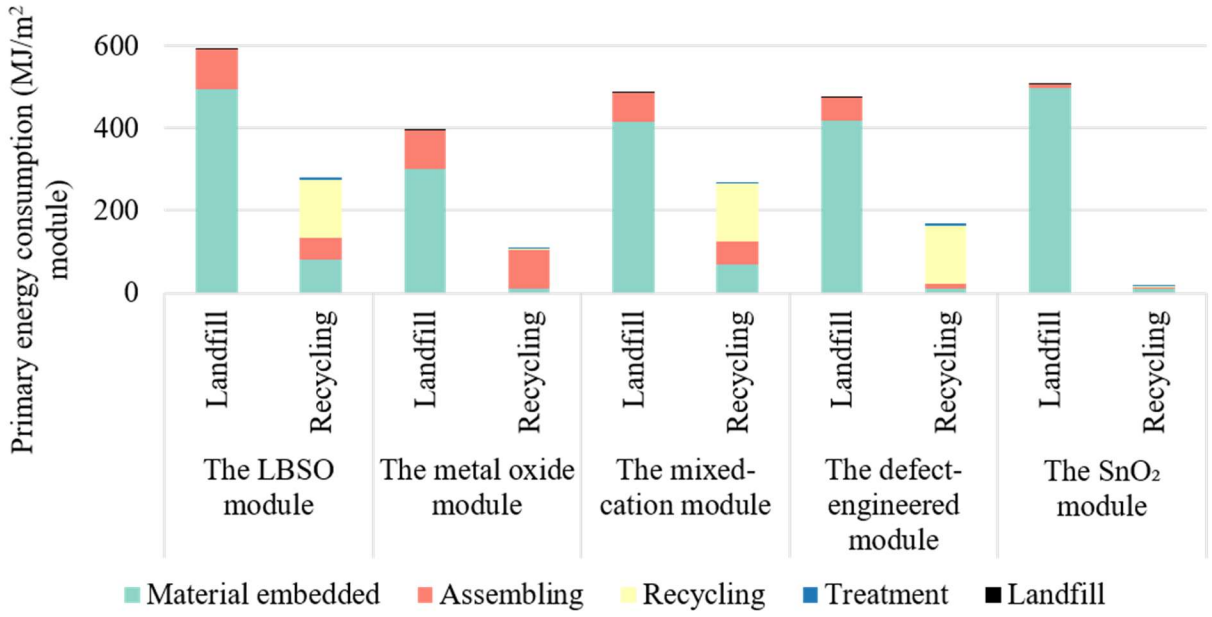

Figure 15. Comparison of primary energy consumption between landfill and recycling scenarios for the five investigated PSCs.

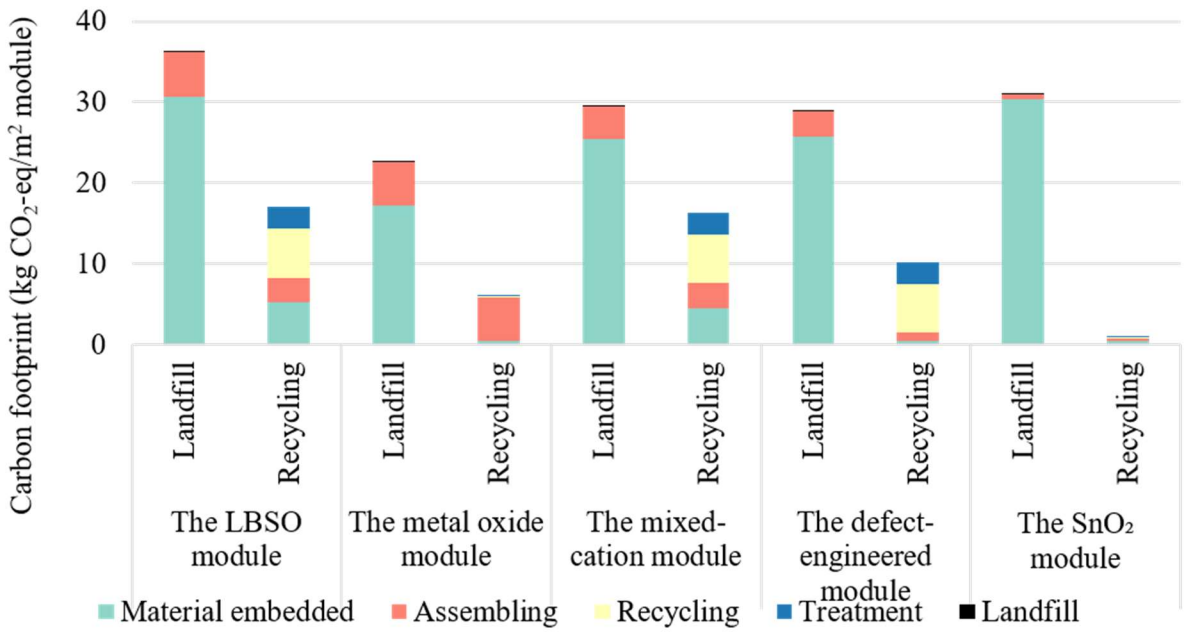

Figure 16. Comparison of carbon footprint between landfill and recycling scenarios for the five investigated PSCs.

We also find that the treatment phase in recycling case induces much more GHG emissions than the landfill scenario for the LBSO module, the mixed-cation module, and the defect-engineered module, because the spent organic solvent is assumed to be incinerated as hazardous waste in this work. This environmental issue, however, would be largely mitigated if effective recycling strategies are implemented for recovering the spent solvent in the PSC recycling infrastructure in the future.

3.5 Comparison with existing PV technologies

Based on the primary energy consumption and carbon footprint results obtained from the previous subsections, we compare the energy and environmental performances of the five perovskite PV modules investigated in this work with those of seven existing modules reported in

the literature, including mono-crystalline silicon (c-Si) module,[55] poly-crystalline silicon (p-Si) module,[56] ribbon silicon (ribbon-Si) module,[57] CdTe module,[56, 58, 59] OPV module,[34] and two alternative perovskite modules (the TiO_2 module and the ZnO module).[60, 61] The comparison is based on the assumption that all the modules are tested based on rooftop-mounted installation in Southern Europe, with annual irradiation of 1,700 kWh/m^2 and a performance ratio of 75%.[10, 34] The comparative results of EPBT and GHG emission factor are shown in Figure 17 and Figure 18, where the shaded bars reflect the influence of recycling on the EPBT and GHG emission factors of the PSCs. We note that the recycling of CdTe panels has been pioneered by First Solar, a major manufacturer of CdTe thin film PV, which runs large-scale recycling plants in the United States, German, and Malaysia.[62] The company reported that approximately 95% of cadmium and 90% of glass could be reused via exhaustive material recycling, and an EPBT reduction of 0.5 years could be achieved.[12, 62]

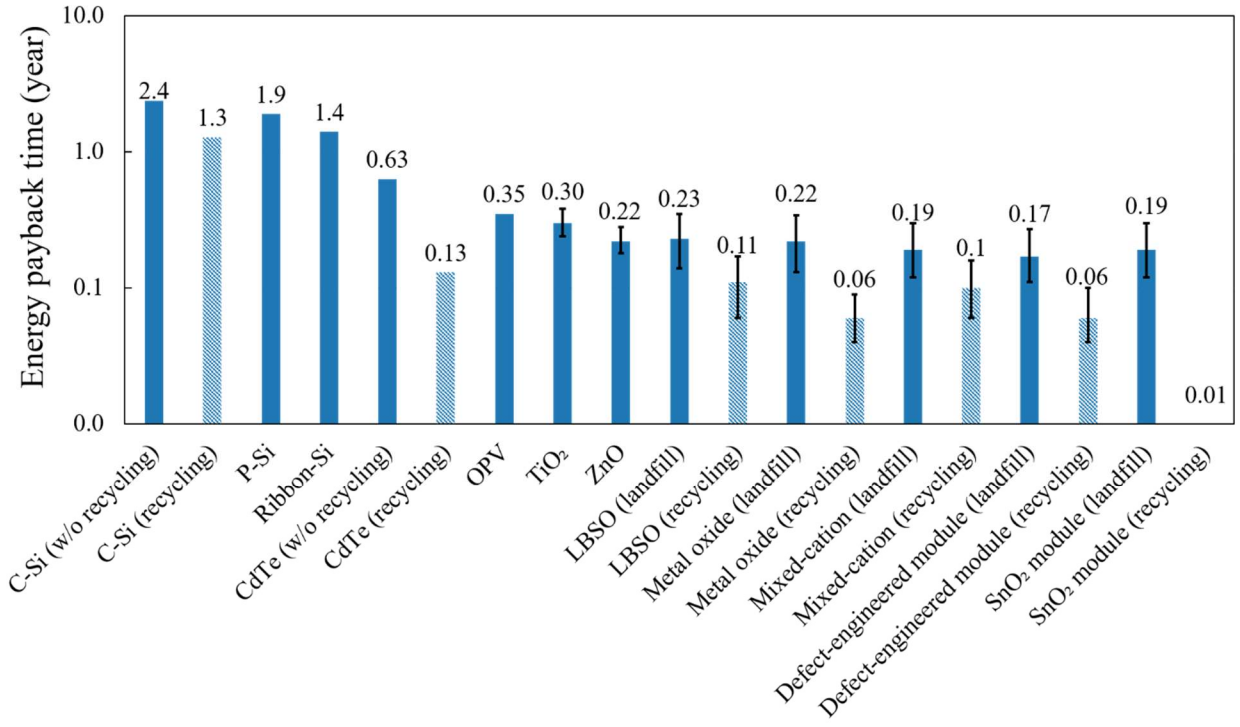

Figure 17. EPBT comparison among 12 PV modules. The evaluations are based on rooftop-

mounted installation in Southern Europe, with annual irradiation of 1,700 kWh/m^2 and a performance ratio of 75%. The data for the first five modules are retrieved from the literature.[34] The data for TiO_2 and ZnO modules are extracted from the literature.[10] The error bars refer to 95% confidence regions.

Figure 17 demonstrates the EPBT for the 12 PV modules. We also calculate the 95% confidence intervals for the five perovskite PV modules investigated in this study. The relevant data for the first seven PSCs are retrieved from existing publications.[34, 37, 38, 55-61, 63] Recycling reduces EPBT by 0.5 years for CdTe and 1.1 years for c-Si.[63] Perovskite PV modules achieve relatively shorter EPBT among all PV alternatives, varying from 0.17 years to 0.30 years, considering landfill as the end-of-life scenario. We notice that the nominal EPBT of the five novel PSCs are comparable or shorter than that of the TiO_2 and ZnO PSC modules, because the increased module efficiency of those investigated here overshadows the increase of primary energy consumption, and the EPBT is further shortened in the recycling case. Furthermore, the recycled metal oxide module demonstrates a promising EPBT as short as 0.06 years in spite of its relatively lower module efficiency. We also note that recycling reduces EPBT to 0.01 years for the SnO_2 module, which is much lower than those of other PVs. This result can be attributed to two major reasons: 1) the energy consumption in recycling phase is very small due to the use of aqueous NaOH instead of energy-intensive organic solvents; 2) the energy consumption during assembling is much lower than other PV technologies due to the use of scalable processing steps.

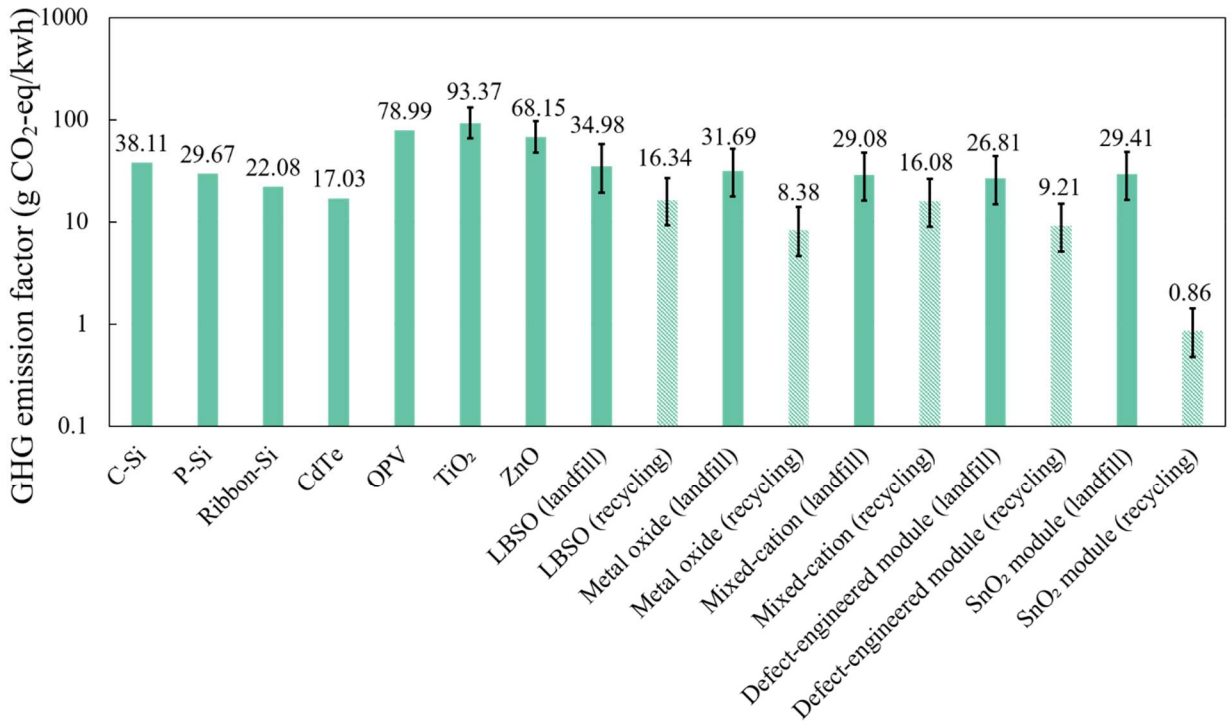

Figure 18. GHG emission factor comparison among the 12 PV modules. The evaluations are based on rooftop-mounted installation in Southern Europe, with annual irradiation of 1,700 kWh/m^2 and a performance ratio of 75%. The data for the first five modules are retrieved from the literature.[34] The data for TiO_2 and ZnO modules are extracted from the literature.[10] The error bars refer to 95% confidence regions.

The GHG emission factors of the 12 PV modules are compared and visualized in Figure 18. The nominal GHG emission factors for the five perovskite PV modules in the landfill scenario are comparable to that of the conventional PV technologies, ranging from 26.81 to 34.98 g CO_2-eq/kWh. Notably, the results are much lower than that of the TiO_2 and ZnO PSCs, because a longer lifetime of five years is used in the calculation of the nominal GHG emission factors. High GHG emission factor is mainly attributed to a high carbon footprint, low module efficiency, poor performance ratio, insufficient irradiation, and a short lifetime. These are common issues for

current PSCs, as well as OPV modules. Despite the five-year lifetime being overestimated in the current situation, the results show that a promisingly low GHG emission factor for PSC could be attained if the lifetime issue is addressed. Conventional silicon-based PV technologies usually have a lifetime of more than 20 years, so the corresponding GHG emission factors are relatively small. In addition, effective recycling of the investigated PSCs results in significant amelioration of the life cycle GHG emissions.

New device architectures of PSCs do not necessarily demonstrate better EPBT and GHG emission factors, because the research focus is more directed toward the stability enhancement and PCE improvement. However, the recycling work would significantly improve the environmental performance of the new PSCs. In addition, the large error bar of the PSCs is due to the immaturity of technology. With the development of the relevant PSC materials and process technologies, the EPBT and the GHG emission factor may attain the lower bound of the error bar. From this perspective, we can envisage great potential of the five innovative PSCs. Both EPBT and GHG emission factors are determined by multiple factors, and the synergistic effects of these parameters should be carefully investigated, in order to efficiently improve these two prevalent sustainability metrics.

3.6 Uncertainty and sensitivity analysis

A number of important input parameters, such as the performance ratio, module efficiency, annual irradiation, primary energy consumption, carbon footprint, and lifetime, are subject to uncertainty.[38, 64] Thus, we perform systematic sensitivity analysis by assigning specific distribution to these parameters. A normal distribution is assigned to irradiation and lognormal distributions are assigned to other parameters, following the assumption of an existing study.[10] The mean value for each parameter is assumed according to the rooftop-mounted installation scenario in Southern

Europe.[34] A pedigree method is used to calculate the geometric standard deviation.[65] Based on the probability distribution of the parameters, we run Monte Carlo simulation to forecast the resulting distribution of EPBT and GHG emission factor for the LBSO module, as shown in Figure 19. For EPBT, the mean value is 0.23 years, the 95% confidence region is [0.14, 0.35], and the standard deviation is 0.05. In contrast, the mean value of GHG emission factor is 34.98, the 95% confidence region is [19.59, 57.89], and the standard deviation is 9.9, indicating that the GHG emission factor is much less robust than EPBT, which is also verified by the error bar in Figure 17 and Figure 18 (comparison results of EPBT and GHG emission factors among 12 PV modules).

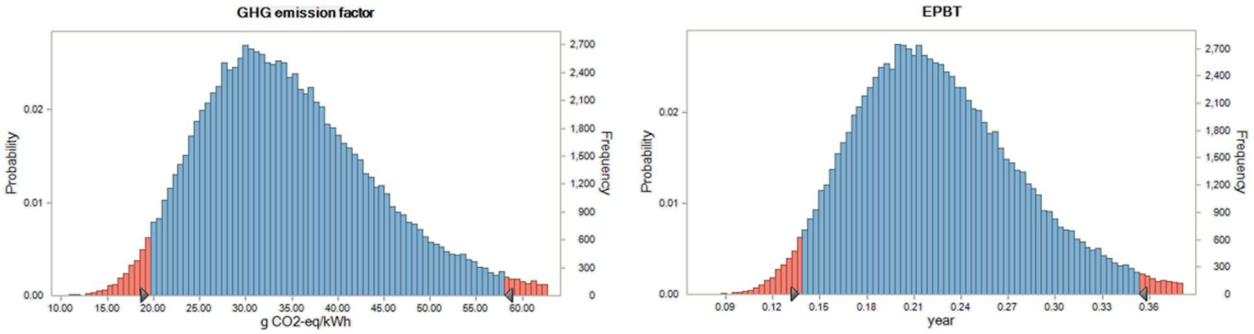

Figure 19. Uncertainty analysis for the LBSO module in terms of EPBT and GHG emission factor.

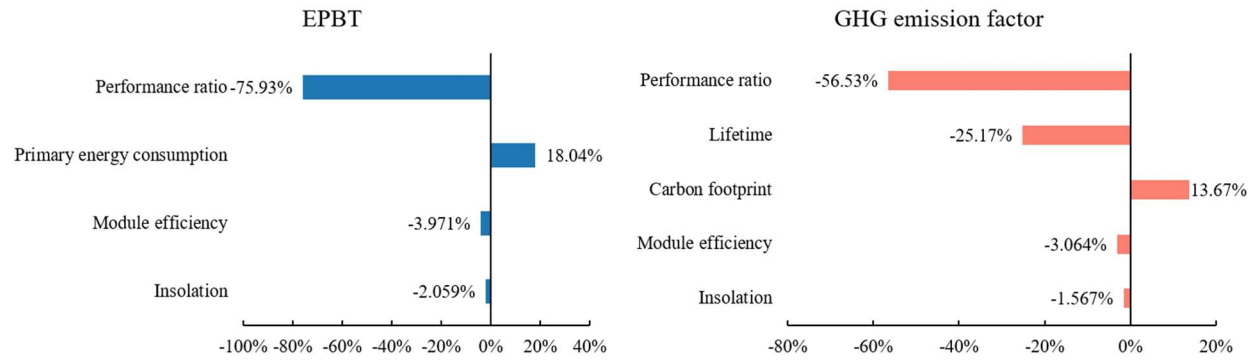

Figure 20. Sensitivity analysis for the LBSO module in terms of EPBT and GHG emission factor.

Furthermore, sensitivity analyses are conducted based on the simulation results. In Figure 20, performance ratio can be intuitively identified as the most influential factor for both EPBT (-75.93%) and GHG emission factor (-56.53%). Lifetime has secondary impacts on the GHG emission factor. In comparison, the fluctuations of annual irradiation and module efficiency show much less influence. The negative sign represents that the target metrics are in negative correlation with the uncertain parameters. Even though performance ratio is confirmed to be the most influential factors for both EPBT and GHG emission factors, the potential of improving these two metrics by improving the performance ratio is very limited (from 75% to 90%). Lifetime, however, could be extended substantially from hundreds of hours to many thousands of hours,[18, 19] or even longer with proper encapsulation (several years for scaled modules in industry). So, prolonging the lifetime is a much more efficient approach to reducing the GHG emission factor. In any case, it is likely that commercial PSC modules will ultimately need to exhibit operating lifetimes approaching those of silicon modules, and thus the GHG emissions will reduce further. Uncertainty and sensitivity analyses are also conducted for the other four modules. Further results for the other modules are presented in the Supplementary Information.

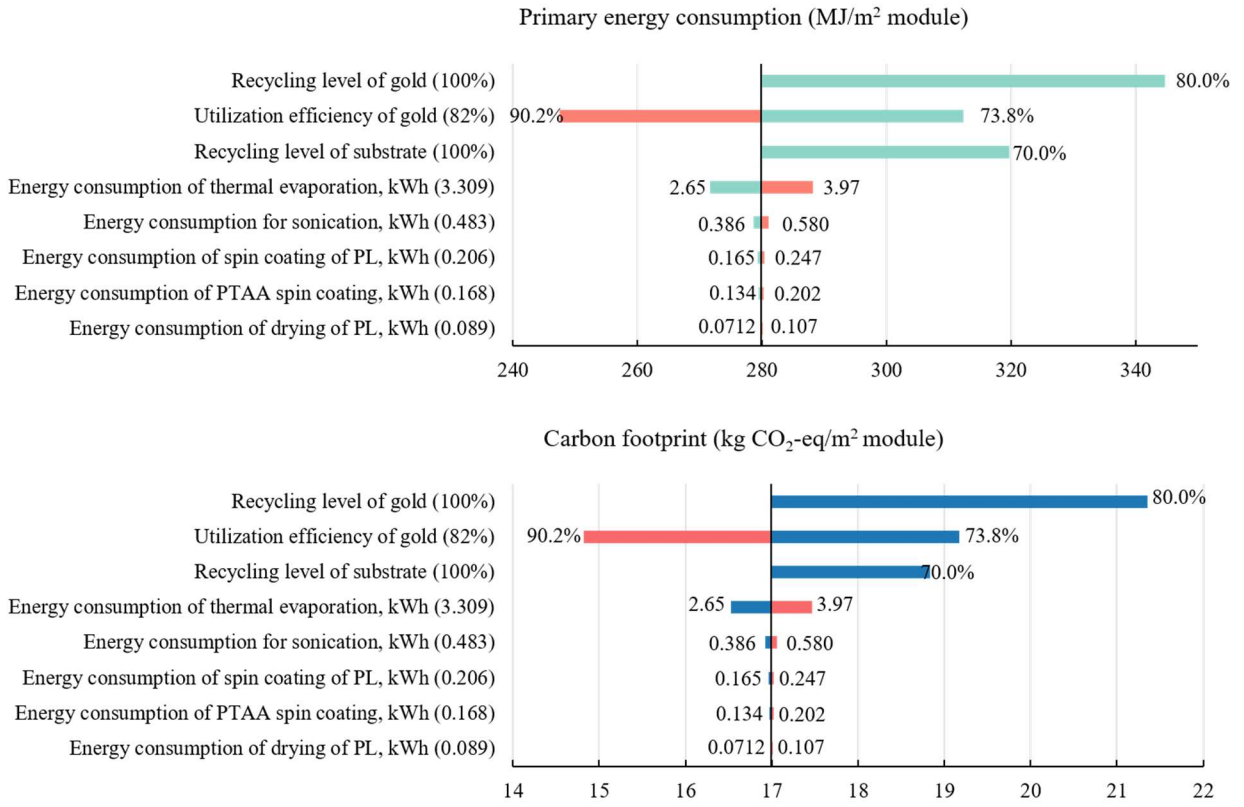

Figure 21. Sensitivity analysis for recycling the LBSO module in terms of primary energy consumption and carbon footprint.

In addition to the sensitivity analysis based on Monte Carlo simulation, the sensitivity of recycling strategy is also quantified in terms of primary energy consumption and carbon footprint, as shown in Figure 21. A resemblance can be observed between the sensitivities of primary energy consumption and carbon footprint to model inputs. The utilization efficiency of gold and recycling levels of electrodes and substrates are in negative correlation with the sustainability metrics, while other input parameters demonstrate positive impacts. Besides the recycling levels, the energy consumption of key manufacturing processes should arouse great attention, because the assessment of this work was performed with the "best available" data,[31] which involves personal assumptions for each LCA phase. Uncertainty analysis on these issues may somehow reveal the

limitation of the individual factors and provide insights for cautious selection of energy-intensive manufacturing processes in the future.

The results of the sensitivity analyses for the other modules are presented in the Supplementary Information due to the length limit of this paper.

CHAPTER 4

CONCLUSIONS

In this work, we studied device architectures and recycling strategies of PSCs using "cradle-to-grave/cradle" comparative LCA for five solvent-processed PSCs. It was almost certain that industry would optimize the laboratory-scale PSCs for scaled modules by reducing material consumption and adopting processing steps with lower energy intensity. Therefore, our calculation based on laboratory-scale data would provide conservative insights and serve as upper bounds on EPBT, GHG emissions, etc. Recycling and stability were two essential starting points to improve the sustainability of PSCs, which provided insightful directions for the development of commercial-scale perovskite PVs in future research. At first sight, however, it seemed that there was no necessity to simultaneously account for these two concepts. Actually, enhanced stability could reduce the frequency of recycling work, mitigating the energy intensity due to the immature recycling manipulations. Additionally, higher stability reduced the dependence on rigid encapsulation, further facilitating the recycling process. PSCs possessed great potential to becoming more energetically and environmentally sustainable by simultaneously considering high stabilities and increasing recycling efforts. By implementing material recycling to the identified environmental hotspots, the primary energy consumption and carbon footprint were confirmed to be drastically reduced by over 40% for most of the investigated modules, indicating significant reduction of EPBT and GHG emission factors correspondingly. Different recycling levels were assigned to the investigated PSCs, and the corresponding impacts on the primary energy consumption and carbon footprint were quantified. A momentary glimpse at the future of PSCs informed that proper policy and recycling infrastructure development strategies would mitigate the detrimental environmental impacts and facilitate the sustainable manufacturing of recycled PSCs.

Furthermore, blindly focusing on the primary environmental hotspots identified based on LCA results may overlook public concerns about the potential risks associated with lead. Thus, toward large-scale PSC deployment, the significance of public perception must be taken into consideration; indeed, the real value of an effective PSC recycling program may lie in mitigating this risk, and thus be invaluable.

REFERENCES

1. H. J. Snaith, *The Journal of Physical Chemistry Letters*, 2013, **4**, 3623-3630.
2. N. T. Energy, Best Research-Cell Efficiency Chart, https://www.nrel.gov/pv/cell-efficiency.html, (accessed May 1st, 2019).
3. J. J. Berry, J. van de Lagemaat, M. M. Al-Jassim, S. Kurtz, Y. Yan and K. Zhu, *ACS Energy Letters*, 2017, **2**, 2540-2544.
4. C. K. L., P. P. D. and D. V., *Progress in Photovoltaics: Research and Applications*, 2004, **12**, 69-92.
5. D. Bonnet, *International Journal of Solar Energy*, 1992, **12**, 1-14.
6. S. Yun, J. Lee and S. Lee, *Energy Policy*, 2019, **124**, 206-214.
7. A. Kojima, K. Teshima, Y. Shirai and T. Miyasaka, *Journal of the American Chemical Society*, 2009, **131**, 6050-6051.
8. Z. Li, T. R. Klein, D. H. Kim, M. Yang, J. J. Berry, M. F. A. M. van Hest and K. Zhu, *Nature Reviews Materials*, 2018, **3**, 18017.
9. R. Brenes, D. Guo, A. Osherov, N. K. Noel, C. Eames, E. M. Hutter, S. K. Pathak, F. Niroui, R. H. Friend, M. S. Islam, H. J. Snaith, V. Bulović, T. J. Savenije and S. D. Stranks, *Joule*, 2017, **1**, 155-167.
10. J. Gong, S. B. Darling and F. You, *Energy & Environmental Science*, 2015, **8**, 1953-1968.
11. B. J. Kim, D. H. Kim, S. L. Kwon, S. Y. Park, Z. Li, K. Zhu and H. S. Jung, *Nature Communications*, 2016, **7**, 11735.
12. J. M. Kadro and A. Hagfeldt, *Joule*, 2017, **1**, 29-46.
13. M. Chen, M.-G. Ju, A. D. Carl, Y. Zong, R. L. Grimm, J. Gu, X. C. Zeng, Y. Zhou and N. P. Padture, *Joule*, 2018, **2**, 558-570.
14. Q. Wang, X. Zheng, Y. Deng, J. Zhao, Z. Chen and J. Huang, *Joule*, 2017, **1**, 371-382.
15. Z. Zhu, D. Zhao, C.-C. Chueh, X. Shi, Z. Li and A. K. Y. Jen, *Joule*, 2018, **2**, 168-183.
16. J.-A. Alberola-Borràs, J. A. Baker, F. De Rossi, R. Vidal, D. Beynon, K. E. A. Hooper, T. M. Watson and I. Mora-Seró, *iScience*, 2018, **9**, 542-551.
17. Z. Song, C. L. McElvany, A. B. Phillips, I. Celik, P. W. Krantz, S. C. Watthage, G. K. Liyanage, D. Apul and M. J. Heben, *Energy & Environmental Science*, 2017, **10**, 1297-1305.
18. S. S. Shin, E. J. Yeom, W. S. Yang, S. Hur, M. G. Kim, J. Im, J. Seo, J. H. Noh and S. I. Seok, *Science*, 2017, **356**, 167-171.
19. Y. C. Kim, T. Y. Yang, N. J. Jeon, J. Im, S. Jang, T. J. Shin, H. W. Shin, S. Kim, E. Lee, S. Kim, J. H. Noh, S. I. Seok and J. Seo, *Energy & Environmental Science*, 2017, **10**, 2109-2116.
20. J. You, L. Meng, T.-B. Song, T.-F. Guo, Y. M. Yang, W.-H. Chang, Z. Hong, H. Chen, H. Zhou and Q. Chen, *Nature Nanotechnology*, 2016, **11**, 75.
21. M. Saliba, T. Matsui, J.-Y. Seo, K. Domanski, J.-P. Correa-Baena, M. K. Nazeeruddin, S. M. Zakeeruddin, W. Tress, A. Abate, A. Hagfeldt and M. Gratzel, *Energy & Environmental Science*, 2016, **9**, 1989-1997.
22. S. Yang, W. Fu, Z. Zhang, H. Chen and C.-Z. Li, *Journal of Materials Chemistry A*, 2017, **5**, 11462-11482.
23. D. Bi, W. Tress, M. I. Dar, P. Gao, J. Luo, C. Renevier, K. Schenk, A. Abate, F. Giordano, J.-P. Correa Baena, J.-D. Decoppet, S. M. Zakeeruddin, M. K. Nazeeruddin, M. Grätzel and A. Hagfeldt, *Science Advances*, 2016, **2**.

24. D. P. McMeekin, G. Sadoughi, W. Rehman, G. E. Eperon, M. Saliba, M. T. Hörantner, A. Haghighirad, N. Sakai, L. Korte, B. Rech, M. B. Johnston, L. M. Herz and H. J. Snaith, *Science*, 2016, **351**, 151-155.
25. Y. Zhao and K. Zhu, *Chemical Society Reviews*, 2016, **45**, 655-689.
26. A. Binek, M. L. Petrus, N. Huber, H. Bristow, Y. Hu, T. Bein and P. Docampo, *ACS Applied Materials & Interfaces*, 2016, **8**, 12881-12886.
27. M. T. Dang, J. Lefebvre and J. D. Wuest, *ACS Sustainable Chemistry & Engineering*, 2015, **3**, 3373-3381.
28. J. M. Kadro, N. Pellet, F. Giordano, A. Ulianov, O. Muntener, J. Maier, M. Gratzel and A. Hagfeldt, *Energy & Environmental Science*, 2016, **9**, 3172-3179.
29. G. Rebitzer, T. Ekvall, R. Frischknecht, D. Hunkeler, G. Norris, T. Rydberg, W.-P. Schmidt, S. Suh, B. P. Weidema and D. W. Pennington, *Environment International*, 2004, **30**, 701-720.
30. D. Pennington, J. Potting, G. Finnveden, E. Lindeijer, O. Jolliet, T. Rydberg and G. Rebitzer, *Environment International*, 2004, **30**, 721-739.
31. N. Espinosa, L. Serrano-Luján, A. Urbina and F. C. Krebs, *Solar Energy Materials and Solar Cells*, 2015, **137**, 303-310.
32. R. Frischknecht, *The International Journal of Life Cycle Assessment*, 2010, **15**, 666-671.
33. M. Goedkoop, R. Heijungs, M. Huijbregts, A. De Schryver, J. Struijs and R. Van Zelm, *ReCiPe 2008.* , 2009.
34. S. B. Darling and F. You, *RSC Advances*, 2013, **3**, 17633-17648.
35. R. García-Valverde, J. A. Cherni and A. Urbina, *Progress in Photovoltaics: Research and Applications*, 2010, **18**, 535-558.
36. N. Espinosa, R. García-Valverde and F. C. Krebs, *Energy & Environmental Science*, 2011, **4**, 1547-1557.
37. N. Espinosa, M. Hösel, D. Angmo and F. C. Krebs, *Energy & Environmental Science*, 2012, **5**, 5117-5132.
38. D. Yue, P. Khatav, F. You and S. B. Darling, *Energy & Environmental Science*, 2012, **5**, 9163-9172.
39. W. S. Yang, B.-W. Park, E. H. Jung, N. J. Jeon, Y. C. Kim, D. U. Lee, S. S. Shin, J. Seo, E. K. Kim, J. H. Noh and S. I. Seok, *Science*, 2017, **356**, 1376.
40. Q. Jiang, Z. Chu, P. Wang, X. Yang, H. Liu, Y. Wang, Z. Yin, J. Wu, X. Zhang and J. You, *Advanced Materials*, 2017, **29**, 1703852.
41. Ecoinvent version 3.5, https://www.ecoinvent.org/, (accessed Jul 1, 2019).
42. W. Siefert, *Thin Solid Films*, 1984, **120**, 267-274.
43. A. A. Gentile, C. Rocco, S. Modeo and T. Romano, *Journal of Cleaner Production*, 2014, **83**, 473-482.
44. T. Stocker, D. Qin, G. Plattner, M. Tignor, S. Allen, J. Boschung, A. Nauels, Y. Xia, V. Bex and P. Midgley, *IPCC, 2013: Climate Change 2013: The Physical Science Basis. Contribution of Working Group I to the Fifth Assessment Report of the Intergovernmental Panel on Climate Change*, Cambridge Univ. Press, Cambridge, UK, and New York, 2013.
45. M. Goedkoop, The Eco-indicator 99 A damage oriented method for Life Cycle Impact Assessment-Methodology report, Pre consultants, http://www.pre-sustainability.com/content/reports, (accessed May 27th, 2018).
46. E. A. Alsema and E. Nieuwlaar, *Energy Policy*, 2000, **28**, 999-1010.
47. V. M. Fthenakis, H. C. Kim and E. Alsema, *Environmental Science & Technology*, 2008,

42, 2168-2174.
48. M. A. Huijbregts, L. J. Rombouts, S. Hellweg, R. Frischknecht, A. J. Hendriks, D. van de Meent, A. M. Ragas, L. Reijnders and J. Struijs, *Environmental Science & Technology*, 2006, **40**, 641-648.
49. M. M. de Wild-Scholten, *Solar Energy Materials and Solar Cells*, 2013, **119**, 296-305.
50. N. Stylos and C. Koroneos, *Journal of Cleaner Production*, 2014, **64**, 639-645.
51. G. M. Mudd, *Resources Policy*, 2007, **32**, 42-56.
52. A. Akcil and S. Koldas, *Journal of Cleaner Production*, 2006, **14**, 1139-1145.
53. L. Wang, G.-R. Li, Q. Zhao and X.-P. Gao, *Energy Storage Materials*, 2017, **7**, 40-47.
54. J. B. Dunn, L. Gaines, J. C. Kelly, C. James and K. G. Gallagher, *Energy & Environmental Science*, 2015, **8**, 158-168.
55. E. Alsema and M. J. de Wild, *MRS Proceedings*, 2005, **895**, 0895-G0803-0805.
56. M. Raugei, S. Bargigli and S. Ulgiati, *Energy*, 2007, **32**, 1310-1318.
57. E. Alsema, M. de Wild-Scholten and V. Fthenakis, 21st European photovoltaic solar energy conference, 2006.
58. V. M. Fthenakis, *Renewable and Sustainable Energy Reviews*, 2004, **8**, 303-334.
59. V. Fthenakis, M. Fuhrmann, J. Heiser, A. Lanzirotti, J. Fitts and W. Wang, *Progress in Photovoltaics: Research and Applications*, 2005, **13**, 713-723.
60. F. Matteocci, L. Cinà, F. Di Giacomo, S. Razza, A. L. Palma, A. Guidobaldi, A. D'Epifanio, S. Licoccia, T. M. Brown and A. Reale, *Progress in Photovoltaics: Research and Applications*, 2016, **24**, 436-445.
61. D. Liu and T. L. Kelly, *Nature Photonics*, 2014, **8**, 133-138.
62. Y. Xu, J. Li, Q. Tan, A. L. Peters and C. Yang, *Waste Management*, 2018, **75**, 450-458.
63. M. Goe and G. Gaustad, *Applied Energy*, 2014, **120**, 41-48.
64. S. B. Darling, F. You, T. Veselka and A. Velosa, *Energy & Environmental Science*, 2011, **4**, 3133-3139.
65. B. P. Weidema, C. Bauer, R. Hischier, C. Mutel, T. Nemecek, J. Reinhard, C. Vadenbo and G. Wernet, *Overview and Methodology: Data Quality Guideline for the Ecoinvent Database Version 3*, 2013.
66. A. Anctil, C. W. Babbitt, R. P. Raffaelle and B. J. Landi, *Environmental Science & Technology*, 2011, **45**, 2353-2359.
67. N. W. Ayer, P. H. Tyedmers, N. L. Pelletier, U. Sonesson and A. Scholz, *The International Journal of Life Cycle Assessment*, 2007, **12**, 480.
68. S. Mukhopadhyay, M. Zerella, A. T. Bell, R. V. Srinivas and G. S. Smith, *Chemical Communications*, 2004, 472-473.
69. J. Foropoulos Jr and D. D. DesMarteau, *Inorganic Chemistry*, 1984, **23**, 3720-3723.
70. L. Xue, C. W. Padgett, D. D. DesMarteau and W. T. Pennington, *Solid state sciences*, 2002, **4**, 1535-1545.
71. I. McCulloch and M. Heeney, *Application of Solution Processable Organic Semiconductors in Organic Electronics*, Aldrich Chemical Co., Inc. Sigma-Aldrich Corporation, 6000 N. Teutonia Ave. Milwaukee, WI 53209, USA, 2009.
72. B. Souharce, Universität Wuppertal, Fakultät für Mathematik und Naturwissenschaften» Chemie» Dissertationen, 2008.
73. C. R. Conard and M. A. Dolliver, http://www.orgsyn.org/demo.aspx?prep=cv2p0167, (accessed February 18th, 2018).
74. Y. Takahashi, T. Ito, S. Sakai and Y. Ishii, *Journal of the Chemical Society D: Chemical*

Communications, 1970, 1065-1066.
75. C. Nataro and S. M. Fosbenner, *Journal of Chemical Education*, 2009, **86**, 1412-1415.
76. V. L. Hansley and P. J. Carlisle, *Chemical and Engineering News*, 1945, **23**, 1379-1380.
77. H. C. Brown, E. J. Mead and C. J. Shoaf, *Journal of the American Chemical Society*, 1956, **78**, 3613-3614.
78. Wikipedia, Lead(II) bromide, https://en.wikipedia.org/wiki/Lead(II)_bromide, (accessed March 21th, 2018).
79. Wikipedia, Potassium bromide, https://en.wikipedia.org/wiki/Potassium_bromide#cite_note-2, (accessed May 13th, 2018).

APPENDIX

This supplementary information file covers: (1) Material inventory and energy inventory for the metal oxide module, the mixed-cation module, and the SnO_2 module; (2) Material inventory and energy inventory for recycling phase (3) Life cycle impact assessment (LCIA) results for key raw materials, such as LBSO nanoparticle solution, LiTFSI, PTAA solution, ZnO precursor solution, FAI, MABr, and $PbBr_2$, which are needed during production of the investigated modules; (4) LCIA results for other key components and the corresponding life cycle inventories (LCIs) are retrieved from existing literature,[10, 66] which are then converted by multiplying with updated characterization factors; (5) Lists of LCIA data extracted from Ecoinvent database;[41] (6) Environmental profile of the metal oxide module, the mixed-cation module, and the SnO_2 module; (7) Primary energy consumption comparison between landfill and recycling end-of-life scenarios; (8) Uncertainty and sensitivity analysis results; (9) Impacts of recycling levels on the primary energy consumption and carbon footprint; (10) Sensitivity analysis results for recycling.

S1. Material inventory and energy inventory for the metal oxide module, the mixed-cation module, and the SnO_2 module

Table S1. Material inventory of 1 m^2 of the metal oxide module with an 80% active area.[20]

	Mass (kg)	Notes
Substrate patterning		
ITO glass	1.540E+00	Substrate
Ethanol	2.577E-02	Cleaning solvent
Deionized water	3.266E-02	Cleaning solvent
HTL deposition		
$Ni(NO_3)_2 \cdot 6H_2O$	5.662E-03	80 nm of HTL
Ethylene glycol	1.656E-02	Solvent of $Ni(NO_3)_2 \cdot 6H_2O$
Ethylenediamine	4.093E-03	Solvent of $Ni(NO_3)_2 \cdot 6H_2O$
Perovskite layer deposition		
PbI_2	1.682E-03	102 nm
Dimethylformamide	3.467E-03	Solvent of PbI_2
CH_3NH_3I	5.803E-04	218 nm
Isopropanol	9.110E-03	Solvent of CH_3NH_3I
ETL deposition		

ZnO powder	1.047E-03	70 nm of ETL
Chlorobenzene	5.131E-02	Solvent of ZnO, concentration 2%
Cathode deposition		
Al	2.634E-04	70 nm of electrode
Direct emissions		
$Ni(NO_3)_2 \cdot 6H_2O$	3.963E-03	Wasted effective component of NiO_x ink
Ethylene glycol	1.656E-02	Solvent in NiO_x ink
Ethylenediamine	4.093E-03	Solvent in NiO_x ink
PbI_2	1.177E-03	Wasted PbI_2
Dimethylformamide	3.467E-03	Solvent of PbI_2
CH_3NH_3I	4.062E-04	Wasted CH_3NH_3I
Isopropanol	9.110E-03	Solvent of CH_3NH_3I
ZnO powder	7.330E-04	Wasted effective component of ZnO ink
Chlorobenzene	5.131E-02	Solvent in ZnO ink
Al	4.741E-05	Wasted aluminum
Mass of module	**1.543**	Landfill

Table S2. Energy inventory of 1 m^2 of the metal oxide module with an 80% active area.[20]

	Power (W)	Time (s)	Electricity (kWh)
Substrate patterning			
Sonication	1.449E+03	1,200	4.831E-01
HTL deposition			
NiO_x spin coating	1.683E+04	90	4.208E-01
Post-annealing	1.953E+03	3,600	1.953E+00
Perovskite layer deposition			
1^{st}-step spin coating	6.733E+03	10	1.870E-02
Drying	3.196E+02	600	5.327E-02
2^{nd}-step spin coating	3.367E+04	20	1.870E-01
Annealing	5.327E+02	7,200	1.065E+00
ETL deposition			
ZnO spin coating	2.020E+04	30	1.683E-01
Electrode deposition			
Thermal evaporation			3.180E+00
Total			**7.530**

Table S3. Material inventory of 1 m^2 of the mixed-cation module with an 80% active area.[23]

	Mass (kg)	Notes
Substrate patterning		
FTO glass	5.040E+00	Substrate
Ethanol	2.577E-02	Cleaning solvent
Deionized water	3.266E-02	Cleaning solvent
BL deposition		
BL-TiO_2 ink	6.266E-03	30 nm of blocking layer
Ethanol	2.577E-02	Cleaning solvent
Deionized water	3.266E-02	Cleaning solvent
ETL deposition		
TiO_2	2.256E-03	200 nm of ETL
Ethanol	4.102E-04	Solvent of TiO_2 paste
Perovskite layer deposition		
FAI	8.236E-04	287 nm of FAI
PbI_2	2.318E-03	141 nm of PbI_2
MABr	9.938E-05	53 nm of MABr
$PbBr_2$	3.256E-04	18 nm of $PbBr_2$
DMF	3.288E-03	Solvent of mixed-cation mixtures
DMSO	9.577E-04	Solvent of mixed-cation mixtures
Chlorobenzene	1.221E-04	Additive
HTL deposition		
Spiro-OMeTAD	9.707E-04	200 nm of HTL
HTFSI	1.137E-04	Additive
Acetonitrile	5.255E-04	Solvent of HTFSI
FK209	3.571E-05	Additive
4-tert-Butylpyridine	3.564E-04	Additive
Chlorobenzene	1.465E-02	Solvent of Spiro-OMeTAD
Cathode deposition		
Au	1.506E-03	80 nm of electrode
Direct emissions		
Ethanol	6.100E-03	Solvent of BL-TiO_2 ink and TiO_2 paste
$TiCl_4$	6.028E-05	Wasted effective component of BL-TiO_2 ink
Isopropanol	3.810E-04	Solvent of BL-TiO_2 ink
Acetone	1.842E-04	Solvent of BL-TiO_2 ink
Acetic anhydride	3.246E-04	Solvent of BL-TiO_2 ink
TiO_2	1.579E-03	Wasted TiO_2 paste
FAI	5.766E-04	Wasted FAI

PbI_2	1.623E-03	Wasted PbI_2
MABr	6.956E-05	Wasted MABr
$PbBr_2$	2.279E-04	Wasted $PbBr_2$
DMF	3.288E-03	Solvent of mixed-cation mixtures
DMSO	9.577E-04	Solvent of mixed-cation mixtures
Chlorobenzene	1.478E-02	Solvent of Spiro-OMeTAD and waste from spin coating
Spiro-OMeTAD	6.795E-04	Wasted Spiro-OMeTAD
HTFSI	7.956E-05	Wasted Li-TFSI
Acetonitrile	5.255E-04	Solvent of HTFSI
FK209	2.500E-05	Wasted FK209
4-tert-Butylpyridine	2.495E-04	Wasted 4-tert-Butylpyridine
Au	2.711E-04	Wasted gold
Mass of module	**5.043**	Landfill

Table S4. Energy inventory of 1 m^2 of the mixed-cation module with an 80% active area.[23]

	Power (W)	Time (s)	Electricity (kWh)
Substrate patterning			
Sonication	1.449E+03	1,200	4.831E-01
BL deposition			
Spray pyrolysis	1.300E+02	7	2.868E-04
ETL deposition			
MP-TiO_2 spin coating	2.801E+04	15	1.167E-01
Calcining	3.409E+03	1,200	1.136E+00
Perovskite layer deposition			
1^{st}-step spin coating	6.733E+03	10	1.870E-02
2^{nd}-step spin coating	3.838E+04	30	3.198E-01
Drying	5.682E+02	5,400	8.524E-01
HTL deposition			
Spiro-OMeTAD spin coating	2.020E+04	20	1.122E-01
Electrode deposition			
Thermal evaporation			2.647E+00
Total			**5.687**

Table S5. Material inventory of 1 m^2 of the SnO_2 module with an 80% active area.[40]

	Mass (kg)	Notes

Substrate		
ITO glass	1.540E+00	Substrate
ETL deposition		
SnO_2	1.390E-04	25 nm of HTL
H_2O	5.067E-03	Solvent
Perovskite layer deposition		
PbI_2	1.105E-03	224 nm
Dimethylformamide	1.660E-03	Solvent
DMSO	1.014E-04	Solvent
FAI	2.927E-04	340 nm
MABr	2.927E-05	52 nm
MACl	2.927E-05	33 nm
Isopropanol	3.834E-03	Solvent
HTL deposition		
Spiro-OMeTAD	2.621E-04	180 nm of HTL
LiTFSI	3.299E-05	Additive
acetonitrile	9.972E-05	
4-tert butylpyridine	1.004E-04	
chlorobenzene	4.024E-03	Solvent
Cathode deposition		
Au	9.264E-04	60 nm of electrode
Encapsulation		
Adhesive	2.020E-02	
PET	6.170E-02	
Direct emissions		
H2O	5.067E-03	
DMF	1.660E-03	
DMSO	1.014E-04	
IPA	3.834E-03	
acetonitrile	9.972E-05	
chlorobenzene	4.024E-03	
Mass of module	**1.543**	Landfill

Table S6. Energy inventory of 1 m^2 of the SnO_2 module with an 80% active area.[40]

	Power (W)	Time (s)	Electricity (kWh)
Substrate treatment			

UV/O_3 cleaning	1.390E+02	600	2.300E-02
HTL deposition			
SnO_2 slot-die coating	2.976E+03	60	4.960E-02
Annealing	8.879E+02	1,800	4.439E-01
Perovskite layer deposition			
1^{st}-step slot-die coating	2.976E+03	60	4.960E-02
Annealing	3.196E+02	60	5.327E-03
2^{nd}-step slot-die coating	2.976E+03	60	4.960E-02
Annealing	8.879E+02	900	2.220E-01
HTL deposition			
Spiro-OMeTAD slot-die coating	2.976E+03	60	4.960E-02
Electrode deposition			
Sputtering	5.000E+01	240	3.333E-03
Encapsulation			
Lamination	1.500E+03	30	1.250E-02
Total			**0.908**

S2. Material inventory and energy inventory for recycling phase

Table S7. Material inventory of recycling 1 m^2 of the module with FTO substrate.

	Mass (kg)	Notes
The LBSO module		
DMF	1.264E+00	Solvent for selective dissolution
Deionized water	3.280E-02	Cleaning solvent
The mixed-cation module		
DMF	1.264E+00	Solvent for selective dissolution
Deionized water	3.277E-02	Cleaning solvent

Table S8. Energy inventory of recycling 1 m^2 of the module with FTO substrate.

	Power (W)	Time (s)	Electricity (kWh)
The LBSO module			
Annealing at 500 ℃	3.409E+03	3,600	3.409E+00
The mixed-cation module			
Annealing at 500 ℃	3.409E+03	3,600	3.409E+00

Table S9. Material inventory of recycling 1 m^2 of the module with ITO substrate.

	Mass (kg)	Notes
The metal oxide module		
NaOH (50%)	6.902E-04	Solvent for aqueous base
Deionized water	4.307E-01	Diluent

Table S10. Energy inventory of recycling 1 m^2 of the module with ITO substrate.

	Power (W)	Time (s)	Electricity (kWh)
The metal oxide module			
Ultrasonic cleaning	8.810E+02	900	2.203E-01

S3. LCIA results for key raw materials

In this section, blue inflows in the charts represent raw materials, items in green refer to intermediate products, purple outflows represent by-products, and outflows in red represent the target products. The flame symbols in the box mean that heating utility is needed in the procedures, the lightning suggests the procedures consume electricity, and snowflake represents that cooling utility is required in the corresponding steps. In order to accurately reveal the individual contribution of target product to the overall environmental impacts of the studied system, mass-based allocation method is employed, which is frequently used in recent life cycle assessment (LCA) studies.[67]

S3.1 LBSO nanoparticle solution

Figure S1 shows the manufacturing route of LBSO nanoparticle solution, which is based on the description of Shin et al.[18] The LCI and the corresponding LCIA results of 1 kg of LBSO nanoparticle solution are available in Table S11 and Table S12, respectively. Water consumption is reflected in the LCI, and energy consumed for distilled water generation is embraced in the total heat consumption.

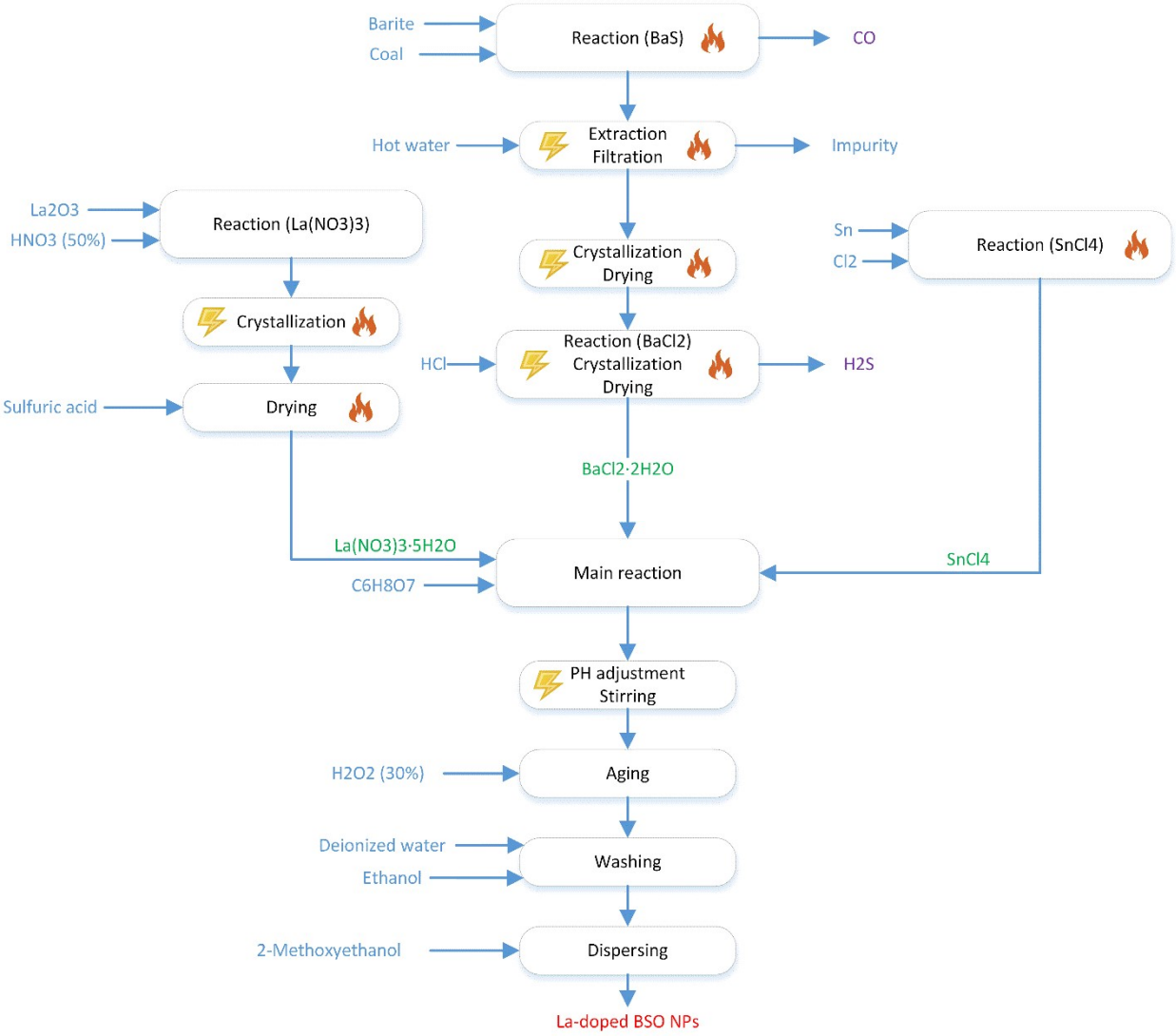

Figure S1. Manufacturing route for LBSO nanoparticle solution.

Table S11. LCI for 1 kg of LBSO nanoparticle solution.

	Value	**Unit**
Process input		
$C_6H_8O_7$	3.431E-01	kg
H_2O_2 (50%)	4.020E-02	kg
2-Methoxyethanol	6.664E-01	kg
H_2O	1.169E+00	kg
La_2O_3	2.922E-02	kg

HNO_3 (50%)	6.776E-02	kg
Barite	8.791E-01	kg
Coal	2.264E-01	kg
HCl	8.263E-01	kg
Sn	4.253E-01	kg
Cl_2	5.076E-01	kg
heat	7.880E+00	MJ
electricity	1.125E-01	kWh
Process output		
$Ba_{0.95}La_{0.05}SnO_3$	1.000E+00	kg
2-Methoxyethanol	6.664E-01	kg
CO	3.803E-01	kg
H_2S	1.155E-01	kg
wastewater	1.556E+00	kg
waste	1.462E+00	kg

Table S12. LCIA results for 1 kg of LBSO nanoparticle solution.

Impact categories (Unit)	**Value**
GHG emissions (kg CO_2-Eq)	7.712E+00
Cumulative energy demand (MJ-Eq)	1.242E+02
Agricultural land occupation (m^2a)	1.572E+00
Climate change (kg CO_2-Eq)	6.925E+00
Fossil depletion (kg oil-Eq)	2.285E+00
Freshwater ecotoxicity (kg 1,4-DCB-Eq)	1.662E-01
Freshwater eutrophication (kg P-Eq)	4.205E-03
Human toxicity (kg 1,4-DCB-Eq)	1.885E+02
Ionising radiation (kg U235-Eq)	6.452E-01
Marine ecotoxicity (kg 1,4-DCB-Eq)	1.515E+02
Marine eutrophication (kg N-Eq)	1.584E-02
Metal depletion (kg Fe-Eq)	2.928E+02
Natural land transformation (m^2)	1.743E-02

Ozone depletion (kg CFC-11-Eq)	7.642E-07
Particulate matter formation (kg PM10-Eq)	7.226E-02
Photochemical oxidant formation (kg NMVOC)	5.003E-02
Terrestrial acidification (kg SO_2-Eq)	1.108E-01
Terrestrial ecotoxicity (kg 1,4-DCB-Eq)	6.143E-03
Urban land occupation (m^2a)	3.059E-01
Water depletion (m^3)	8.075E-02
Ecosystem quality (points)	1.649E+00
Human health (points)	1.706E+00
Resources (points)	1.387E+01

S3.2 LiTFSI

Figure S2 shows the complete manufacturing route of Lithium bis (trifluoromethylsulphonyl) imide (LiTFSI). Methanesulfonyl chloride (MSC) is synthesized from methane and sulfuryl chloride following Sudip Mukhopadhyay's method.[68] The synthesis method of Bis ((trifluoromethyl) sulfonyl) imide (HTFSI) is extracted from existing literature.[69] HTFSI is then converted to the desired salt (LiTFSI) via neutralizing with lithium carbonate.[70] The LCI and the corresponding LCIA results of 1 kg of LiTFSI are shown in Table S13 and Table S14. Note that water consumption is reflected in the LCI, and energy consumed for distilled water generation is embraced in the total heat consumption.

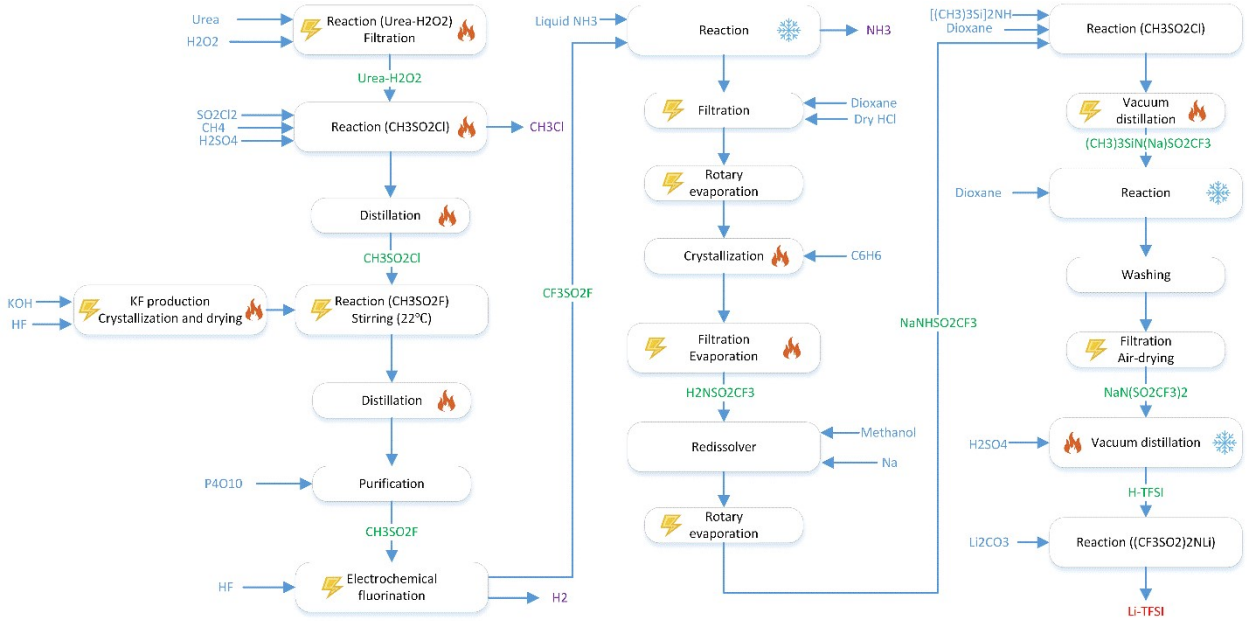

Figure S2. Manufacturing route for LiTFSI.

Table S13. LCI for 1 kg of LiTFSI.

	Value	Unit
Process input		
H_2O	2.879E+00	kg
methanol	2.546E+00	kg
Li_2CO_3	1.289E-01	kg
H_2SO_4	7.267E+01	kg
dioxane	8.959E+00	kg
$[(CH_3)_3Si]_2NH$	4.761E+00	kg
Na	1.266E-01	kg
SO_2Cl_2	1.283E+01	kg
CH_4	3.961E+01	kg
urea	3.148E-01	kg
H_2O_2	3.568E-01	kg
KOH	1.624E+00	kg
HF	1.283E+00	kg
liquid NH_3	3.747E+00	kg

dry HCl	2.011E-01	kg
C_6H_6	1.563E+00	kg
cooling	1.250E+00	MJ
heat	2.922E+01	MJ
electricity	2.851E+02	kWh
Process output		
$(CF_3SO_2)_2NLi$	1.000E+00	kg
H_2	7.028E-02	kg
CH_3Cl	7.102E+00	kg
NH_3	3.466E+00	kg
CO_2	7.666E-02	kg
wastewater	4.600E+00	kg
waste	1.373E+02	kg

Table S14. LCIA results for 1 kg of LiTFSI.

Impact categories (Unit)	**Value**
GHG emissions (kg CO_2-Eq)	4.441E+01
Cumulative energy demand (MJ-Eq)	6.967E+02
Agricultural land occupation (m^2a)	3.681E+00
Climate change (kg CO_2-Eq)	3.771E+01
Fossil depletion (kg oil-Eq)	1.497E+01
Freshwater ecotoxicity (kg 1,4-DCB-Eq)	2.171E+00
Freshwater eutrophication (kg P-Eq)	4.137E-02
Human toxicity (kg 1,4-DCB-Eq)	1.860E+03
Ionising radiation (kg U235-Eq)	2.025E+00
Marine ecotoxicity (kg 1,4-DCB-Eq)	1.529E+03
Marine eutrophication (kg N-Eq)	4.527E-02
Metal depletion (kg Fe-Eq)	1.353E+00
Natural land transformation (m^2)	6.327E-03
Ozone depletion (kg CFC-11-Eq)	5.283E-06
Particulate matter formation (kg PM10-Eq)	9.033E-02

Photochemical oxidant formation (kg NMVOC)	1.323E-01
Terrestrial acidification (kg SO_2-Eq)	2.842E-01
Terrestrial ecotoxicity (kg 1,4-DCB-Eq)	3.511E-02
Urban land occupation (m^2a)	3.567E-01
Water depletion (m^3)	9.077E-02
Ecosystem quality (points)	1.767E+00
Human health (points)	1.425E+01
Resources (points)	1.858E+00

S3.3 PTAA solution

Figure S3 demonstrates the manufacturing route of Poly(bis(4-phenyl)(2,4,6-trimethylphenyl)amine) (PTAA) solution. PTAA is synthesized via Suzuki coupling according to the description in the literature.[71] N,N-bis(4-bromophenyl)-2,4,6-trimethylaniline (MTPA3) is one of the key precursors for PTAA production, whose synthesis mechanism is found in a doctoral dissertation.[72] The manufacturing processes of Dibenzylideneacetone,[73] $Pd_2(dba)_3$,[74] DPPF,[75] NaH,[76] and Isopropyl borate,[77] are retrieved from existing publications. Finally, the PTAA solution is prepared by mixing 5 different reagents which is detailed by Shin et al.[18] The LCI and the corresponding LCIA results of 1 kg of PTAA solution are listed in Table S15 and Table S16. Water consumption is reflected in the LCI, and energy consumed for distilled water generation is embraced in the total heat consumption.

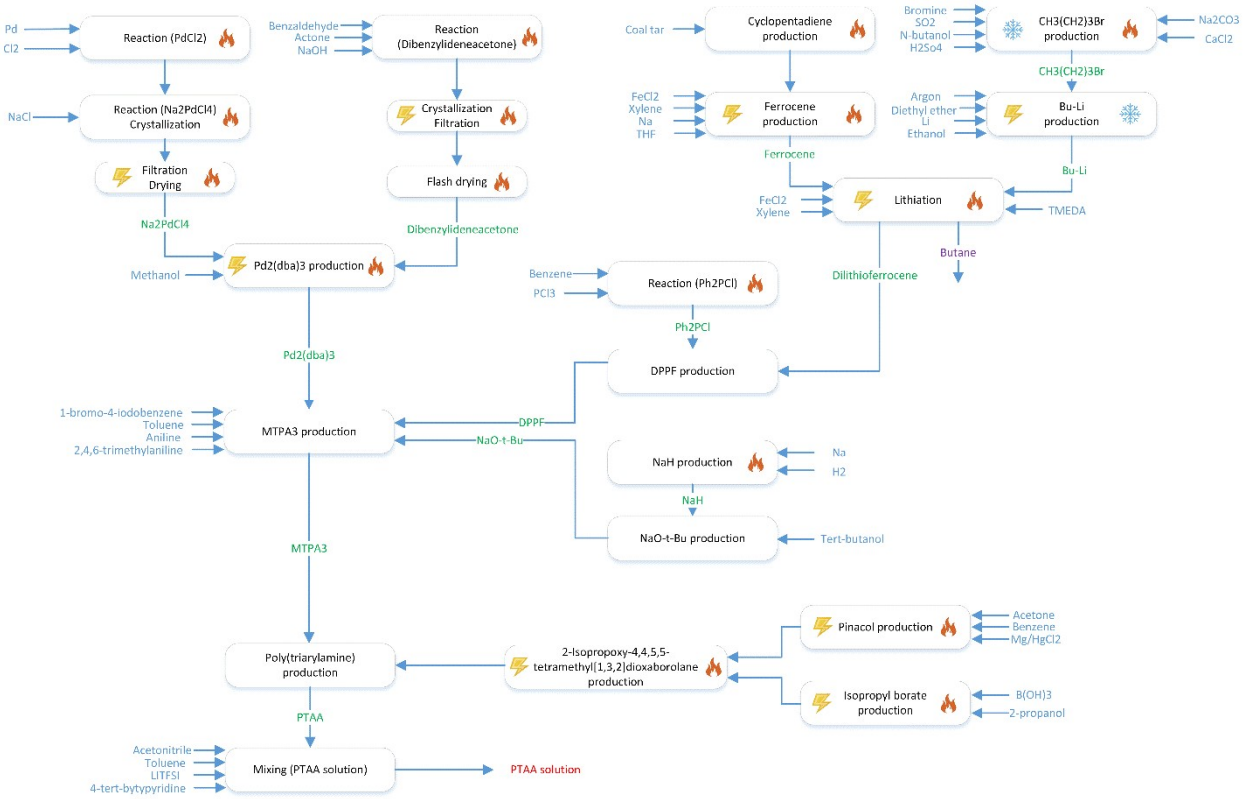

Figure S3. Manufacturing route for PTAA solution.

Table S15. LCI for 1 kg of PTAA solution.

	Value	Unit
Process input		
Benzaldehyde	9.234E-05	kg
NaOH (50%)	1.835E-04	kg
NaCl	3.058E-05	kg
Pd	2.770E-05	kg
Cl_2	1.856E-05	kg
xylene	5.175E-04	kg
tetrahydrofuran	5.349E-04	kg
$FeCl_2$	9.514E-05	kg
coal tar	3.971E-04	kg
hexanes	1.546E-03	kg
Ar	2.266E-06	kg

diethyl ether	5.429E-04	kg
bromine	1.336E-04	kg
sulfur dioxide	5.343E-05	kg
n-butanol	9.884E-05	kg
sodium carbonate	5.566E-06	kg
calcium chloride	1.670E-06	kg
Li	2.183E-05	kg
ethanol	2.103E-04	kg
TMEDA	6.589E-05	kg
PCl_3	1.220E-04	kg
1-bromo-4-iodobenzene	1.117E-02	kg
tert-butanol	3.493E-03	kg
H_2	4.720E-05	kg
aniline	1.749E-03	kg
ethyl acetate	7.712E-02	kg
EDTA	3.676E-02	kg
2,4,6-trimethylaniline	2.539E-03	kg
Trimethyl borate	7.578E-03	kg
Isopropyl alcohol	3.552E-03	kg
Mg	2.189E-04	kg
acetone	1.667E-03	kg
Hg	1.820E-04	kg
HNO_3 (50%)	1.141E-04	kg
HCl (30%)	2.203E-04	kg
N_2	2.435E-05	kg
toluene	1.711E-01	kg
H_2O	1.528E-01	kg
methanol	5.318E-02	kg
Li_2CO_3	2.384E-03	kg
H_2SO_4	1.344E+00	kg
dioxane	1.657E-01	kg

$[(CH_3)_3Si]_2NH$	8.804E-02	kg
Na	3.461E-03	kg
SO_2Cl_2	2.372E-01	kg
CH_4	7.325E-01	kg
urea	5.821E-03	kg
H_2O_2	6.597E-03	kg
KOH	3.002E-02	kg
HF	2.372E-02	kg
liquid NH_3	6.929E-02	kg
dry HCl	3.718E-03	kg
C_6H_6	3.276E-02	kg
acetonitrile	8.549E-02	kg
4-tert-butylpyridine	7.529E-01	kg
cooling	2.322E-02	MJ
heat	6.848E-01	MJ
electricity	1.371E+01	kWh
Process output		
PTAA solution	1.000E+00	kg
H_2	1.299E-03	kg
CH_3Cl	1.313E-01	kg
NH_3	6.419E-02	kg
CO_2	1.417E-03	kg
C_3H_8O	8.530E-04	kg
azeotrope	4.311E-03	kg
$Mg(OH)_2$	2.457E-04	kg
butane	5.095E-05	kg
N_2	2.435E-05	kg
Ar	2.266E-06	kg
NO_2	4.164E-05	kg
wastewater	1.847E-01	kg
waste	2.723E+00	kg

Table S16. LCIA results for 1 kg of PTAA solution.

Impact categories (Unit)	Value
GHG emissions (kg CO_2-Eq)	2.113E+01
Cumulative energy demand (MJ-Eq)	3.576E+02
Agricultural land occupation (m^2a)	1.140E+00
Climate change (kg CO_2-Eq)	1.892E+01
Fossil depletion (kg oil-Eq)	7.781E+00
Freshwater ecotoxicity (kg 1,4-DCB-Eq)	5.382E-01
Freshwater eutrophication (kg P-Eq)	1.111E-02
Human toxicity (kg 1,4-DCB-Eq)	5.676E+02
Ionising radiation (kg U235-Eq)	1.026E+00
Marine ecotoxicity (kg 1,4-DCB-Eq)	4.281E+02
Marine eutrophication (kg N-Eq)	2.253E-02
Metal depletion (kg Fe-Eq)	1.316E+00
Natural land transformation (m^2)	2.969E-03
Ozone depletion (kg CFC-11-Eq)	3.218E-06
Particulate matter formation (kg PM10-Eq)	5.734E-02
Photochemical oxidant formation (kg NMVOC)	6.765E-02
Terrestrial acidification (kg SO_2-Eq)	1.871E-01
Terrestrial ecotoxicity (kg 1,4-DCB-Eq)	5.573E-02
Urban land occupation (m^2a)	1.322E-01
Water depletion (m^3)	4.260E-02
Ecosystem quality (points)	8.024E-01
Human health (points)	4.672E+00
Resources (points)	9.903E-01

S3.4 NiO_x precursor solution

The NiO_x precursor solution is prepared according to the technical details in a paper by You et al.[20] Table S17 and Table S18 exhibit the LCI and the corresponding LCIA results of 1 kg of NiO_x precursor solution. Water consumption is reflected in the LCI, and energy consumed for distilled water generation is embraced in the total heat consumption.

Table S17. LCI for 1 kg of NiO_x precursor solution.

	Value	Unit
Process input		
ethylene glycol	6.293E-01	kg
ethylenediamine	1.555E-01	kg
HNO_3 (50%)	1.863E-01	kg
$NiSO_4$	1.146E-01	kg
KOH	8.280E-02	kg
H_2O	1.303E+00	kg
heat	6.197E+00	MJ
electricity	5.077E-03	kWh
Process output		
NiO_x precursor solution	1.000E+00	kg
K_2SO_4	1.286E-01	kg
wastewater	1.343E+00	kg

Table S18. LCIA results for 1 kg of NiO_x precursor solution.

Impact categories (Unit)	Value
GHG emissions (kg CO_2-Eq)	3.266E+00
Cumulative energy demand (MJ-Eq)	6.471E+01
Agricultural land occupation (m^2a)	7.461E-01
Climate change (kg CO_2-Eq)	2.847E+00
Fossil depletion (kg oil-Eq)	1.259E+00
Freshwater ecotoxicity (kg 1,4-DCB-Eq)	1.177E-01
Freshwater eutrophication (kg P-Eq)	2.210E-03
Human toxicity (kg 1,4-DCB-Eq)	1.383E+02
Ionising radiation (kg U235-Eq)	2.423E-01
Marine ecotoxicity (kg 1,4-DCB-Eq)	1.363E+02
Marine eutrophication (kg N-Eq)	5.890E-03
Metal depletion (kg Fe-Eq)	1.677E+00

Natural land transformation (m^2)	3.903E-04
Ozone depletion (kg CFC-11-Eq)	4.301E-07
Particulate matter formation (kg PM10-Eq)	2.891E-02
Photochemical oxidant formation (kg NMVOC)	2.067E-02
Terrestrial acidification (kg SO_2-Eq)	1.172E-01
Terrestrial ecotoxicity (kg 1,4-DCB-Eq)	9.879E-03
Urban land occupation (m^2a)	3.762E-02
Water depletion (m^3)	1.619E-02
Ecosystem quality (points)	1.751E-01
Human health (points)	1.113E+00
Resources (points)	2.207E-01

S3.5 ZnO precursor solution

We derive the manufacturing procedure following the method of You et al.[20] The LCI and the corresponding LCIA results of 1 kg of NiO_x precursor solution are demonstrated in Table S19 and Table S20. Water consumption is reflected in the LCI, and energy consumed for distilled water generation is embraced in the total heat consumption.

Table S19. LCI for 1 kg of ZnO precursor solution.

	Value	**Unit**
Process input		
chlorobenzene	9.800E-01	kg
KOH	2.765E-02	kg
H_2O	1.325E-01	kg
CH_3COOH	3.023E-02	kg
Zn	1.605E-02	kg
heat	7.244E-01	MJ
electricity	1.123E-02	kWh
Process output		
ZnO precursor solution	1.000E+00	kg
KAc	4.840E-02	kg
H_2	4.938E-04	kg

wastewater	1.370E-01	kg
waste	6.047E-04	kg

Table S20. LCIA results for 1 kg of ZnO precursor solution.

Impact categories (Unit)	**Value**
GHG emissions (kg CO_2-Eq)	3.248E+00
Cumulative energy demand (MJ-Eq)	7.748E+01
Agricultural land occupation (m^2a)	1.928E-01
Climate change (kg CO_2-Eq)	2.772E+00
Fossil depletion (kg oil-Eq)	1.695E+00
Freshwater ecotoxicity (kg 1,4-DCB-Eq)	9.913E-02
Freshwater eutrophication (kg P-Eq)	1.386E-03
Human toxicity (kg 1,4-DCB-Eq)	5.612E+01
Ionising radiation (kg U235-Eq)	1.597E-01
Marine ecotoxicity (kg 1,4-DCB-Eq)	4.397E+01
Marine eutrophication (kg N-Eq)	2.895E-03
Metal depletion (kg Fe-Eq)	1.723E-01
Natural land transformation (m^2)	2.807E-04
Ozone depletion (kg CFC-11-Eq)	6.835E-07
Particulate matter formation (kg PM10-Eq)	8.530E-03
Photochemical oxidant formation (kg NMVOC)	2.157E-02
Terrestrial acidification (kg SO_2-Eq)	1.550E-02
Terrestrial ecotoxicity (kg 1,4-DCB-Eq)	2.961E-03
Urban land occupation (m^2a)	2.853E-02
Water depletion (m^3)	9.696E-03
Ecosystem quality (points)	1.279E-01
Human health (points)	5.002E-01
Resources (points)	2.113E-01

S3.6 FAI

$NH{=}CHNH_3I$ (FAI) is synthesized according to the technical details in a recent publication

by Bi et al.[23] The LCI and the corresponding LCIA results of 1 kg of FAI are demonstrated in Table S21 and Table S22. Water consumption is reflected in the LCI, and energy consumed for distilled water generation is embraced in the total heat consumption.

Table S21. LCI for 1 kg of FAI.

	Value	**Unit**
Process input		
H_2O	5.763E+01	kg
iodine	3.442E+01	kg
H_2S	4.611E+00	kg
chloroform	1.828E+02	kg
Na	7.721E+01	kg
HOAc	2.039E+01	kg
NH_3	7.560E+00	kg
Ethanol	9.581E+02	kg
cooling	5.729E+00	MJ
heat	9.754E+02	MJ
electricity	1.053E+05	kWh
Process output		
$NH{=}CHNH_3I$	1.000E+00	kg
H_2	3.357E+00	kg
NaCl	1.963E+02	kg
Ethanol (chloroform)	7.460E+02	kg
wastewater	1.129E+02	kg
waste	2.114E+02	kg
Ethanol (emitted to air)	7.171E+01	kg

Table S22. LCIA results for 1 kg of FAI.

Impact categories (Unit)	**Value**
GHG emissions (kg CO_2-Eq)	8.167E+01
Cumulative energy demand (MJ-Eq)	2.768E+01

Agricultural land occupation (m^2a)	1.409E+03
Climate change (kg CO_2-Eq)	6.952E-02
Fossil depletion (kg oil-Eq)	6.784E+00
Freshwater ecotoxicity (kg 1,4-DCB-Eq)	5.129E-02
Freshwater eutrophication (kg P-Eq)	3.462E-03
Human toxicity (kg 1,4-DCB-Eq)	2.606E+00
Ionising radiation (kg U235-Eq)	3.157E-01
Marine ecotoxicity (kg 1,4-DCB-Eq)	1.447E+03
Marine eutrophication (kg N-Eq)	1.369E+00
Metal depletion (kg Fe-Eq)	7.671E+01
Natural land transformation (m^2)	3.356E+01
Ozone depletion (kg CFC-11-Eq)	3.557E-01
Particulate matter formation (kg PM10-Eq)	2.704E-03
Photochemical oxidant formation (kg NMVOC)	6.397E+02
Terrestrial acidification (kg SO_2-Eq)	6.245E-01
Terrestrial ecotoxicity (kg 1,4-DCB-Eq)	2.198E+02
Urban land occupation (m^2a)	7.560E-02
Water depletion (m^3)	4.317E-01
Ecosystem quality (points)	1.349E-02
Human health (points)	1.478E-04
Resources (points)	8.962E-02

S3.7 MABr

CH_3NH_3Br (MABr) is prepared based on the method depicted by Bi et al.[23] The LCI and the corresponding LCIA results of 1 kg of FAI are summarized in Table S23 and Table S24, respectively. Water consumption is reflected in the LCI, and energy consumed for distilled water generation is included in the total heat consumption.

Table S23. LCI for 1 kg of MABr.

	Value	**Unit**
Process input		
H_2O	1.543E+03	kg

S	5.614E+01	kg
Bromine	8.421E+02	kg
CH_3NH_2	3.220E+02	kg
methanol	4.830E+02	kg
cooling	9.662E+01	MJ
heat	6.871E+03	MJ
electricity	8.725E+05	kWh
Process output		
MABr	1.000E+00	kg
H_2SO_4	1.719E+02	kg
waste	2.580E+03	kg
wastewater	4.928E+02	kg

Table S24. LCIA results for 1 kg of MABr.

Impact categories (Unit)	**Value**
GHG emissions (kg CO_2-Eq)	3.619E+03
Cumulative energy demand (MJ-Eq)	2.320E+02
Agricultural land occupation (m^2a)	6.318E+04
Climate change (kg CO_2-Eq)	2.312E+00
Fossil depletion (kg oil-Eq)	2.358E+02
Freshwater ecotoxicity (kg 1,4-DCB-Eq)	2.856E-01
Freshwater eutrophication (kg P-Eq)	2.656E-02
Human toxicity (kg 1,4-DCB-Eq)	9.355E+01
Ionising radiation (kg U235-Eq)	1.036E+01
Marine ecotoxicity (kg 1,4-DCB-Eq)	6.376E+04
Marine eutrophication (kg N-Eq)	3.184E+01
Metal depletion (kg Fe-Eq)	3.416E+03
Natural land transformation (m^2)	1.505E+03
Ozone depletion (kg CFC-11-Eq)	1.497E+01
Particulate matter formation (kg PM10-Eq)	9.919E-02
Photochemical oxidant formation (kg NMVOC)	2.848E+04

Terrestrial acidification (kg SO_2-Eq)	2.324E+01
Terrestrial ecotoxicity (kg 1,4-DCB-Eq)	9.592E+03
Urban land occupation (m^2a)	3.138E+00
Water depletion (m^3)	1.620E+01
Ecosystem quality (points)	5.629E-01
Human health (points)	3.044E-04
Resources (points)	3.851E+00

S3.8 $PbBr_2$

$PbBr_2$ is prepared by treating solution of lead nitrate with potassium bromide,[78] whose manufacturing route is shown in Figure S4. A conventional method for manufacturing KBr is the reaction of potassium carbonate with Fe_3Br_8, obtained by treating scrap iron under water with excess bromine.[79] The LCI and the corresponding LCIA results of 1 kg of $PbBr_2$ are summed up in Table S25 and Table S26. Water consumption is reflected in the LCI, and energy consumed for distilled water generation is included in the total heat consumption.

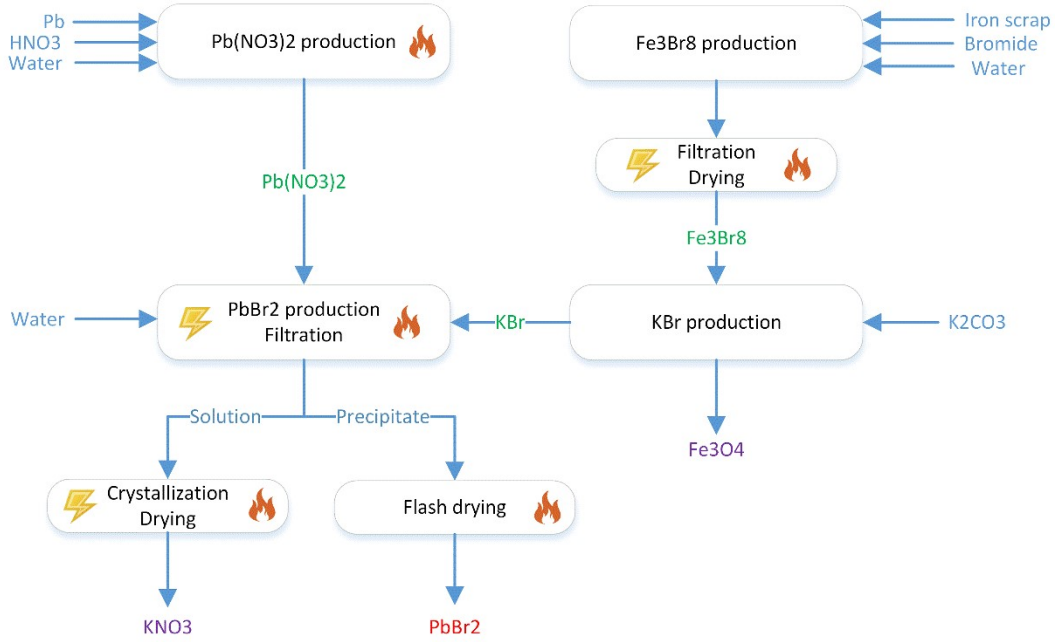

Figure S4. Manufacturing route for $PbBr_2$.

Table S25. LCI for 1 kg of $PbBr_2$.

	Value	Unit

Process input		
K_2CO_3	3.760E-01	kg
iron scrap	1.144E-01	kg
bromine	4.360E-01	kg
HNO_3 (50%)	5.640E-01	kg
Pb	9.155E-01	kg
H_2O	3.777E+00	kg
heat	1.524E+01	MJ
electricity	2.399E-01	kWh
Process output		
$PbBr_2$	1.000E+00	kg
KNO_3	5.504E-01	kg
Fe_3O_4	1.580E-01	kg
CO_2	1.199E-01	kg
NO	5.450E-02	kg
wastewater	4.301E+00	kg

Table S26. LCIA results for 1 kg of $PbBr_2$.

Impact categories (Unit)	**Value**
GHG emissions (kg CO_2-Eq)	3.850E+00
Cumulative energy demand (MJ-Eq)	8.288E+00
Agricultural land occupation (m^2a)	3.840E+01
Climate change (kg CO_2-Eq)	2.888E-02
Fossil depletion (kg oil-Eq)	2.540E+00
Freshwater ecotoxicity (kg 1,4-DCB-Eq)	4.831E-03
Freshwater eutrophication (kg P-Eq)	2.110E-03
Human toxicity (kg 1,4-DCB-Eq)	1.070E+00
Ionising radiation (kg U235-Eq)	1.466E-01
Marine ecotoxicity (kg 1,4-DCB-Eq)	5.048E+01
Marine eutrophication (kg N-Eq)	1.141E+00
Metal depletion (kg Fe-Eq)	3.537E+00

Natural land transformation (m^2)	9.154E-01
Ozone depletion (kg CFC-11-Eq)	8.717E-02
Particulate matter formation (kg PM10-Eq)	2.607E-03
Photochemical oxidant formation (kg NMVOC)	2.352E+02
Terrestrial acidification (kg SO_2-Eq)	2.037E-01
Terrestrial ecotoxicity (kg 1,4-DCB-Eq)	1.012E+02
Urban land occupation (m^2a)	7.144E-03
Water depletion (m^3)	1.114E+00
Ecosystem quality (points)	5.770E-04
Human health (points)	3.507E-07
Resources (points)	1.946E-02

S4. LCIA results for other key components

In this section, LCIs for other key components, namely PbI_2, CH_3NH_3I, FTO glass, ITO glass, BL-TiO_2 ink, and spiro-OMeTAD are retrieved from existing publication.[10] LCI data are then converted into various impact categories by employing the LCIA method used in this work. Because the LCI for all aforementioned components are easily accessible in the literature, technical details are omitted, and only the LCIA results are summarized as follows.

S4.1 PbI_2

Table S27. LCIA results for 1 kg of PbI_2.

Impact categories (Unit)	**Value**
GHG emissions (kg CO_2-Eq)	4.564E+00
Cumulative energy demand (MJ-Eq)	5.427E+01
Agricultural land occupation (m^2a)	1.047E+00
Climate change (kg CO_2-Eq)	3.898E+00
Fossil depletion (kg oil-Eq)	1.035E+00
Freshwater ecotoxicity (kg 1,4-DCB-Eq)	7.126E-02
Freshwater eutrophication (kg P-Eq)	1.978E-03
Human toxicity (kg 1,4-DCB-Eq)	1.559E+02

Ionising radiation (kg U235-Eq)	1.916E-01
Marine ecotoxicity (kg 1,4-DCB-Eq)	7.820E+01
Marine eutrophication (kg N-Eq)	5.158E-03
Metal depletion (kg Fe-Eq)	6.322E-01
Natural land transformation (m^2)	6.631E-04
Ozone depletion (kg CFC-11-Eq)	4.463E-07
Particulate matter formation (kg PM10-Eq)	1.105E-02
Photochemical oxidant formation (kg NMVOC)	1.555E-02
Terrestrial acidification (kg SO_2-Eq)	3.125E-02
Terrestrial ecotoxicity (kg 1,4-DCB-Eq)	5.377E-03
Urban land occupation (m^2a)	4.020E-02
Water depletion (m^3)	1.174E-02
Ecosystem quality (points)	1.912E-01
Human health (points)	1.221E+00
Resources (points)	1.534E-01

S4.2 CH_3NH_3I (MAI)

Table S28. LCIA results for 1 kg of MAI.

Impact categories (Unit)	**Value**
GHG emissions (kg CO_2-Eq)	1.615E+02
Cumulative energy demand (MJ-Eq)	3.431E+03
Agricultural land occupation (m^2a)	1.614E+01
Climate change (kg CO_2-Eq)	1.478E+02
Fossil depletion (kg oil-Eq)	6.818E+01
Freshwater ecotoxicity (kg 1,4-DCB-Eq)	5.572E+00
Freshwater eutrophication (kg P-Eq)	1.312E-01
Human toxicity (kg 1,4-DCB-Eq)	6.537E+03
Ionising radiation (kg U235-Eq)	1.580E+01
Marine ecotoxicity (kg 1,4-DCB-Eq)	4.973E+03
Marine eutrophication (kg N-Eq)	2.100E-01
Metal depletion (kg Fe-Eq)	1.181E+01

Natural land transformation (m^2)	3.118E-02
Ozone depletion (kg CFC-11-Eq)	5.345E-05
Particulate matter formation (kg PM10-Eq)	4.825E-01
Photochemical oxidant formation (kg NMVOC)	6.497E-01
Terrestrial acidification (kg SO_2-Eq)	1.224E+00
Terrestrial ecotoxicity (kg 1,4-DCB-Eq)	2.323E-01
Urban land occupation (m^2a)	2.232E+00
Water depletion (m^3)	2.899E+00
Ecosystem quality (points)	9.257E+00
Human health (points)	5.102E+01
Resources (points)	8.723E+00

S4.3 FTO glass

Table S29. LCIA results for 1 kg of FTO glass.

Impact categories (Unit)	**Value**
GHG emissions (kg CO_2-Eq)	6.901E-01
Cumulative energy demand (MJ-Eq)	1.687E+01
Agricultural land occupation (m^2a)	1.230E+00
Climate change (kg CO_2-Eq)	7.116E-01
Fossil depletion (kg oil-Eq)	1.660E-01
Freshwater ecotoxicity (kg 1,4-DCB-Eq)	1.921E-02
Freshwater eutrophication (kg P-Eq)	4.022E-04
Human toxicity (kg 1,4-DCB-Eq)	2.478E+01
Ionising radiation (kg U235-Eq)	4.365E-02
Marine ecotoxicity (kg 1,4-DCB-Eq)	1.755E+01
Marine eutrophication (kg N-Eq)	2.106E-03
Metal depletion (kg Fe-Eq)	7.486E+00
Natural land transformation (m^2)	5.284E-04
Ozone depletion (kg CFC-11-Eq)	4.482E-08
Particulate matter formation (kg PM10-Eq)	6.202E-03
Photochemical oxidant formation (kg NMVOC)	9.550E-03

Terrestrial acidification (kg SO_2-Eq)	1.242E-02
Terrestrial ecotoxicity (kg 1,4-DCB-Eq)	1.474E-03
Urban land occupation (m^2a)	2.931E-02
Water depletion (m^3)	1.535E-03
Ecosystem quality (points)	1.012E-01
Human health (points)	2.037E-01
Resources (points)	3.674E-01

S4.4 ITO glass

Table S30. LCIA results for 1 m^2 of ITO glass.

Impact categories (Unit)	**Value**
GHG emissions (kg CO_2-Eq)	1.684E+01
Cumulative energy demand (MJ-Eq)	2.922E+02
Agricultural land occupation (m^2a)	5.404E-02
Climate change (kg CO_2-Eq)	1.586E+01
Fossil depletion (kg oil-Eq)	6.871E+00
Freshwater ecotoxicity (kg 1,4-DCB-Eq)	8.252E-02
Freshwater eutrophication (kg P-Eq)	1.055E-03
Human toxicity (kg 1,4-DCB-Eq)	1.655E+02
Ionising radiation (kg U235-Eq)	1.673E-01
Marine ecotoxicity (kg 1,4-DCB-Eq)	6.653E+01
Marine eutrophication (kg N-Eq)	1.505E-02
Metal depletion (kg Fe-Eq)	6.412E-01
Natural land transformation (m^2)	2.606E-03
Ozone depletion (kg CFC-11-Eq)	1.375E-06
Particulate matter formation (kg PM10-Eq)	1.995E-02
Photochemical oxidant formation (kg NMVOC)	4.886E-02
Terrestrial acidification (kg SO_2-Eq)	7.217E-02
Terrestrial ecotoxicity (kg 1,4-DCB-Eq)	7.877E-03
Urban land occupation (m^2a)	1.584E-02
Water depletion (m^3)	1.015E-02

Ecosystem quality (points)	4.891E-01
Human health (points)	1.724E+00
Resources (points)	8.537E-01

S4.5 BL-TiO_2 ink

Table S31. LCIA results for 1 kg of BL-TiO_2 ink.

Impact categories (Unit)	**Value**
GHG emissions (kg CO_2-Eq)	1.817E+00
Cumulative energy demand (MJ-Eq)	4.924E+01
Agricultural land occupation (m^2a)	1.032E+00
Climate change (kg CO_2-Eq)	1.572E+00
Fossil depletion (kg oil-Eq)	5.645E-01
Freshwater ecotoxicity (kg 1,4-DCB-Eq)	3.649E-02
Freshwater eutrophication (kg P-Eq)	6.776E-04
Human toxicity (kg 1,4-DCB-Eq)	2.217E+01
Ionising radiation (kg U235-Eq)	1.100E-01
Marine ecotoxicity (kg 1,4-DCB-Eq)	1.826E+01
Marine eutrophication (kg N-Eq)	6.090E-03
Metal depletion (kg Fe-Eq)	6.899E-02
Natural land transformation (m^2)	1.068E-03
Ozone depletion (kg CFC-11-Eq)	1.436E-07
Particulate matter formation (kg PM10-Eq)	4.574E-03
Photochemical oxidant formation (kg NMVOC)	5.793E-03
Terrestrial acidification (kg SO_2-Eq)	1.415E-02
Terrestrial ecotoxicity (kg 1,4-DCB-Eq)	7.737E-03
Urban land occupation (m^2a)	5.909E-02
Water depletion (m^3)	3.417E-01
Ecosystem quality (points)	3.290E-01
Human health (points)	2.157E-01
Resources (points)	7.162E-02

S4.6 Spiro-OMeTAD

Table S32. LCIA results for 1 kg of spiro-OMeTAD.

Impact categories (Unit)	Value
GHG emissions (kg CO_2-Eq)	1.215E+02
Cumulative energy demand (MJ-Eq)	1.958E+03
Agricultural land occupation (m^2a)	2.977E+01
Climate change (kg CO_2-Eq)	1.099E+02
Fossil depletion (kg oil-Eq)	3.547E+01
Freshwater ecotoxicity (kg 1,4-DCB-Eq)	7.422E+00
Freshwater eutrophication (kg P-Eq)	1.279E-01
Human toxicity (kg 1,4-DCB-Eq)	6.548E+03
Ionising radiation (kg U235-Eq)	1.118E+01
Marine ecotoxicity (kg 1,4-DCB-Eq)	5.538E+03
Marine eutrophication (kg N-Eq)	1.230E-01
Metal depletion (kg Fe-Eq)	5.050E+00
Natural land transformation (m^2)	9.585E-03
Ozone depletion (kg CFC-11-Eq)	1.034E-05
Particulate matter formation (kg PM10-Eq)	6.201E-01
Photochemical oxidant formation (kg NMVOC)	4.377E-01
Terrestrial acidification (kg SO_2-Eq)	5.987E-01
Terrestrial ecotoxicity (kg 1,4-DCB-Eq)	1.241E-01
Urban land occupation (m^2a)	1.625E+00
Water depletion (m^3)	3.610E-01
Ecosystem quality (points)	6.379E+00
Human health (points)	4.999E+01
Resources (points)	4.487E+00

S4.7 PCBM

Table S33. LCIA results for 1 kg of PCBM.[66]

Impact categories (Unit)	Value

GHG emissions (kg CO_2-Eq)	6.819E+02
Cumulative energy demand (MJ-Eq)	2.096E+04
Agricultural land occupation (m^2a)	7.640E+02
Climate change (kg CO_2-Eq)	5.971E+02
Fossil depletion (kg oil-Eq)	3.481E+02
Freshwater ecotoxicity (kg 1,4-DCB-Eq)	5.378E+00
Freshwater eutrophication (kg P-Eq)	1.327E-01
Human toxicity (kg 1,4-DCB-Eq)	7.165E+03
Ionising radiation (kg U235-Eq)	2.537E+01
Marine ecotoxicity (kg 1,4-DCB-Eq)	4.742E+03
Marine eutrophication (kg N-Eq)	1.195E+00
Metal depletion (kg Fe-Eq)	1.262E+01
Natural land transformation (m^2)	8.921E-02
Ozone depletion (kg CFC-11-Eq)	4.186E-05
Particulate matter formation (kg PM10-Eq)	2.336E+00
Photochemical oxidant formation (kg NMVOC)	4.199E+00
Terrestrial acidification (kg SO_2-Eq)	3.911E+00
Terrestrial ecotoxicity (kg 1,4-DCB-Eq)	6.000E-01
Urban land occupation (m^2a)	1.271E+01
Water depletion (m^3)	1.439E+00
Ecosystem quality (points)	4.171E+01
Human health (points)	7.317E+01
Resources (points)	4.232E+01

S5. LCIA data from Ecoinvent database[41]

Table S34. Characterization factors extracted from Ecoinvent database (Part I).

item	value	unit	IPCC 2013/kg CO2-Eq	cumulative energy demand/MJ-Eq	ReCiPe Midpoint (E)								
					agricultural land occupation	climate change	fossil depletion	freshwater ecotoxicity	freshwater eutrophication	human toxicity	ionising radiation	marine ecotoxicity	marine eutrophication
1-Bromo-4-iodobenzene (BrC6H4I)	1	kg	3.01E+00	6.67E+01	1.18E-01	2.61E+00	1.45E+00	1.17E-01	1.31E-03	5.02E+01	1.78E-01	4.06E+01	2.65E-03
2,4,6-Trimethylaniline (C9H13N)	1	kg	5.24E+00	9.47E+01	1.31E-01	4.05E+00	2.12E+00	5.12E-02	1.47E-03	7.02E+01	1.88E-01	5.25E+01	5.66E-03
2-Methoxyethanol (C3H8O2)	1	kg	2.34E+00	6.58E+01	8.03E-02	2.08E+00	1.46E+00	1.82E-02	7.81E-04	2.75E+01	1.22E-01	2.16E+01	1.69E-03
4-tert-Butylpyridine (C9H13N)	1	kg	1.11E+01	1.82E+02	6.17E-01	1.02E+01	3.73E+00	1.45E-01	4.76E-03	2.15E+02	9.00E-01	1.70E+02	1.25E-02
Acetic acid (CH3COOH, 98%)	1	kg	1.87E+00	5.09E+01	7.77E-02	1.57E+00	1.13E+00	2.49E-02	7.47E-04	3.94E+01	2.01E-01	2.64E+01	1.57E-03
Acetic anhydride (C4H6O3)	1	kg	3.97E+00	7.90E+01	1.94E-01	3.54E+00	1.72E+00	4.33E-02	1.30E-03	6.58E+01	3.41E-01	4.62E+01	2.93E-03
Acetone (C3H6O)	1	kg	2.32E+00	6.74E+01	3.82E-04	1.93E+00	1.54E+00	1.63E-02	1.56E-04	1.06E+00	3.09E-04	2.09E+00	1.81E-03
Acetonitrile (C2H3N)	1	kg	4.08E+00	1.10E+02	6.15E-02	3.68E+00	2.54E+00	1.75E-02	4.29E-04	2.87E+01	8.83E-02	2.24E+01	1.68E-02
Alumina (Al2O3)	1	kg	1.26E+00	1.54E+01	2.04E-02	1.19E+00	3.45E-01	4.02E-02	5.43E-04	4.22E+01	5.83E-02	6.23E+01	1.31E-03
Aluminium (Al)	1	kg	2.66E+01	2.48E+02	3.70E-01	2.45E+01	5.51E+00	2.38E-01	6.70E-03	2.99E+02	2.63E-01	3.19E+02	2.36E-02
Aniline (C6H5NH2)	1	kg	5.24E+00	9.47E+01	1.31E-01	4.05E+00	2.12E+00	5.12E-02	1.47E-03	7.02E+01	1.88E-01	5.25E+01	5.66E-03
Argon (Ar)	1	kg	2.69E+00	4.04E+01	1.41E-01	2.49E+00	7.14E-01	3.53E-02	1.46E-03	4.68E+01	4.14E-01	4.03E+01	2.43E-03
Barite (BaSO4)	1	kg	2.90E-01	3.97E+00	1.49E-02	2.68E-01	7.60E-02	3.87E-03	1.50E-04	5.61E+00	2.91E-02	4.51E+00	2.86E-04
Benzaldehyde (C7H6O)	1	kg	5.16E+00	1.10E+02	2.81E-01	4.64E+00	2.33E+00	5.02E-02	1.75E-03	7.68E+01	4.06E-01	5.89E+01	4.15E-03
Benzene (C6H6)	1	kg	1.86E+00	6.76E+01	2.07E-04	1.56E+00	1.56E+00	1.27E-03	1.40E-05	7.03E-01	1.76E-04	2.07E+00	1.10E-03
Bis(trimethylsilyl)amine ([(CH3)3Si]2NH)	1	kg	5.74E+00	1.01E+02	4.98E-01	5.22E+00	2.03E+00	6.16E-02	1.83E-03	8.34E+01	4.31E-01	9.04E+01	1.16E-02
Bromine (Br2)	1	kg	5.02E+00	6.62E+01	1.02E-01	4.72E+00	1.47E+00	3.36E-02	1.20E-03	5.53E+01	2.57E-01	4.15E+01	3.34E-03
Calcium chloride (CaCl2)	1	kg	9.14E-01	1.03E+01	1.19E-01	8.40E-01	2.04E-01	1.51E-02	4.44E-04	1.99E+01	4.76E-02	1.50E+01	1.23E-03
Chlorine (Cl2)	1	kg	2.21E-01	3.02E+00	1.19E-02	2.05E-01	5.96E-02	2.98E-03	1.06E-04	4.56E+00	2.07E-02	3.49E+00	2.34E-04
Chlorobenzene (C6H5Cl)	1	kg	3.24E+00	7.85E+01	1.15E-01	2.76E+00	1.73E+00	1.01E-01	1.33E-03	5.04E+01	1.55E-01	4.10E+01	2.73E-03
Citric acid (C6H8O7)	1	kg	2.85E+00	6.89E+01	1.20E+00	2.56E+00	7.62E-01	5.04E-02	1.37E-03	4.66E+01	4.67E-01	3.76E+01	8.92E-03
Coal	1	kg	2.20E+00	5.75E+01	6.82E+00	7.17E-01	1.76E-01	4.81E-03	9.96E-05	4.25E+00	3.85E-02	4.08E+00	9.02E-04
Coal tar	1	kg	5.11E+02	7.79E+03	2.37E+01	4.59E+02	1.48E+02	1.39E+01	2.87E-01	9.48E+03	6.15E+01	9.83E+03	4.62E-01
Cooling	1	MJ	1.55E-01	2.48E+00	1.82E-03	1.41E-01	5.59E-02	1.24E-03	2.65E-05	1.39E+00	5.35E-03	1.06E+00	5.06E-05
Cullet	1	kg	1.40E-02	1.46E-01	5.89E-04	1.07E-02	2.83E-03	5.99E-04	2.67E-06	2.31E-01	1.27E-03	1.29E+00	3.30E-05
Deionised water	1	kg	1.74E-03	2.40E-02	8.02E-05	1.60E-03	4.61E-04	2.40E-05	8.52E-07	3.19E-02	1.74E-04	2.74E-02	1.72E-06
Diethyl ether ((C2H5)2O)	1	kg	7.01E+00	1.55E+02	4.14E-01	6.39E+00	3.22E+00	1.08E-01	4.09E-03	1.75E+02	7.85E-01	1.27E+02	8.08E-03
Dimethyl sulfate (C2H6O4S)	1	kg	1.36E+00	3.78E+01	8.42E-02	1.22E+00	8.24E-01	2.91E-02	7.86E-04	5.08E+01	1.40E-01	3.16E+01	1.59E-03
Dimethylformamide (C3H7NO, DMF)	1	kg	2.86E+00	7.78E+01	1.16E-01	2.59E+00	1.74E+00	3.64E-02	9.83E-04	5.94E+01	2.56E-01	3.86E+01	1.25E-02
Dioxane (C4H8O2)	1	kg	5.04E+00	1.06E+02	2.29E-01	4.57E+00	2.30E+00	4.35E-02	1.53E-03	6.74E+01	2.97E-01	5.25E+01	3.84E-03
Dolomite	1	kg	4.21E-02	5.16E-01	2.27E-03	3.87E-02	1.03E-02	4.28E-04	1.75E-05	6.16E-01	3.04E-03	5.26E-01	5.39E-05
Electricity	1	kWh	7.10E-01	1.25E+01	8.13E-04	6.70E-01	2.96E-01	2.55E-03	1.24E-05	5.22E+00	4.22E-03	1.57E+00	6.15E-04
Ethanol (C2H6O)	1	kg	1.40E+00	4.16E+01	1.12E+00	1.22E+00	3.43E-01	3.41E-02	5.68E-04	1.67E+01	8.71E-02	1.34E+01	6.24E-03
Ethyl acetate (C4H8O2)	1	kg	2.86E+00	7.37E+01	1.50E-01	2.50E+00	1.64E+00	2.79E-02	1.07E-03	4.50E+01	1.94E-01	3.18E+01	2.30E-03
Ethylene glycol (C2H6O2)	1	kg	1.99E+00	5.39E+01	7.47E-02	1.77E+00	1.17E+00	1.88E-02	6.43E-04	2.79E+01	1.44E-01	2.22E+01	1.53E-03
Ethylenediamine (C2H8N2)	1	kg	6.14E+00	1.19E+02	3.05E-01	5.66E+00	2.44E+00	8.14E-02	2.55E-03	1.17E+02	6.40E-01	9.11E+01	1.74E-02
Ethylenediaminetetraacetic acid (C10H16N2O8, EDTA)	1	kg	4.21E+00	8.17E+01	1.58E-01	3.67E+00	1.74E+00	6.99E-02	1.39E-03	6.65E+01	3.02E-01	4.93E+01	1.38E-02
Ferrous chloride (FeCl2)	1	kg	2.39E-01	3.52E+00	2.60E-02	2.21E-01	6.19E-02	6.28E-03	1.95E-04	1.03E+01	3.24E-02	7.34E+00	2.46E-04
Gold (Au)	1	kg	1.75E+04	2.72E+05	4.00E+02	1.66E+04	5.53E+03	3.19E+04	9.64E+02	7.64E+07	2.59E+03	3.81E+07	1.20E+02
Heat	1	MJ	2.26E-02	1.13E+00	1.12E-01	1.86E-02	6.38E-03	4.35E-04	1.04E-05	5.32E-01	1.83E-03	3.53E-01	1.23E-04
Hexanes (C6H14)	1	kg	6.10E-01	2.40E+01	3.95E-02	5.72E-01	5.49E-01	8.33E-03	2.19E-04	1.46E+01	1.10E-01	9.52E+00	5.52E-04
Hydrochloric acid (HCl, 30%)	1	kg	1.72E+00	2.49E+01	1.01E-01	1.58E+00	4.79E-01	2.67E-02	9.55E-04	4.05E+01	1.75E-01	3.11E+01	1.73E-03
Hydrogen (H2)	1	kg	2.04E+01	2.80E+02	1.10E+00	1.88E+01	5.32E+00	2.95E-01	1.10E-02	4.28E+02	2.14E+00	3.41E+02	2.08E-02
Hydrogen fluoride (HF)	1	kg	3.50E+00	7.43E+01	2.67E-01	3.24E+00	1.51E+00	8.13E-02	2.59E-03	1.43E+02	4.99E-01	9.71E+01	5.45E-03
Hydrogen peroxide (H2O2, 50%)	1	kg	1.25E+00	2.01E+01	5.41E-02	1.11E+00	4.27E-01	3.01E-02	4.49E-04	2.17E+01	7.61E-02	5.02E+01	1.15E-03
Hydrogen sulfide (H2S)	1	kg	4.69E-01	9.75E+00	2.92E-02	4.14E-01	2.05E-01	7.61E-03	2.44E-04	1.22E+01	3.61E-02	8.90E+00	4.08E-04
Incineration of average residue	1	kg	3.69E-01	2.37E+00	6.09E-03	3.59E-01	5.20E-02	1.22E-01	1.86E-03	1.14E+02	1.05E-02	9.15E+01	2.90E-04
Indium (In)	1	kg	2.19E+02	2.55E+03	7.48E+00	2.00E+02	5.18E+01	8.59E+00	2.56E-01	1.82E+04	8.06E+00	1.05E+04	3.69E-01
Iodine (I2)	1	kg	5.01E+00	6.58E+01	1.01E-01	4.71E+00	1.46E+00	3.32E-02	1.18E-03	5.45E+01	2.55E-01	4.09E+01	3.32E-03

Isopropyl alcohol (C3H8O)	**1**	**kg**	1.83E+00	6.04E+01	3.67E-02	1.59E+00	1.38E+00	9.28E-03	2.63E-04	1.53E+01	3.69E-02	1.14E+01	1.12E-03
Lanthanum oxide (La2O3)	**1**	**kg**	1.86E+01	3.89E+02	1.13E+00	1.72E+01	8.46E+00	4.60E-01	8.02E-03	4.51E+02	1.59E+00	2.99E+02	1.52E-02
Lead (Pb)	**1**	**kg**	1.67E+00	1.67E+01	1.18E-01	1.55E+00	3.46E-01	1.17E-01	3.40E-03	3.70E+02	7.03E-02	1.38E+02	4.01E-03
Li (Lithium)	**1**	**kg**	5.99E+01	8.19E+02	3.86E+00	5.57E+01	1.53E+01	8.46E-01	3.67E-02	1.20E+03	6.79E+00	9.41E+02	9.32E-02
Limestone	**1**	**kg**	3.10E-03	4.32E-02	6.60E-05	2.82E-03	9.42E-04	1.60E-05	4.67E-07	2.26E-02	2.02E-04	1.84E-02	2.03E-05
Liquid Ammonia (NH3)	**1**	**kg**	1.87E+00	3.78E+01	2.29E-02	1.78E+00	8.84E-01	1.24E-02	1.76E-04	2.23E+01	6.68E-02	1.43E+01	9.04E-04
Lithium carbonate (Li2CO3)	**1**	**kg**	2.54E+00	3.53E+01	2.52E-01	2.37E+00	7.11E-01	4.08E-02	2.27E-03	5.76E+01	2.07E-01	4.16E+01	9.00E-03
Magnesium (Mg)	**1**	**kg**	1.68E+01	2.77E+02	7.55E-02	1.51E+01	6.47E+00	3.48E-02	8.59E-04	5.24E+01	2.67E-01	3.24E+01	4.85E-03
Mercury (Hg)	**1**	**kg**	1.66E+01	1.51E+02	1.60E+00	1.52E+01	3.27E+00	1.93E+00	4.50E-03	1.97E+05	2.10E-01	1.17E+04	1.38E-02
Methane (CH4)	**1**	**kg**	3.50E+00	2.89E+01	2.62E-01	2.13E+00	5.15E-01	1.56E-01	4.39E-03	5.27E+01	2.28E-01	7.19E+01	3.78E-03
Methanol (CH3OH)	**1**	**kg**	6.93E-01	6.96E+01	8.08E+00	6.39E-01	2.08E-01	1.37E-02	4.67E-04	2.28E+01	7.82E-02	1.34E+01	1.13E-03
Methylamine (CH5N)	**1**	**kg**	2.56E+00	6.86E+01	6.12E-02	2.33E+00	1.58E+00	2.78E-02	5.58E-04	4.79E+01	1.25E-01	2.83E+01	3.94E-03
n-Butanol (C4H10O)	**1**	**kg**	3.14E+00	8.37E+01	1.27E-01	2.76E+00	1.88E+00	2.28E-02	8.21E-04	3.56E+01	1.80E-01	2.80E+01	2.37E-03
Nickel (II) sulfate (NiSO4)	**1**	**kg**	5.18E+00	7.38E+01	3.23E-01	4.82E+00	1.36E+00	8.87E-01	1.30E-02	9.65E+02	4.30E-01	1.04E+03	1.20E-02
Nitric acid (HNO3, 50%)	**1**	**kg**	2.91E+00	1.30E+01	2.51E-02	1.94E+00	2.97E-01	7.93E-03	1.65E-04	1.41E+01	3.65E-02	9.83E+00	2.62E-03
Nitrogen (N2)	**1**	**kg**	4.70E-01	6.40E+00	1.85E-02	4.34E-01	1.23E-01	5.67E-03	2.30E-04	7.67E+00	4.77E-02	6.56E+00	4.29E-04
Oxygen (O2)	**1**	**kg**	1.18E+00	1.61E+01	4.66E-02	1.09E+00	3.09E-01	1.43E-02	5.81E-04	1.93E+01	1.20E-01	1.65E+01	1.08E-03
Palladium (Pd)	**1**	**kg**	4.05E+03	6.56E+04	1.28E+02	3.75E+03	1.27E+03	4.49E+02	3.06E+00	1.82E+05	6.64E+02	4.97E+05	3.61E+00
Phenol (C6H5OH)	**1**	**kg**	4.60E+00	1.20E+02	1.11E-01	3.95E+00	2.69E+00	3.75E-02	1.37E-03	5.22E+01	1.68E-01	4.31E+01	3.24E-03
Phosphorus trichloride (PCl3)	**1**	**kg**	4.53E+00	6.96E+01	2.77E-01	3.91E+00	1.29E+00	7.51E-02	2.62E-03	8.89E+01	6.85E-01	7.29E+01	4.70E-03
Potassium hydroxide (KOH)	**1**	**kg**	2.36E+00	3.21E+01	1.30E-01	2.18E+00	6.42E-01	2.97E-02	1.09E-03	4.49E+01	1.84E-01	3.52E+01	2.13E-03
Potassium iodate (KIO3)	**1**	**kg**	4.94E+00	6.67E+01	2.19E-01	4.52E+00	1.27E+00	8.41E-02	2.50E-03	9.09E+01	5.01E-01	1.16E+02	4.84E-03
Potassium iodide (KI)	**1**	**kg**	5.32E-01	9.49E+00	3.94E-02	4.86E-01	1.94E-01	8.79E-03	2.28E-04	1.47E+01	3.17E-02	9.99E+00	4.67E-04
Silica sand	**1**	**kg**	3.92E-02	4.34E-01	2.80E-03	3.63E-02	9.46E-03	2.39E-04	1.01E-05	4.00E-01	1.45E-03	3.43E-01	5.04E-05
Sodium (Na)	**1**	**kg**	2.02E+00	2.76E+01	1.09E-01	1.88E+00	5.45E-01	2.72E-02	9.65E-04	4.17E+01	1.89E-01	3.19E+01	2.14E-03
Sodium carbonate (Na2CO3)	**1**	**kg**	6.00E-01	6.79E+00	7.83E-02	5.51E-01	1.34E-01	9.89E-03	2.91E-04	1.31E+01	3.12E-02	9.84E+00	8.06E-04
Sodium chloride (NaCl)	**1**	**kg**	2.63E-01	3.39E+00	2.68E-02	2.43E-01	6.36E-02	6.14E-03	1.95E-04	1.02E+01	2.33E-02	7.23E+00	3.63E-04
Sodium hydroxide (NaOH, 50%)	**1**	**kg**	1.45E+00	2.00E+01	7.82E-02	1.34E+00	3.79E-01	2.10E-02	7.82E-04	3.05E+01	1.52E-01	2.43E+01	1.48E-03
Sodium methoxide (CH3ONa)	**1**	**kg**	1.86E+00	4.22E+01	1.01E-01	1.68E+00	8.81E-01	3.00E-02	9.24E-04	4.69E+01	2.08E-01	3.18E+01	1.80E-03
Sodium nitrite (NaNO2)	**1**	**kg**	3.05E+00	4.78E+01	1.56E-01	2.85E+00	9.37E-01	3.92E-02	1.36E-03	5.90E+01	3.62E-01	4.62E+01	5.20E-03
Sulfur dioxide (SO2)	**1**	**kg**	4.94E-01	2.06E+01	3.02E-02	4.54E-01	4.64E-01	8.42E-03	2.58E-04	1.37E+01	9.51E-02	9.61E+00	5.55E-04
Sulfuric acid (H2SO4)	**1**	**kg**	1.14E-01	6.97E+00	1.26E-02	1.04E-01	1.59E-01	3.39E-03	8.21E-05	5.73E+00	2.96E-02	4.08E+00	3.46E-04
Sulfuryl chloride (SO2Cl2)	**1**	**kg**	1.62E+00	3.85E+01	1.13E-01	1.50E+00	7.85E-01	2.82E-02	9.49E-04	4.37E+01	2.67E-01	3.22E+01	1.69E-03
tert-Butyl alcohol (C4H10O)	**1**	**kg**	3.40E+00	8.11E+01	2.15E-01	3.07E+00	1.85E+00	2.24E-02	8.06E-04	4.02E+01	6.85E-02	2.91E+01	2.62E-03
Tetrahydrofuran (C4H8O)	**1**	**kg**	6.71E+00	1.17E+02	4.64E-01	6.12E+00	2.45E+00	7.60E-02	2.57E-03	1.19E+02	4.72E-01	8.67E+01	5.83E-03
Tetramethylethylenediamine (C6H16N2, TMEDA)	**1**	**kg**	6.14E+00	1.19E+02	3.05E-01	5.66E+00	2.44E+00	8.14E-02	2.55E-03	1.17E+02	6.40E-01	9.11E+01	1.74E-02
Tin (Sn)	**1**	**kg**	2.41E+01	3.19E+02	8.40E-01	2.23E+01	6.41E+00	2.44E-01	9.44E-03	3.42E+02	2.07E+00	2.82E+02	6.04E-02
Titanium dioxide (TiO2)	**1**	**kg**	8.60E+00	9.22E+01	3.68E-01	7.43E+00	1.83E+00	1.32E-01	3.41E-03	1.21E+02	4.63E-01	1.52E+02	7.91E-03
Titanium tetrachloride (TiCl4)	**1**	**kg**	3.34E+00	3.60E+01	1.39E-01	2.67E+00	7.19E-01	4.61E-02	1.55E-03	5.43E+01	2.29E-01	6.06E+01	3.12E-03
Toluene (C7H8)	**1**	**kg**	1.56E+00	6.34E+01	1.57E-04	1.28E+00	1.47E+00	8.85E-04	1.03E-05	5.14E-01	1.32E-04	1.32E+00	8.13E-04
Treatment of wastewater	**1**	**t**	2.48E+00	2.07E+01	8.89E-02	2.26E+00	3.91E-01	3.46E-02	1.41E-02	3.20E+01	1.59E-01	3.11E+01	1.30E-01
Trimethyl borate (C3H9BO3)	**1**	**kg**	1.64E+00	5.06E+01	5.96E-02	1.45E+00	1.16E+00	2.65E-02	5.90E-04	4.76E+01	9.60E-02	2.62E+01	2.15E-03
Urea (CH4N2O)	**1**	**kg**	3.32E+00	6.06E+01	7.99E-02	3.13E+00	1.39E+00	2.89E-02	6.03E-04	5.00E+01	1.63E-01	3.55E+01	2.52E-03
Xylene (C8H10)	**1**	**kg**	1.70E+00	6.58E+01	1.81E-04	1.41E+00	1.52E+00	1.38E-03	1.37E-05	6.98E-01	1.59E-04	2.65E+00	9.28E-04
Zinc (Zn)	**1**	**kg**	5.09E+00	5.86E+01	1.71E-01	4.63E+00	1.19E+00	1.92E-01	5.69E-03	4.06E+02	1.72E-01	2.36E+02	8.68E-03

Table S35. Characterization factors extracted from Ecoinvent database (Part II).

item	**ReCiPe Midpoint (E)**									**ReCiPe Endpoint (E,A)**		
	metal depletion	**natural land transformation**	**ozone depletion**	**particulate matter formation**	**photochemical oxidant formation**	**terrestrial acidification**	**terrestrial ecotoxicity**	**urban land occupation**	**water depletion**	**ecosystem quality**	**human health**	**resources**
1-Bromo-4-iodobenzene (BrC6H4I)	1.29E-01	2.65E-04	8.50E-07	8.13E-03	1.80E-02	1.41E-02	2.07E-03	2.55E-02	8.44E-03	1.18E-01	4.53E-01	1.79E-01
2,4,6-Trimethylaniline (C9H13N)	2.55E-01	5.47E-04	3.05E-07	1.09E-02	1.96E-02	3.00E-02	3.43E-03	3.60E-02	7.55E-03	1.70E-01	6.49E-01	2.66E-01
2-Methoxyethanol (C3H8O2)	1.03E-01	1.68E-04	7.69E-08	3.91E-03	8.06E-03	8.48E-03	9.78E-04	1.22E-02	4.41E-03	7.97E-02	2.69E-01	1.80E-01
4-tert-Butylpyridine (C9H13N)	6.75E-01	1.49E-03	2.81E-06	2.87E-02	3.17E-02	5.62E-02	1.04E-02	9.08E-02	3.26E-02	4.59E-01	1.89E+00	4.79E-01
Acetic acid (CH3COOH, 98%)	1.03E-01	7.77E-04	3.63E-07	5.14E-03	7.19E-03	1.08E-02	1.31E-03	1.43E-02	5.93E-03	7.40E-02	3.35E-01	1.40E-01
Acetic anhydride (C4H6O3)	1.82E-01	1.18E-03	5.41E-07	8.34E-03	1.23E-02	1.96E-02	2.55E-03	2.86E-02	1.11E-02	1.53E-01	5.89E-01	2.15E-01
Acetone (C3H6O)	1.24E-03	-1.88E-07	9.56E-10	2.80E-03	9.06E-03	1.02E-02	1.79E-04	1.65E-04	1.38E-04	5.34E-02	8.31E-02	1.85E-01
Acetonitrile (C2H3N)	1.08E-01	4.15E-04	1.99E-07	6.24E-03	9.43E-03	2.64E-02	2.46E-03	9.83E-03	9.46E-03	1.23E-01	3.39E-01	3.09E-01
Alumina (Al2O3)	6.99E-02	1.51E-04	1.49E-07	3.09E-03	4.18E-03	4.18E-03	1.16E-03	1.16E-03	1.91E-03	5.97E-02	3.35E-01	4.46E-02
Aluminium (Al)	2.66E-01	1.65E-03	7.15E-07	5.55E-02	7.19E-02	1.32E-01	6.21E-03	1.95E-01	6.61E-02	1.02E+00	3.02E+00	6.73E-01

Aniline (C6H5NH2)	2.55E-01	5.47E-04	3.05E-07	1.09E-02	1.96E-02	3.00E-02	3.43E-03	3.60E-02	7.55E-03	1.70E-01	6.49E-01	2.66E-01
Argon (Ar)	3.24E-02	2.95E-04	1.49E-07	8.33E-03	6.63E-03	1.31E-02	8.99E-04	1.60E-02	1.05E-02	1.06E-01	4.25E-01	8.71E-02
Barite (BaSO4)	8.77E-03	3.69E-05	1.49E-08	9.88E-04	7.96E-04	1.50E-03	1.31E-04	2.32E-03	1.19E-03	1.24E-02	5.00E-02	9.52E-03
Benzaldehyde (C7H6O)	2.46E-01	4.98E-04	1.18E-06	1.00E-02	1.58E-02	2.21E-02	4.78E-03	3.66E-02	1.09E-02	1.93E-01	7.06E-01	2.90E-01
Benzene (C6H6)	1.03E-03	-2.15E-07	5.38E-10	1.79E-03	5.67E-03	6.23E-03	5.02E-04	1.04E-04	1.56E-04	4.32E-02	6.43E-02	1.87E-01
Bis(trimethylsilyl)amine ([(CH3)3Si]2NH)	3.77E-01	8.64E-04	3.94E-06	1.30E-02	1.72E-02	2.97E-02	4.11E-03	5.03E-02	1.70E-02	2.27E-01	7.81E-01	2.61E-01
Bromine (Br2)	1.17E-01	1.03E-03	8.04E-07	8.44E-03	1.07E-02	2.25E-02	7.13E-03	2.54E-02	8.82E-03	1.79E-01	5.55E-01	1.82E-01
Calcium chloride (CaCl2)	7.90E-02	9.69E-05	4.39E-08	2.63E-03	2.78E-03	9.26E-03	8.81E-04	1.14E-02	1.85E-03	4.25E-02	1.69E-01	2.81E-02
Chlorine (Cl2)	1.46E-02	3.58E-05	1.57E-08	6.12E-04	6.10E-04	1.15E-03	2.34E-04	2.27E-03	6.57E-04	9.67E-03	3.96E-02	7.83E-03
Chlorobenzene (C6H5Cl)	1.33E-01	2.54E-04	7.11E-07	8.27E-03	2.19E-02	1.48E-02	1.90E-03	2.70E-02	8.47E-03	1.23E-01	4.60E-01	2.14E-01
Citric acid (C6H8O7)	1.59E-01	1.07E-03	3.30E-07	6.25E-03	7.71E-03	2.35E-02	7.26E-03	5.98E-02	3.76E-01	3.56E-01	4.20E-01	9.88E-02
Coal	2.10E-02	1.80E-04	7.37E-08	1.66E-03	1.81E-02	2.84E-03	7.21E-04	9.00E-02	8.79E-04	1.91E-01	5.71E-02	2.21E-02
Coal tar	2.47E+01	5.57E-02	3.09E-05	3.45E+00	1.71E+00	2.49E+00	3.01E-01	4.41E+00	1.90E+00	2.17E+01	8.91E+01	1.89E+01
Cooling	5.85E-03	2.37E-05	1.75E-08	1.52E-04	2.24E-04	3.47E-04	4.56E-05	3.15E-04	1.69E-03	4.63E-03	1.47E-02	6.98E-03
Cullet	8.26E-04	-3.44E-07	1.52E-09	2.42E-05	4.41E-05	4.87E-05	2.98E-05	5.49E-04	4.11E-05	9.36E-04	1.99E-03	3.78E-04
Deionised water	1.15E-04	2.21E-07	7.30E-10	5.70E-06	4.90E-06	8.82E-06	1.43E-06	1.53E-05	1.31E-03	7.51E-05	2.87E-04	6.06E-05
Diethyl ether ((C2H5)2O)	5.96E-01	1.30E-03	2.74E-06	2.29E-02	3.04E-02	5.68E-02	7.27E-03	7.83E-02	2.31E-02	3.06E-01	1.48E+00	4.13E-01
Dimethyl sulfate (C2H6O4S)	1.93E-01	4.89E-04	2.27E-07	5.20E-03	6.01E-03	1.54E-02	1.71E-03	1.89E-02	5.16E-03	6.65E-02	4.04E-01	1.08E-01
Dimethylformamide (C3H7NO, DMF)	1.67E-01	1.09E-03	5.20E-07	7.22E-03	8.76E-03	1.84E-02	1.84E-02	2.21E-02	7.74E-03	1.15E-01	5.12E-01	2.17E-01
Dioxane (C4H8O2)	2.03E-01	4.76E-04	1.94E-07	9.72E-03	1.41E-02	2.15E-02	2.36E-03	3.14E-02	1.00E-02	1.84E-01	6.39E-01	2.85E-01
Dolomite	1.35E-03	4.66E-06	1.83E-09	1.90E-04	1.59E-04	2.65E-04	1.67E-05	3.51E-04	1.45E-04	1.63E-03	5.97E-03	1.30E-03
Electricity	3.00E-03	1.10E-04	5.93E-08	7.49E-04	2.01E-03	2.90E-03	5.19E-05	3.20E-04	8.02E-05	1.96E-02	6.05E-02	3.56E-02
Ethanol (C2H6O)	5.45E-02	1.05E-03	8.90E-08	3.92E-03	4.11E-03	1.29E-02	8.21E-03	5.98E-02	3.74E-01	3.41E-01	1.65E-01	4.36E-02
Ethyl acetate (C4H8O2)	1.45E-01	7.19E-04	3.25E-07	5.73E-03	1.19E-02	1.47E-02	1.84E-03	2.12E-02	6.99E-03	1.07E-01	4.05E-01	2.04E-01
Ethylene glycol (C2H6O2)	9.64E-02	1.39E-04	6.81E-08	3.89E-03	6.08E-03	7.62E-03	8.88E-04	1.11E-02	4.06E-03	7.10E-02	2.61E-01	1.45E-01
Ethylenediamine (C2H8N2)	3.77E-01	9.63E-04	2.23E-06	1.53E-02	1.69E-02	3.31E-02	3.92E-02	5.19E-02	1.59E-02	2.58E-01	1.03E+00	3.10E-01
Ethylenediaminetetraacetic acid (C10H16N2O8, EDTA)	2.23E-01	5.78E-04	8.81E-07	8.65E-03	1.14E-02	2.04E-02	9.15E-03	2.94E-02	1.01E-02	1.54E-01	6.02E-01	2.19E-01
Ferrous chloride (FeCl2)	5.01E-02	3.83E-05	1.85E-08	8.08E-04	6.83E-04	1.41E-03	3.20E-04	3.32E-03	9.59E-04	1.39E-02	7.99E-02	9.75E-03
Gold (Au)	7.99E+04	1.13E+01	2.45E-03	8.88E+01	2.20E+02	2.04E+02	3.01E+01	2.56E+03	2.17E+02	1.17E+04	5.23E+05	4.37E+03
Heat	1.18E-03	6.10E-06	1.77E-09	2.40E-04	4.16E-04	3.10E-04	7.43E-05	1.75E-03	5.75E-05	3.97E-03	4.55E-03	8.19E-04
Hexanes (C6H14)	7.44E-02	5.55E-04	2.67E-07	1.33E-03	6.61E-03	3.60E-03	6.29E-04	6.29E-04	1.30E-03	3.00E-02	1.22E-01	6.93E-02
Hydrochloric acid (HCl, 30%)	1.19E-01	2.18E-04	7.36E-07	5.62E-03	4.71E-03	9.00E-03	2.18E-03	1.60E-02	6.08E-03	7.61E-02	3.45E-01	6.30E-02
Hydrogen (H2)	9.98E-01	2.59E-03	1.05E-05	6.76E-02	5.54E-02	1.07E-01	1.23E-02	1.78E-01	7.34E-02	8.83E-01	3.74E+00	6.84E-01
Hydrogen fluoride (HF)	5.39E-01	1.14E-03	5.32E-07	1.78E-02	1.81E-02	5.23E-02	4.78E-03	5.01E-02	1.41E-02	1.81E-01	1.14E+00	2.07E-01
Hydrogen peroxide (H2O2, 50%)	7.88E-02	1.79E-04	9.89E-08	2.81E-03	3.48E-03	5.44E-03	6.23E-04	7.73E-03	5.28E-03	5.51E-02	1.93E-01	5.48E-02
Hydrogen sulfide (H2S)	5.29E-02	5.14E-05	4.50E-08	1.29E-03	1.29E-03	2.21E-03	3.72E-04	4.12E-03	1.35E-03	2.08E-02	1.01E-01	2.70E-02
Incineration of average residue	5.65E-03	-8.05E-05	1.85E-08	4.20E-04	8.72E-04	9.91E-04	1.28E-03	1.26E-02	4.77E-04	3.45E-02	7.91E-01	6.50E-03
Indium (In)	1.18E+02	3.00E-02	8.76E-06	8.53E-01	1.14E+00	2.22E+00	2.85E+00	2.41E+00	3.02E+00	1.37E+01	1.33E+02	1.17E+01
Iodine (I2)	1.13E-01	1.02E-03	8.01E-07	8.35E-03	1.06E-02	2.21E-02	7.09E-03	2.51E-02	8.77E-03	1.79E-01	5.49E-01	1.81E-01
Isopropyl alcohol (C3H8O)	6.46E-02	1.47E-04	6.47E-08	2.41E-03	7.86E-03	6.76E-03	5.24E-04	5.21E-03	4.23E-03	5.49E-02	1.66E-01	1.69E-01
Lanthanum oxide (La2O3)	1.59E+00	6.31E-03	4.23E-06	5.58E-02	5.20E-02	8.89E-02	6.42E-02	1.60E-01	6.94E-02	8.09E-01	3.81E+00	1.09E+00
Lead (Pb)	1.89E+00	2.20E-04	8.35E-08	1.03E-02	1.26E-02	3.83E-02	3.00E-03	2.33E-02	1.88E-02	1.17E-01	2.60E+00	1.29E-01
Li (Lithium)	2.84E+00	9.15E-03	7.41E-06	1.76E-01	1.72E-01	3.33E-01	4.65E-02	1.18E+00	1.92E-01	3.58E+00	1.05E+01	1.97E+00
Limestone	1.66E-04	9.32E-07	4.14E-10	7.47E-05	6.08E-05	5.58E-05	1.55E-06	9.91E-05	1.92E-04	1.06E-04	4.40E-04	1.21E-04
Liquid Ammonia (NH3)	7.00E-02	5.07E-04	2.54E-07	2.40E-03	3.36E-03	7.43E-03	2.57E-03	4.48E-03	9.70E-04	6.14E-02	2.19E-01	1.09E-01
Lithium carbonate (Li2CO3)	1.96E-01	7.00E-04	2.54E-07	7.42E-03	1.10E-02	2.05E-02	3.38E-03	1.44E-01	5.91E-03	2.89E-01	4.90E-01	9.44E-02
Magnesium (Mg)	1.39E-01	2.85E-03	2.10E-06	9.15E-03	2.36E-02	2.94E-02	1.26E-03	2.97E-02	4.68E-02	4.90E-01	8.99E-01	7.82E-01
Mercury (Hg)	6.91E-02	1.05E-03	3.32E-07	3.33E-02	4.39E-02	1.05E-01	2.73E+02	1.15E-01	1.72E-02	6.35E+01	1.35E+03	3.95E-01
Methane (CH4)	1.18E-01	5.49E-04	1.41E-07	6.33E-03	8.23E-03	1.39E-02	2.71E-03	2.70E-02	1.58E-02	1.11E-01	4.48E-01	6.73E-02
Methanol (CH3OH)	4.43E-02	1.83E-04	7.24E-08	2.38E-03	3.64E-03	4.22E-03	1.09E-03	5.58E-02	4.68E-03	2.28E-01	1.71E-01	2.70E-02
Methylamine (CH5N)	1.31E-01	8.45E-04	4.05E-07	5.53E-03	7.18E-03	1.83E-02	3.03E-03	1.48E-02	4.99E-03	9.38E-02	4.21E-01	1.96E-01
n-Butanol (C4H10O)	8.19E-02	6.04E-04	2.82E-07	6.31E-03	1.15E-02	1.44E-02	1.06E-03	1.54E-02	6.82E-03	1.09E-01	3.52E-01	2.29E-01
Nickel (II) sulfate (NiSO4)	1.52E+01	9.62E-04	4.58E-07	2.20E-01	1.10E-01	1.02E+00	3.20E-02	1.15E-01	8.81E-02	5.92E-01	7.31E+00	7.89E-01
Nitric acid (HNO3, 50%)	6.93E-02	2.06E-04	1.02E-07	3.06E-03	6.21E-03	1.40E-02	1.38E-03	4.50E-03	6.77E-04	6.33E-02	1.70E-01	3.89E-02
Nitrogen (N2)	4.80E-03	5.10E-05	2.13E-08	1.58E-03	1.19E-03	2.32E-03	1.49E-04	2.83E-03	1.72E-03	1.80E-02	7.13E-02	1.49E-02
Oxygen (O2)	1.21E-02	1.28E-04	5.37E-08	3.99E-03	2.99E-03	5.85E-03	3.75E-04	7.12E-03	4.34E-03	4.53E-02	1.80E-01	3.77E-02
Palladium (Pd)	2.57E+04	4.73E-01	3.55E-04	6.59E+02	2.73E+02	3.26E+03	9.86E+00	7.11E+01	1.21E+02	3.63E+02	3.04E+03	1.18E+03
Phenol (C6H5OH)	1.39E-01	3.02E-04	1.74E-07	9.13E-03	2.15E-02	1.73E-02	1.80E-03	2.92E-02	8.18E-03	1.58E-01	5.17E-01	3.29E-01
Phosphorus trichloride (PCl3)	1.65E-01	9.52E-04	7.91E-07	1.57E-02	1.51E-02	2.32E-02	4.38E-03	1.01E-01	2.93E-02	1.92E-01	7.80E-01	1.62E-01
Potassium hydroxide (KOH)	1.09E-01	1.91E-04	1.32E-07	6.81E-03	6.22E-03	1.22E-02	1.28E-03	2.97E-02	1.13E-02	9.97E-02	3.97E-01	8.20E-02
Potassium iodate (KIO3)	1.34E-01	5.50E-04	2.64E-07	1.64E-02	1.26E-02	2.46E-02	2.09E-03	3.41E-02	1.79E-02	2.04E-01	8.17E-01	1.59E-01
Potassium iodide (KI)	8.78E-02	-1.56E-04	8.05E-08	9.99E-04	1.57E-03	2.30E-03	6.27E-04	2.96E-02	4.47E-03	2.77E-02	1.19E-01	2.73E-02
Silica sand	9.57E-04	1.25E-05	2.32E-09	9.18E-05	1.58E-04	2.58E-04	4.66E-05	1.08E-03	6.10E-05	5.82E-03	4.10E-03	1.18E-03
Sodium (Na)	1.34E-01	3.27E-04	1.43E-07	5.59E-03	5.58E-03	1.05E-02	2.14E-03	2.08E-02	6.00E-03	8.83E-02	3.62E-01	7.15E-02

Sodium carbonate (Na2CO3)	5.19E-02	6.36E-05	2.88E-08	1.72E-03	1.83E-03	6.08E-03	5.78E-04	7.49E-03	1.22E-03	2.79E-02	1.11E-01	1.85E-02
Sodium chloride (NaCl)	5.09E-02	3.91E-05	1.80E-08	8.40E-04	7.48E-04	1.57E-03	3.40E-04	3.75E-03	8.94E-04	1.48E-02	8.00E-02	9.99E-03
Sodium hydroxide (NaOH, 50%)	7.12E-02	1.85E-04	7.45E-07	4.82E-03	3.95E-03	7.60E-03	8.78E-04	1.27E-02	5.23E-03	6.29E-02	2.66E-01	4.88E-02
Sodium methoxide (CH3ONa)	1.30E-01	4.32E-04	7.27E-07	5.39E-03	5.90E-03	1.12E-02	1.60E-03	1.84E-02	6.77E-03	8.05E-02	3.91E-01	1.12E-01
Sodium nitrite (NaNO2)	1.73E-01	5.63E-04	7.02E-07	8.12E-03	9.29E-03	1.77E-02	3.56E-03	2.52E-02	8.68E-03	1.27E-01	5.20E-01	1.20E-01
Sulfur dioxide (SO2)	5.49E-02	3.99E-04	1.87E-07	1.10E-02	5.73E-03	5.04E-02	4.64E-04	5.56E-03	1.66E-03	2.58E-02	1.55E-01	5.82E-02
Sulfuric acid (H2SO4)	3.30E-02	1.49E-04	7.08E-08	1.67E-03	1.54E-03	7.24E-03	2.20E-04	2.21E-03	3.73E-04	7.95E-03	4.92E-02	2.06E-02
Sulfuryl chloride (SO2Cl2)	1.55E-01	5.77E-04	6.52E-07	1.51E-02	9.11E-03	6.02E-02	2.14E-03	1.72E-02	6.05E-03	7.82E-02	4.07E-01	1.01E-01
tert-Butyl alcohol (C4H10O)	7.02E-02	4.26E-04	1.70E-07	6.57E-03	1.26E-02	1.99E-02	1.30E-03	1.92E-02	5.63E-03	1.21E-01	3.90E-01	2.26E-01
Tetrahydrofuran (C4H8O)	2.77E-01	1.15E-03	5.37E-07	1.72E-02	2.08E-02	3.74E-02	4.96E-03	5.21E-02	2.09E-02	2.68E-01	1.06E+00	3.07E-01
Tetramethylethylenediamine (C6H16N2, TMEDA)	3.77E-01	9.63E-04	2.23E-06	1.53E-02	1.69E-02	3.31E-02	3.92E-02	5.19E-02	1.59E-02	2.58E-01	1.03E+00	3.10E-01
Tin (Sn)	1.49E+03	8.65E-02	1.55E-06	3.31E-01	1.98E-01	4.89E-01	8.19E-03	1.31E+00	7.27E-02	7.41E+00	3.93E+00	6.98E+01
Titanium dioxide (TiO2)	2.30E-01	1.72E-03	7.61E-07	1.98E-02	2.91E-02	4.11E-02	4.33E-03	1.13E-01	7.90E-02	3.28E-01	1.12E+00	2.52E-01
Titanium tetrachloride (TiCl4)	1.27E-01	9.23E-04	6.41E-07	7.41E-03	1.41E-02	1.55E-02	2.28E-03	6.23E-02	3.21E-02	1.27E-01	4.78E-01	1.07E-01
Toluene (C7H8)	7.43E-04	-1.52E-07	4.16E-10	1.18E-03	4.37E-03	3.75E-03	2.26E-04	7.70E-05	2.15E-04	3.54E-02	5.13E-02	1.77E-01
Treatment of wastewater	1.75E-01	1.82E-04	1.84E-07	5.06E-03	5.95E-03	1.04E-02	1.38E-03	2.34E-02	1.06E-02	1.01E-01	3.07E-01	5.50E-02
Trimethyl borate (C3H9BO3)	1.68E-01	7.40E-04	3.01E-07	6.93E-03	8.25E-03	1.62E-02	1.42E-03	2.40E-02	5.26E-03	5.70E-02	3.93E-01	1.47E-01
Urea (CH4N2O)	1.98E-01	9.40E-04	4.42E-07	7.92E-03	6.93E-03	2.54E-02	5.34E-03	1.60E-02	3.84E-03	1.22E-01	4.69E-01	1.76E-01
Xylene (C8H10)	8.31E-04	-2.45E-07	4.76E-10	1.38E-03	4.80E-03	4.46E-03	9.61E-04	9.86E-05	2.55E-04	3.94E-02	5.76E-02	1.82E-01
Zinc (Zn)	2.73E+00	6.98E-04	2.01E-07	1.98E-02	2.48E-02	5.27E-02	6.91E-02	5.59E-02	7.23E-02	3.19E-01	2.98E+00	2.70E-01

S6. Environmental profile of the metal oxide module, the mixed-cation module, and the SnO_2 module

The environmental profiles of the metal oxide module, the mixed-cation module, and the SnO_2 module in terms of 21 impact categories are shown in Figure S5 to Figure S7.

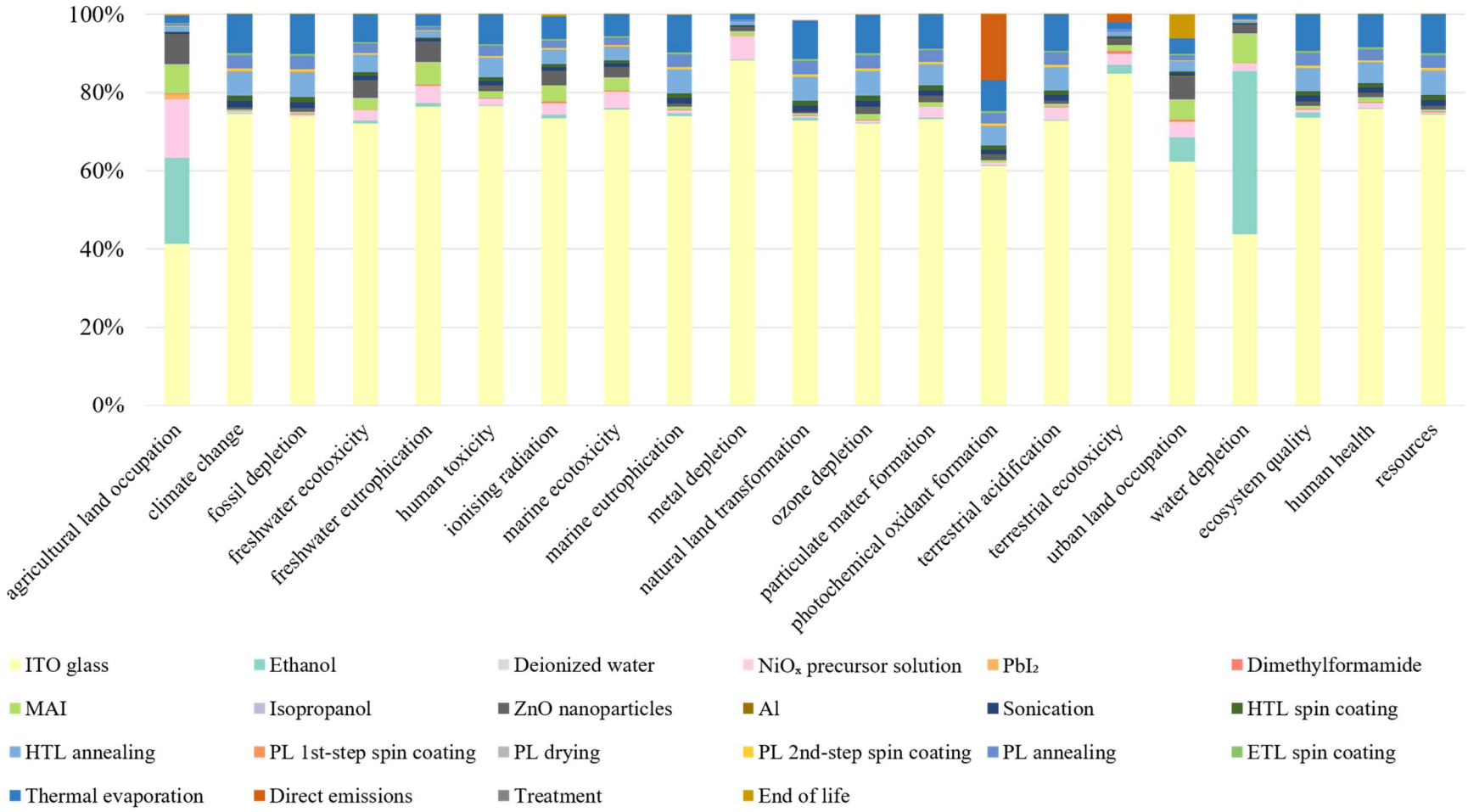

Figure S5. Environmental profile of 1 m^2 of the metal oxide module.

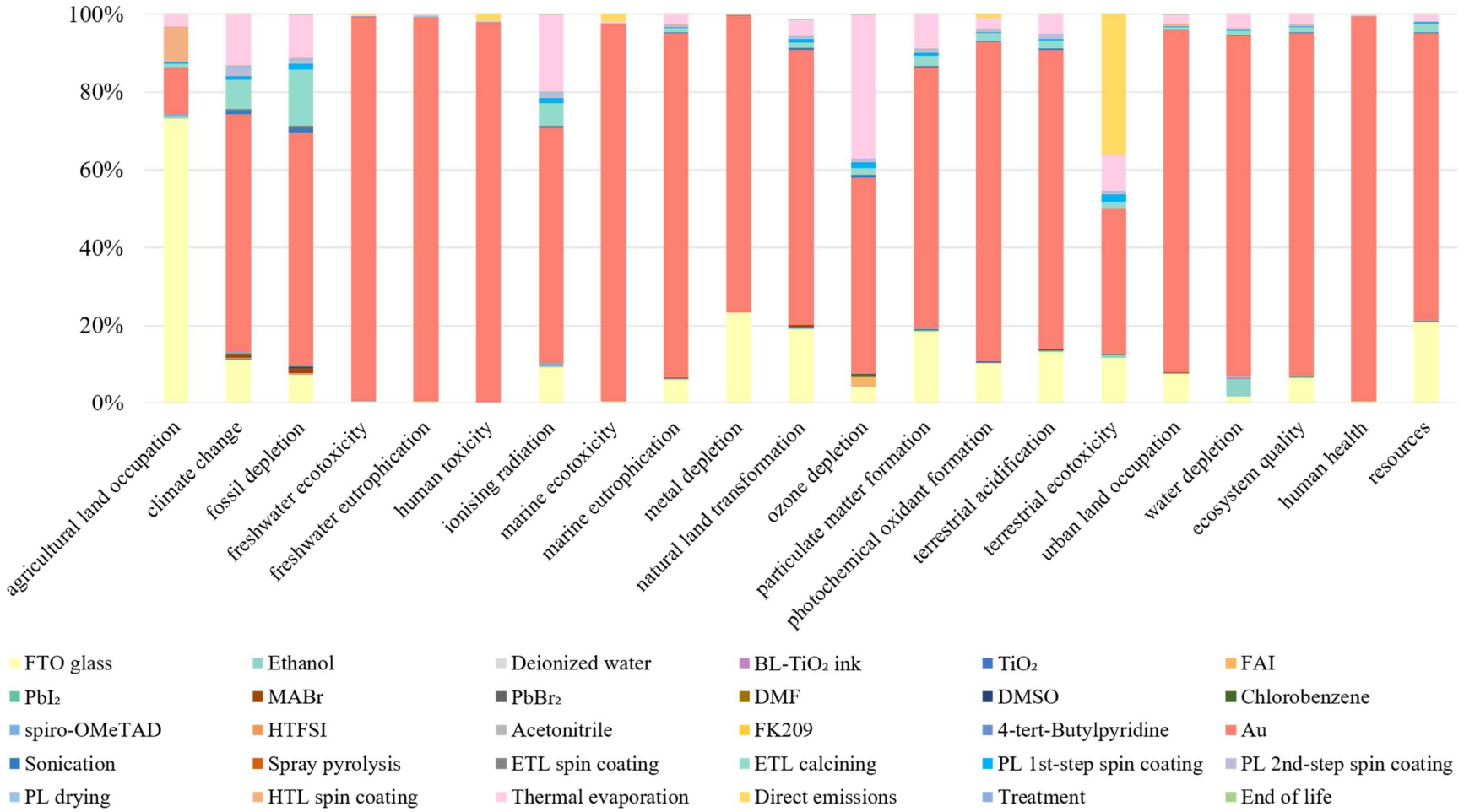

Figure S6. Environmental profile of 1 m^2 of the mixed-cation module.

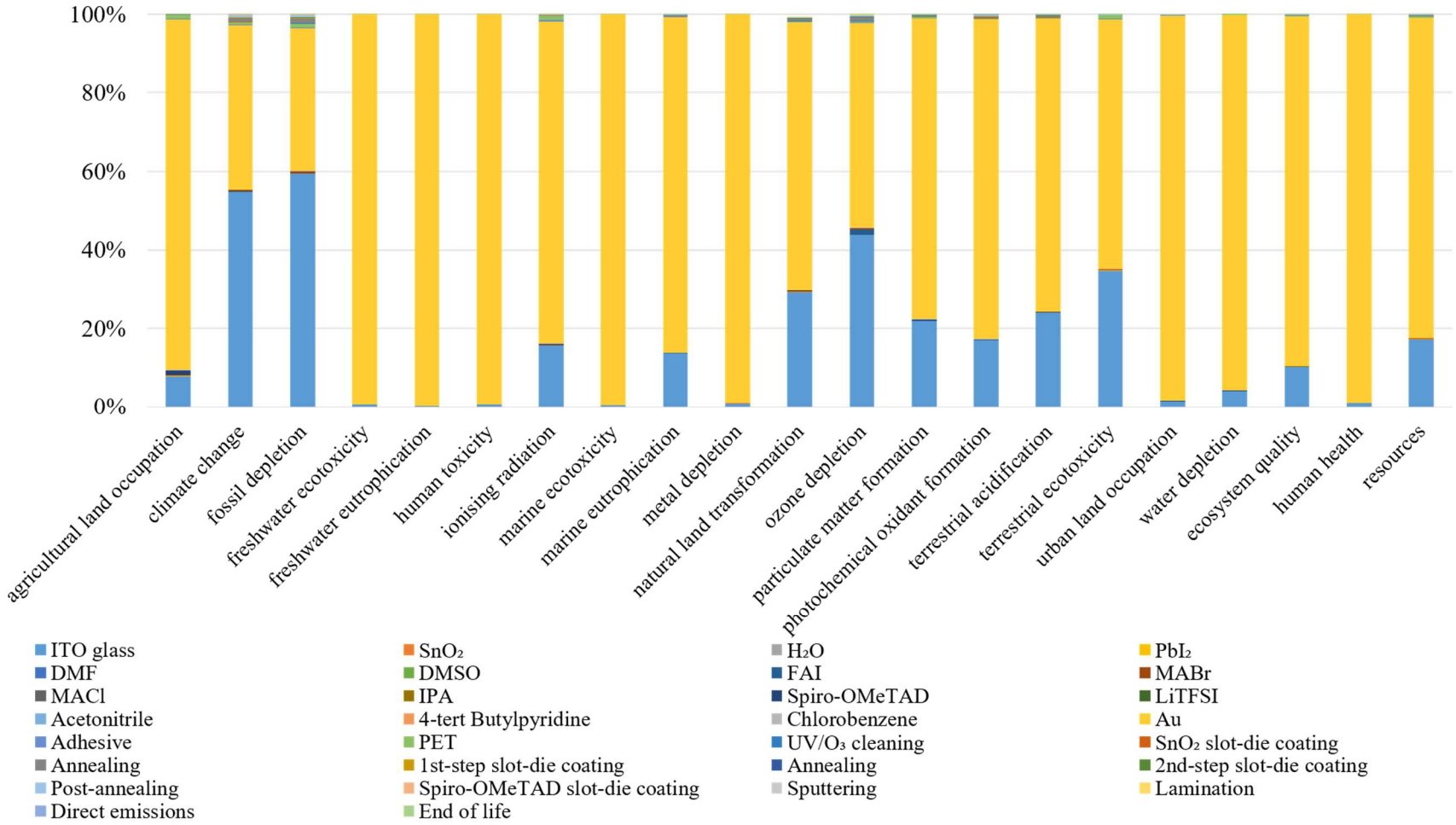

Figure S7. Environmental profile of 1 m^2 of the SnO_2 module.

S7. Primary energy consumption comparison between landfill and recycling end-of-life scenarios

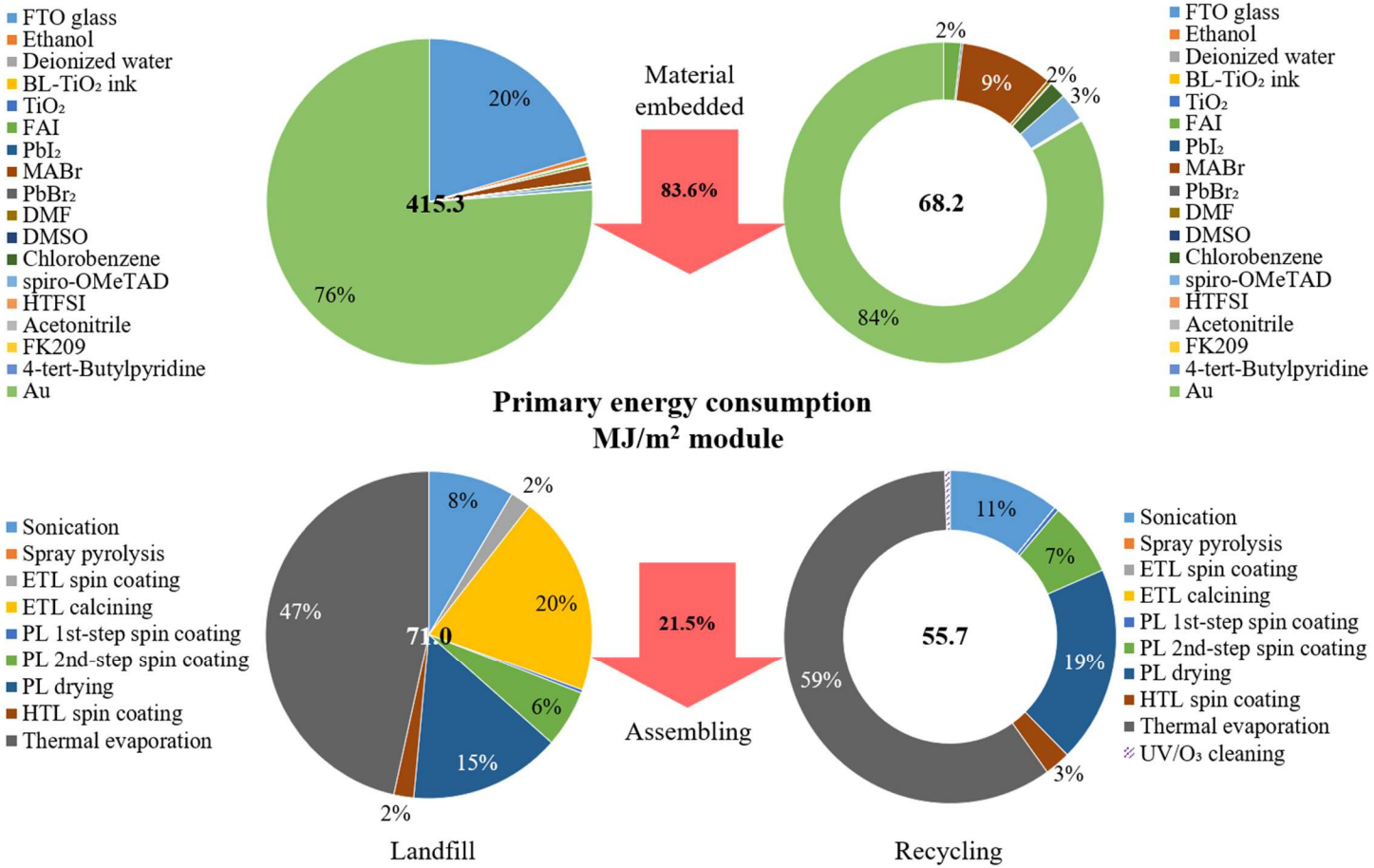

Figure S8. Primary energy consumption comparison between landfill (pie charts on the left) and recycling (donut charts on the right) end-of-life scenarios for the mixed-cation module (The upper two charts refer to the primary energy consumption in material acquisition, while the lower two charts represent the energy consumption during the assembling phase of PSC preparation. The arrows in the middle

reflect the variation of primary energy consumption relative to the landfill scenario).

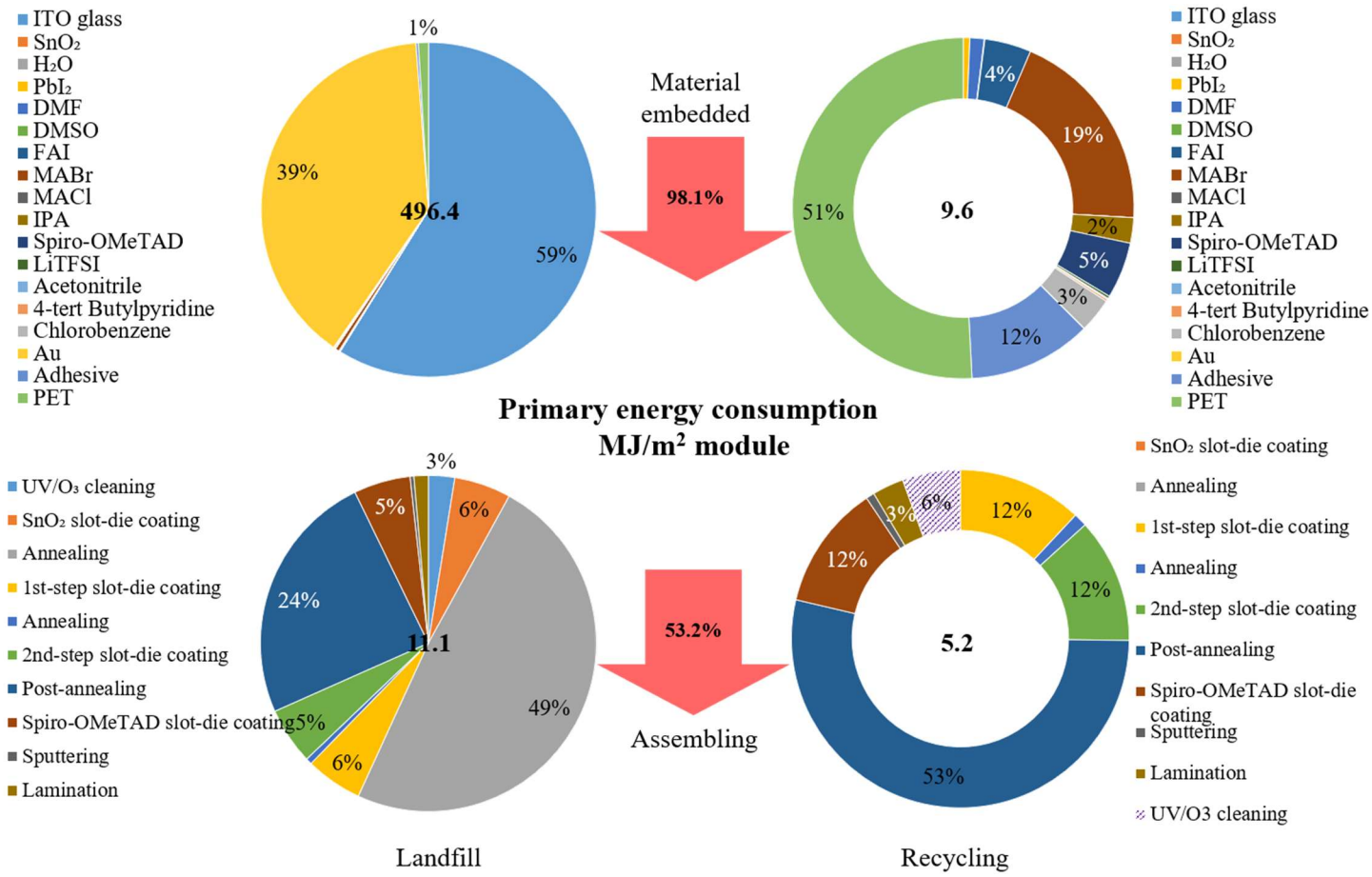

Figure S9. Primary energy consumption comparison between landfill (pie charts on the left) and recycling (donut charts on the right) end-of-life scenarios for the SnO_2 module (The upper two charts refer to the primary energy consumption in material acquisition, while the lower two charts represent the energy consumption during the assembling phase of PSC preparation. The arrows in the middle reflect

the variation of primary energy consumption relative to the landfill scenario).

S8. Uncertainty and sensitivity analysis results

The uncertainty and sensitivity analysis results for the metal oxide module, the mixed-cation module, the defect-engineered module, and the SnO_2 module are shown in Figure S10 to Figure S17.

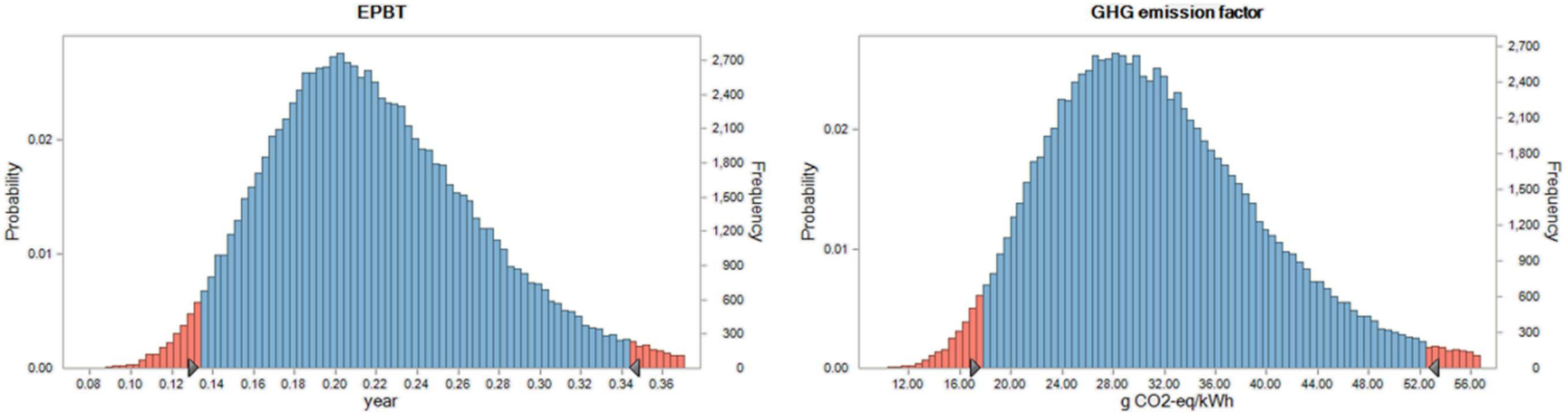

Figure S10. Uncertainty analysis for the metal oxide module in terms of EPBT and GHG emission factor.

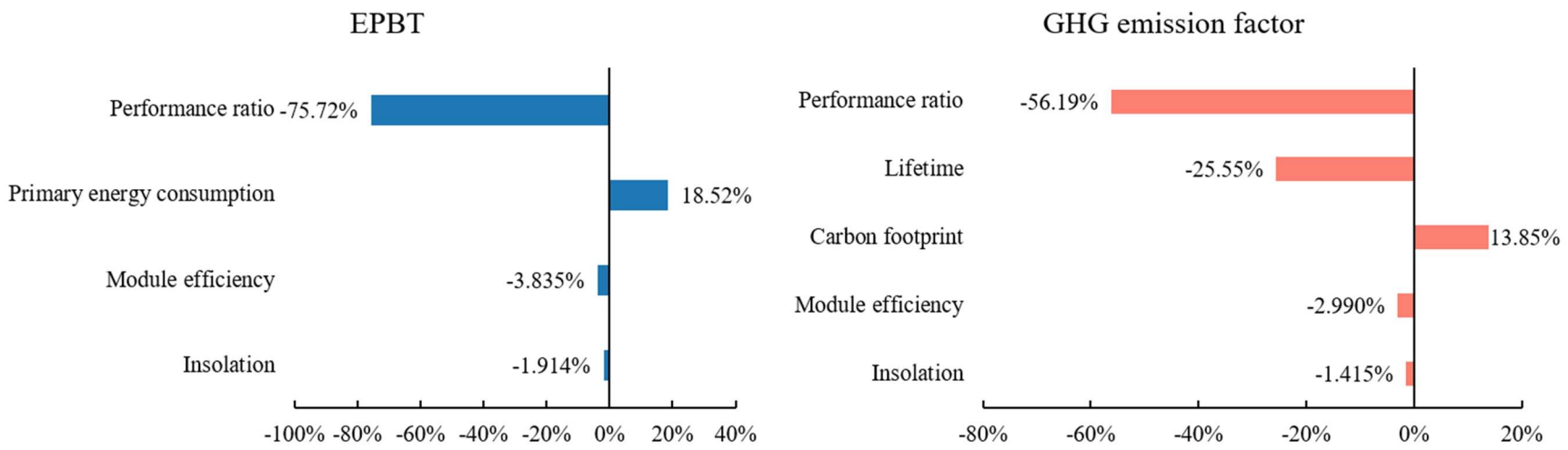

Figure S11. Sensitivity analysis for the metal oxide module in terms of EPBT and GHG emission factor.

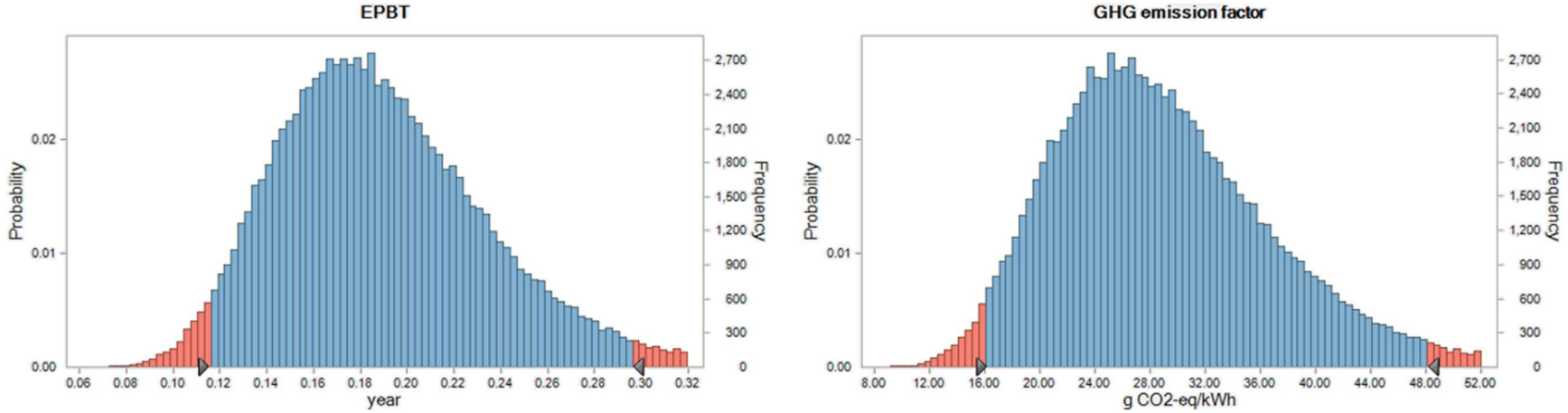

Figure S12. Uncertainty analysis for the mixed-cation module in terms of EPBT and GHG emission factor.

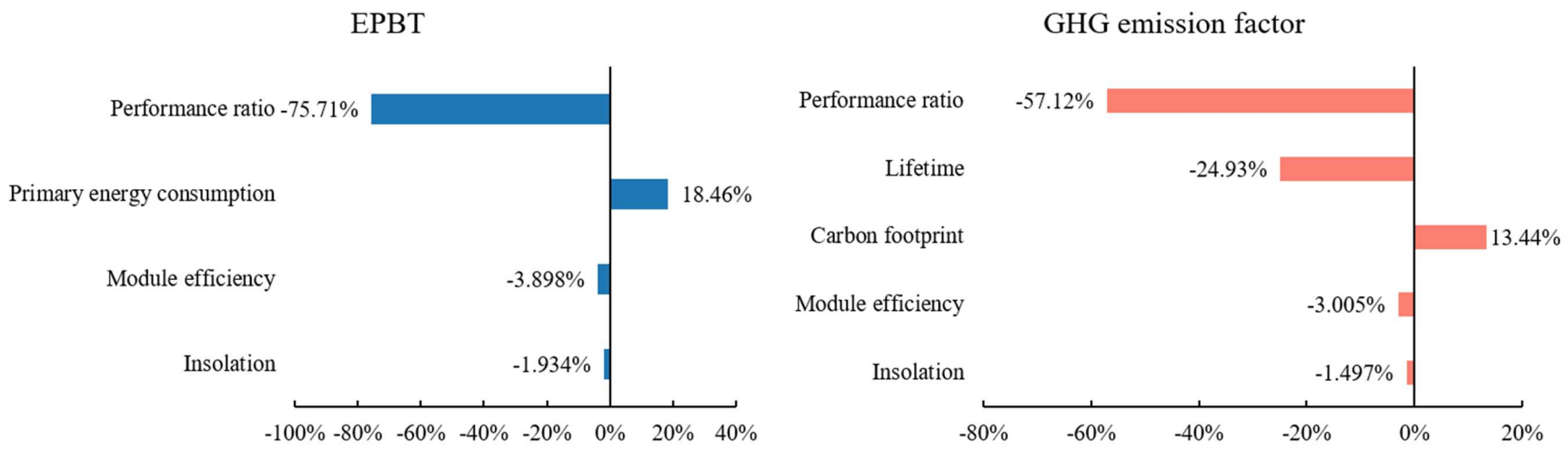

Figure S13. Sensitivity analysis for the mixed-cation module in terms of EPBT and GHG emission factor.

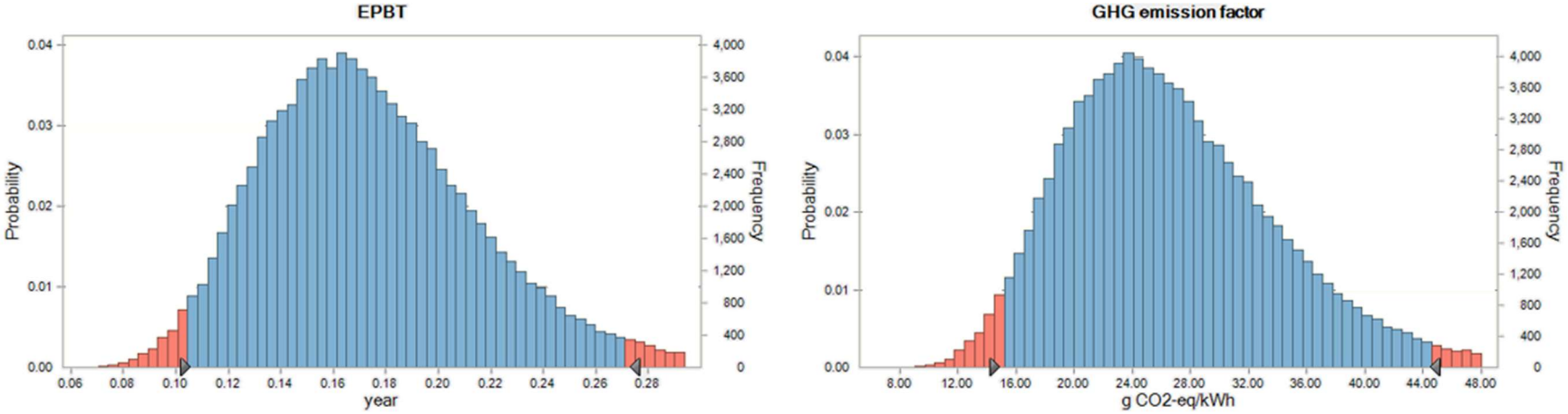

Figure S14. Uncertainty analysis for the defect-engineered module in terms of EPBT and GHG emission factor.

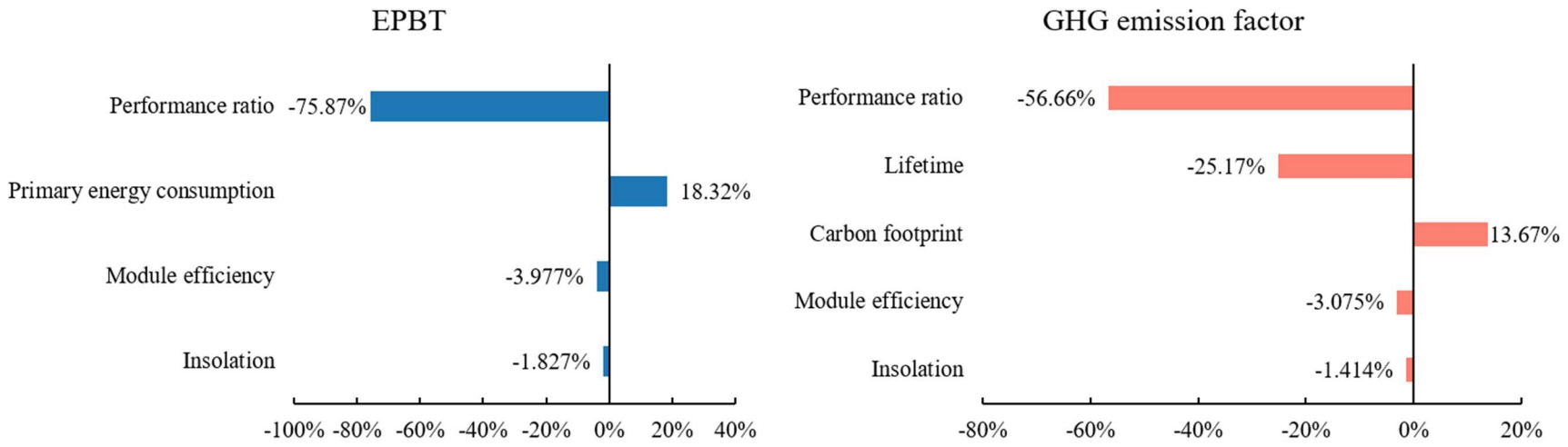

Figure S15. Sensitivity analysis for the defect-engineered module in terms of EPBT and GHG emission factor.

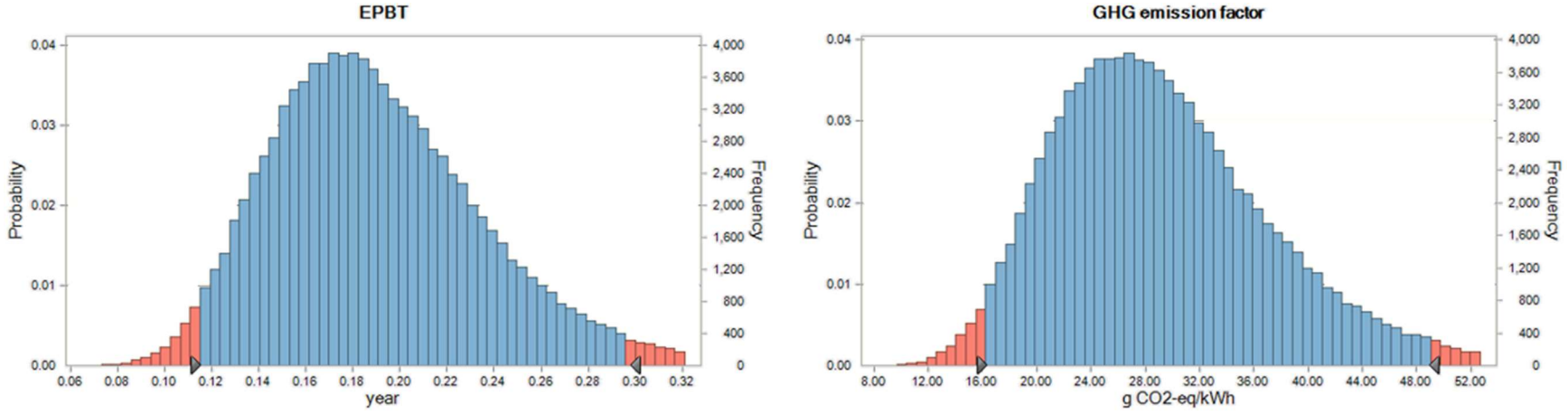

Figure S16. Uncertainty analysis for the SnO_2 module in terms of EPBT and GHG emission factor.

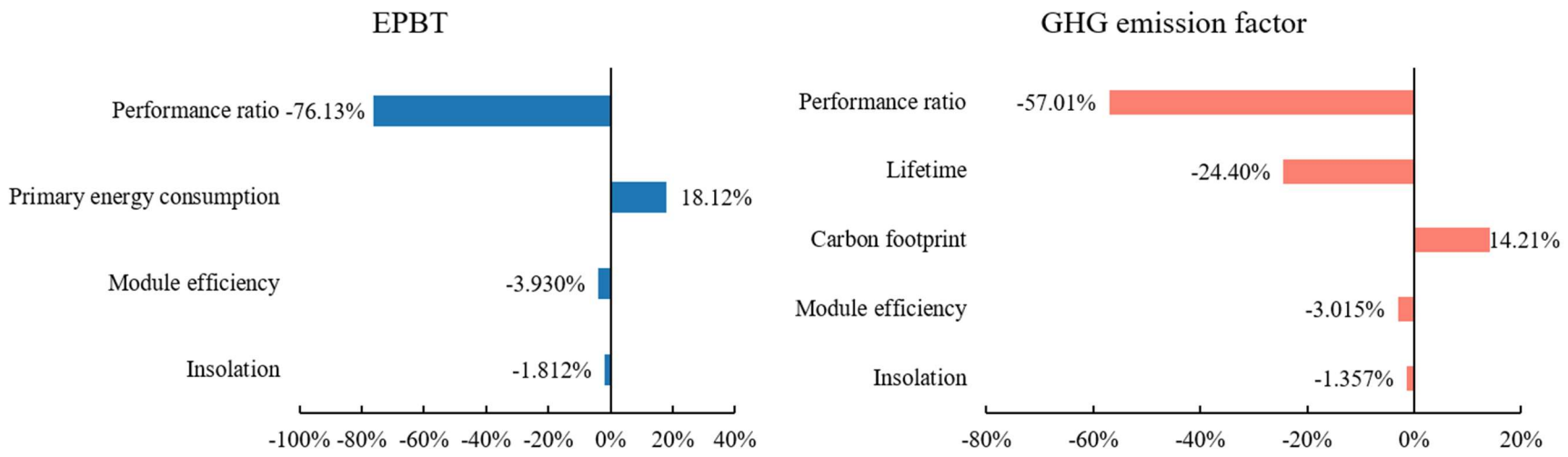

Figure S17. Sensitivity analysis for the SnO_2 module in terms of EPBT and GHG emission factor.

S9. Impacts of recycling levels on the primary energy consumption and carbon footprint

For the rest of the investigated perovskite PV modules, the impacts of recycling levels on the primary energy consumption and carbon footprint are quantified in Figure S18 to Figure S21, respectively. Note that for the metal oxide module, only the recycling level of ITO glass is considered, so the corresponding heat map is unidimensional.

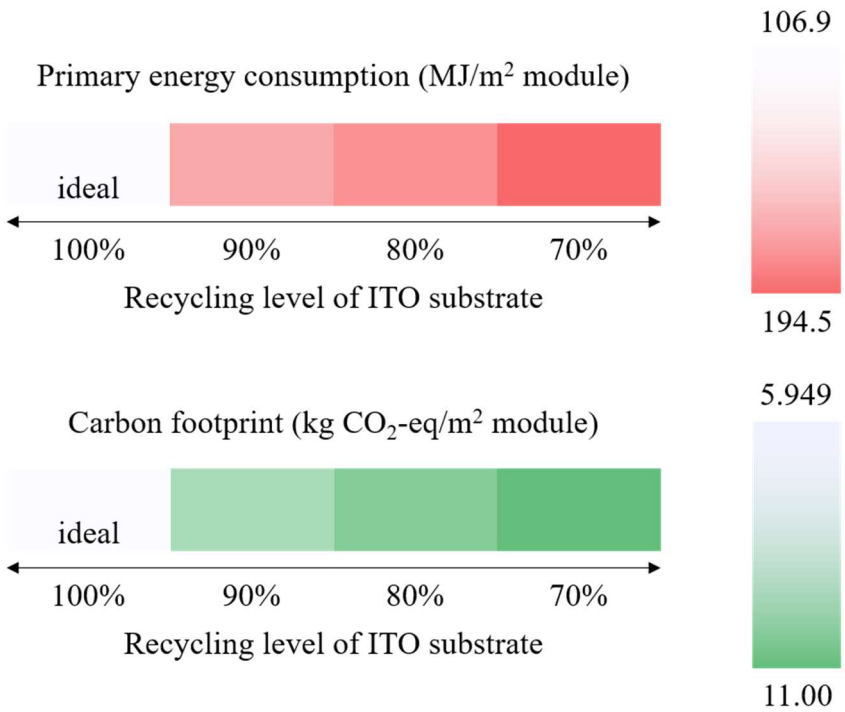

Figure S18. Impacts of recycling levels on the primary energy consumption and carbon footprint for the metal oxide module (The ideal recycling scenario can be intuitively identified on upper left corner of this heat map; the lower right corner refers to the "worst" recycling strategy).

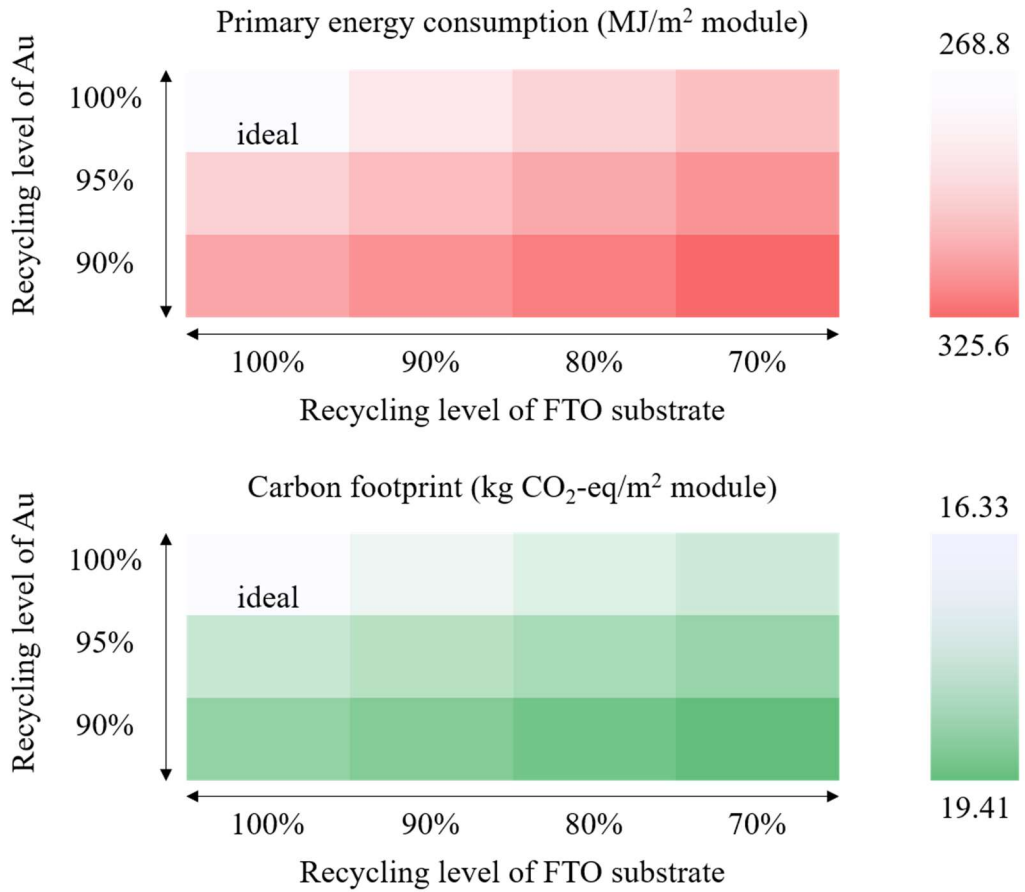

Figure S19. Impacts of recycling levels on the primary energy consumption and carbon footprint for the mixed-cation module (The ideal recycling scenario can be intuitively identified on upper left corner of this heat map; the lower right corner refers to the "worst" recycling strategy).

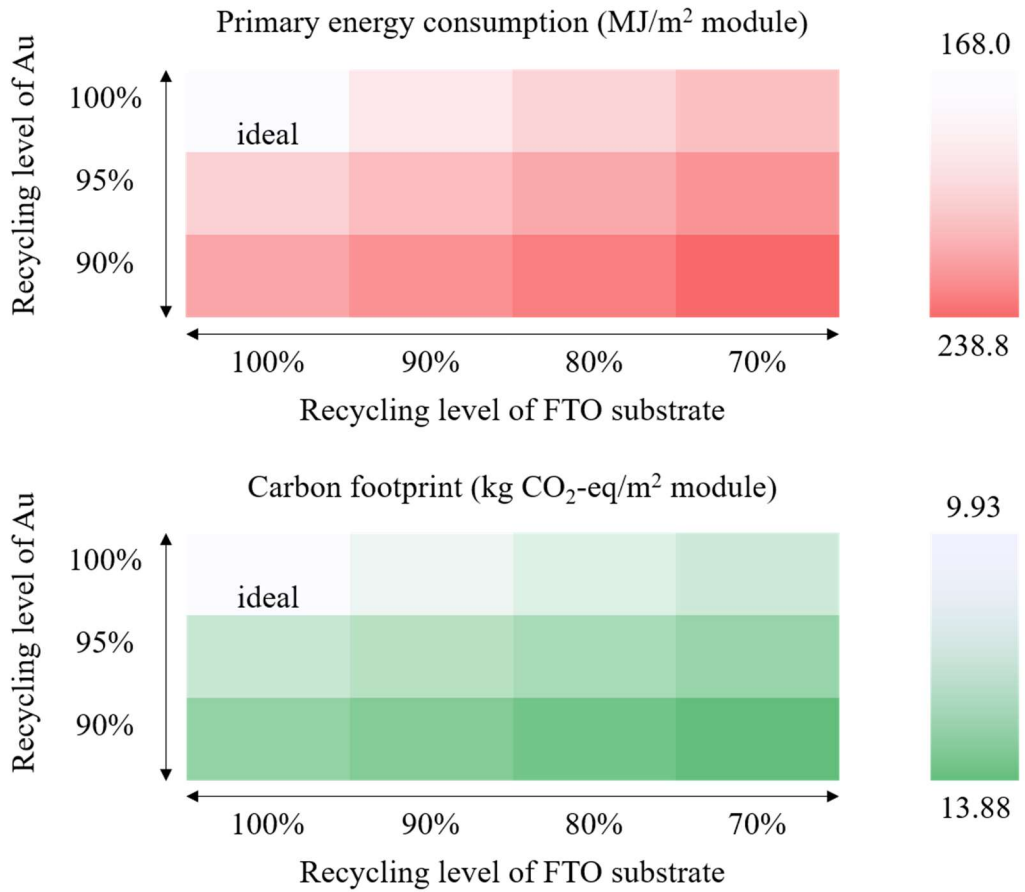

Figure S20. Impacts of recycling levels on the primary energy consumption and carbon footprint for the defect-engineered module (The ideal recycling scenario can be intuitively identified on upper left corner of this heat map; the lower right corner refers to the "worst" recycling strategy).

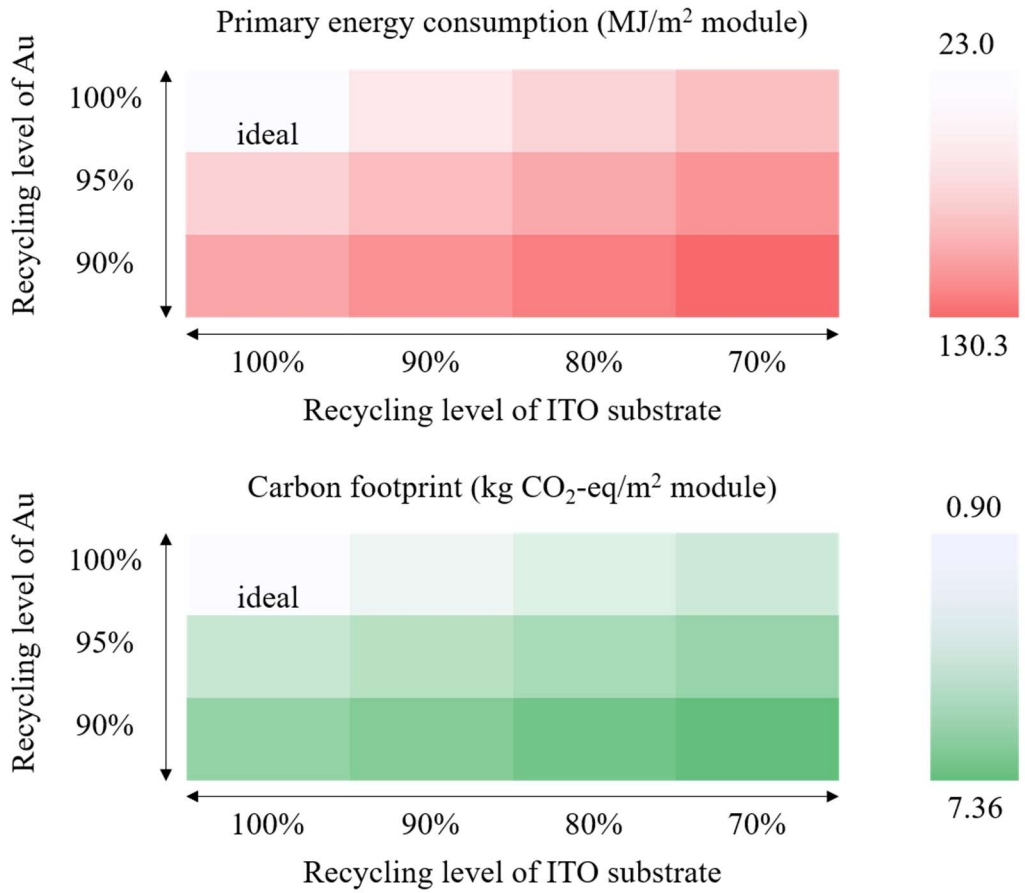

Figure S21. Impacts of recycling levels on the primary energy consumption and carbon footprint for the SnO_2 module (The ideal recycling scenario can be intuitively identified on upper left corner of this heat map; the lower right corner refers to the "worst" recycling strategy).

S10. Sensitivity analysis results for recycling

The sensitivity of recycling strategy is also quantified in terms of primary energy consumption as well as carbon footprint for the rest of the modules.

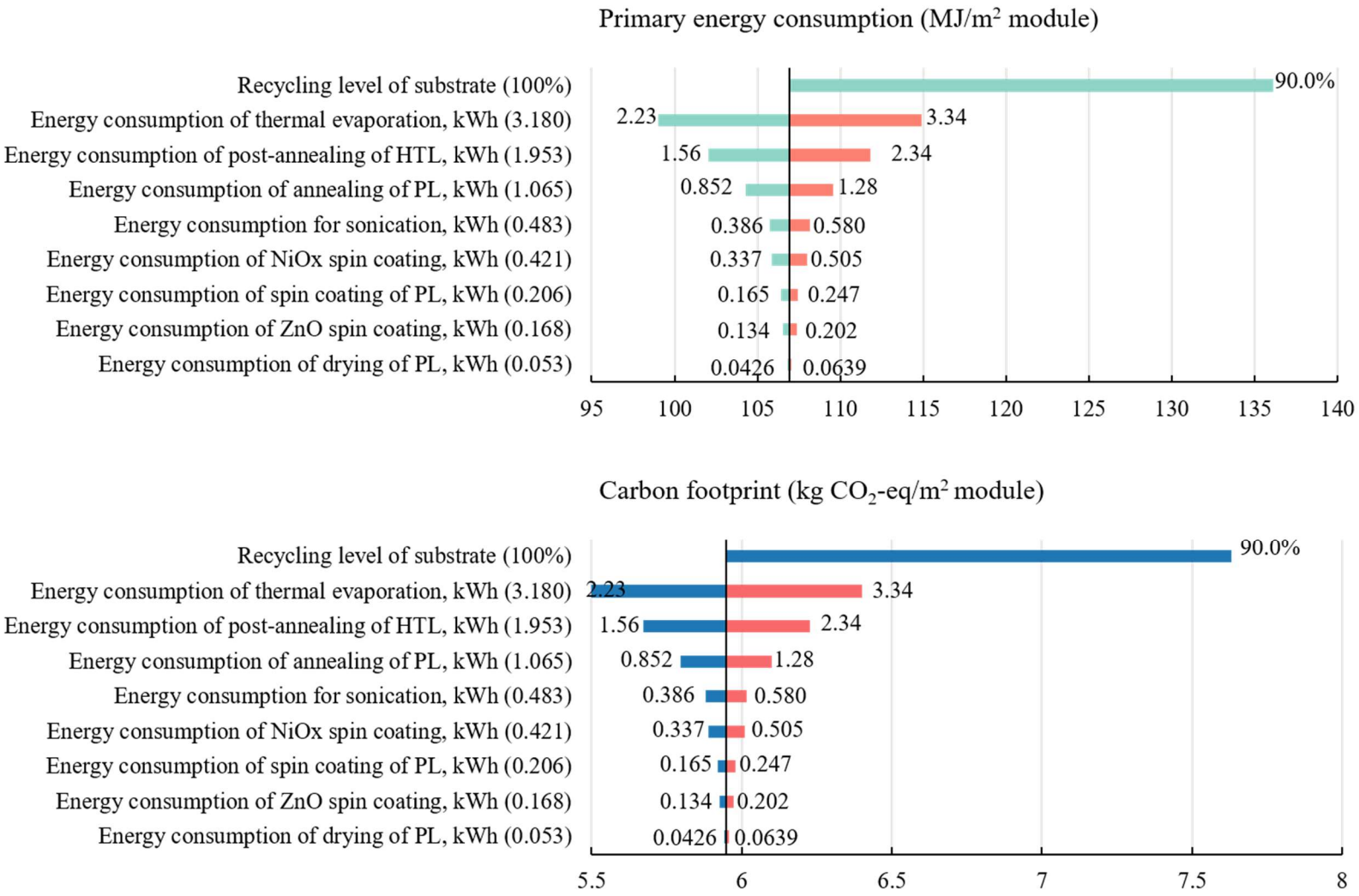

Figure S22. Sensitivity analysis for recycling the metal oxide module in terms of primary energy consumption and carbon footprint.

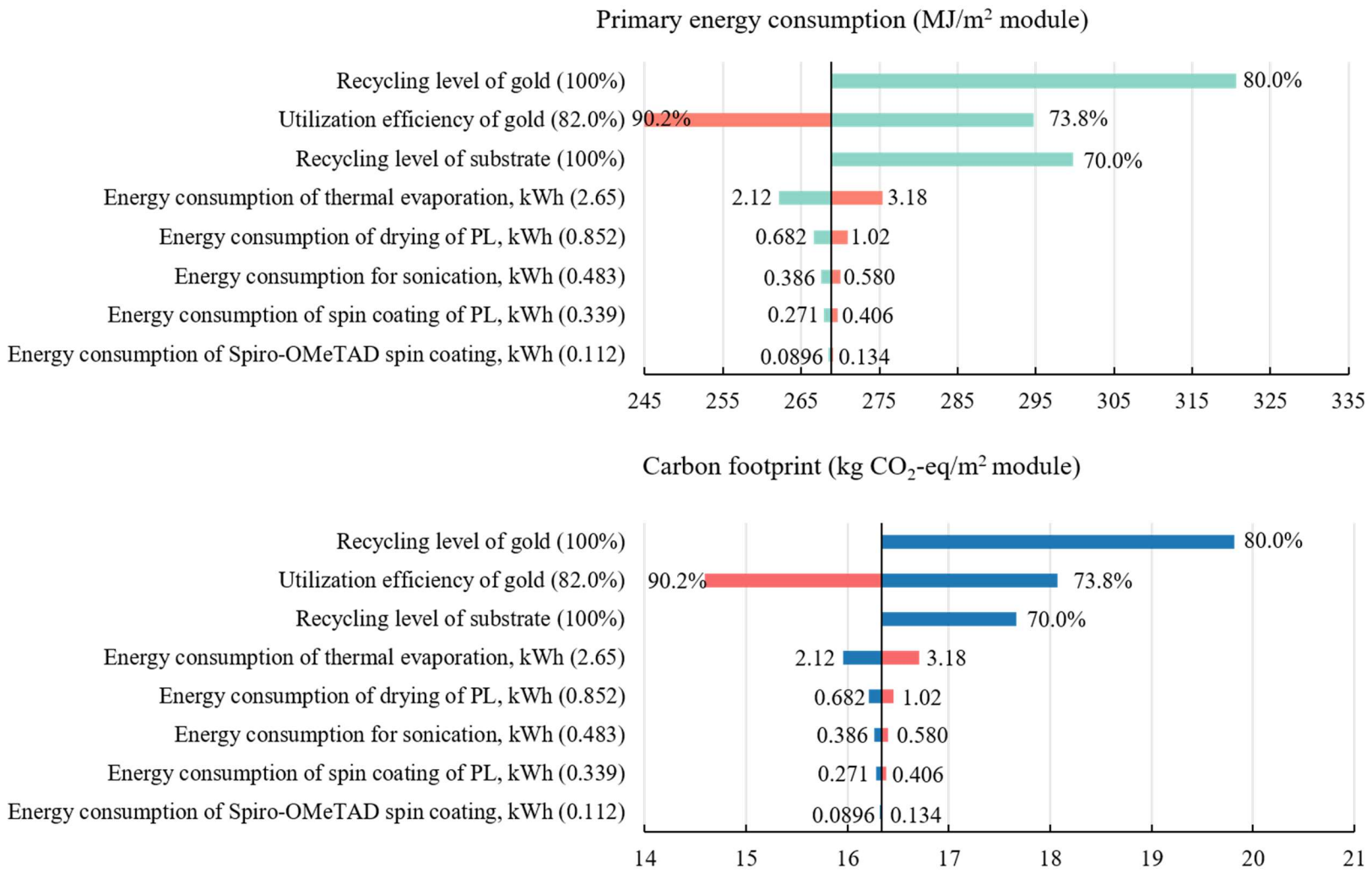

Figure S23. Sensitivity analysis for recycling the mixed-cation module in terms of primary energy consumption and carbon footprint.

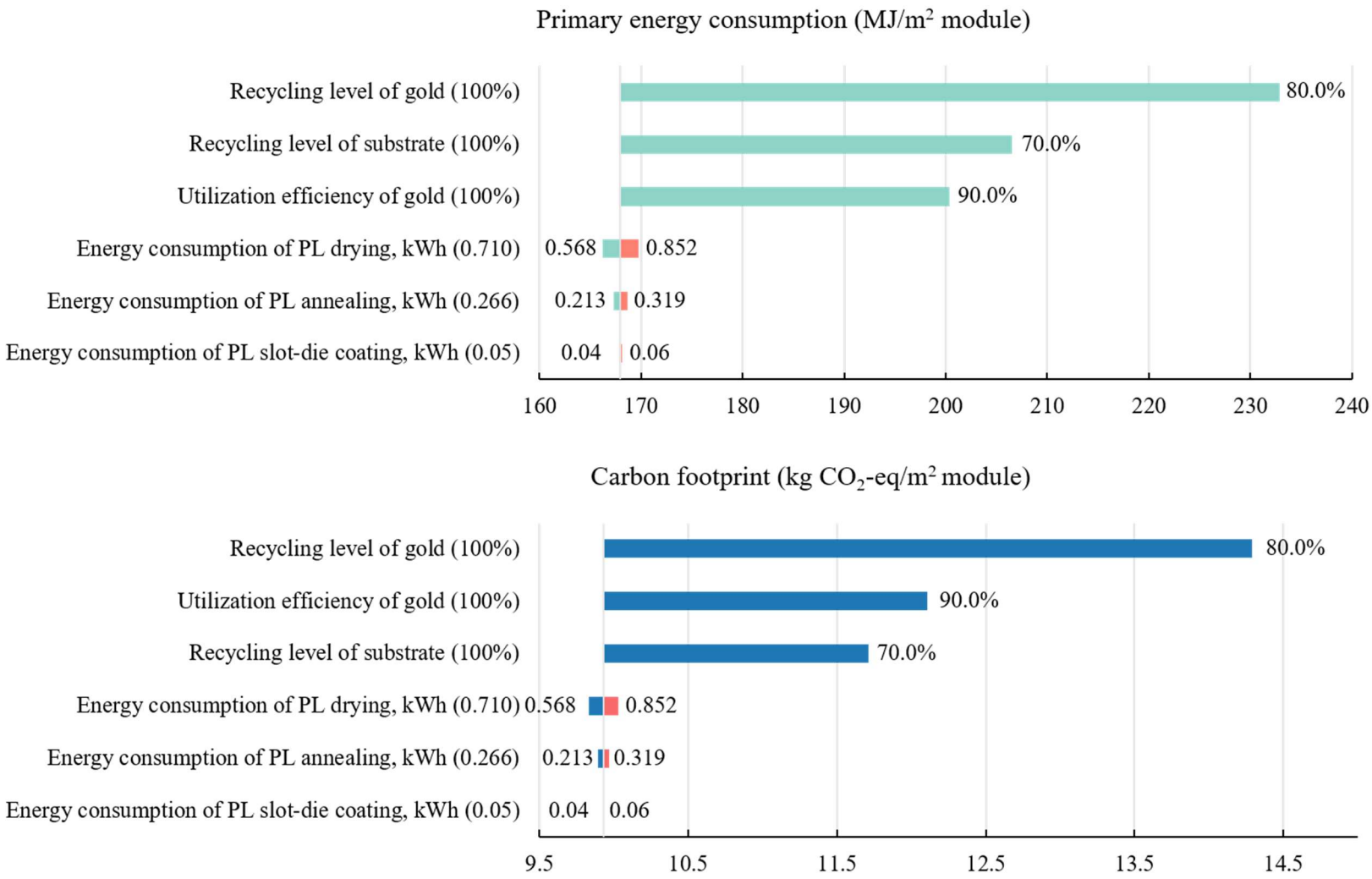

Figure S24. Sensitivity analysis for recycling the defect-engineered module in terms of primary energy consumption and carbon footprint.